Axonal wiring in the mouse olfactory system

By

Dipl.Biol. Olaf Christian Bressel

from Gross-Gerau, Germany

Performed at the Max Planck Research Unit for Neurogenetics in Frankfurt am Main and the Faculty of Biology at Technische Universität in Darmstadt

Approved Dissertation to receive the academic title of
Doctor rerum naturalium

Instructors
At the Max Planck Research Unit for Neurogenetics:
Peter Mombaerts, M.D., P.h.D.

At the Technische Universität Darmstadt:
1. Referent: Professor Bodo Laube
2. Referent: Professor Paul G. Layer

Date of submission: 16.07.2015

Date of oral defense: 15.10.2015

Darmstadt 2016

D17

Table of contents

Abbreviation

Abbreviation	Full name
(i)OSN	(immature) olfactory sensory neuron
(M)OB	(main) olfactory bulb
(T-)PBS	(Triton-) Phosphate buffered saline
AC3	Adenylyl cyclase 3
AOB	Accessory olfactory bulb
ATP	Adenosine triphosphate
Big2	Brain-derived, immunoglobulin superfamily molecule-2
bp	Base pairs
BSA	Bovine serum albumin
caGs	Constitutively active $G_{\alpha s}$ subunit
cAMP	Cyclic adenosine monophosphate
CIP	Calf intestine phosphatase
CNGC	Cyclic nucleotide gated channel
CV	Coefficient of variation
DNA	Deoxyribonucleic acid
E(number)	Embryonic age ()
EPL	External plexiform layer
ES	Embryonic stem cell
EtBr	Ethidium bromide
GAP43	Growth associated protein 43
GFP	Green fluorescent protein
GG	Grüneberg ganglion
Glom	Glomerular layer
GPCR	G protein coupled receptors
GrL	Granule layer
GTP	Guanine triphosphate
iOSN	Immature OSN
IPL	Internal plexiform layer
IRES	Internal ribosomal entry site
lacZ	β-galactosidase
LB	Lysogeny broth
LB-Crab	LB with carbenicilin
MOE	Main olfactory epithelium
MT	Mitral layer
NaCl	Sodium Chloride
NCAM	Neural cell adhesion molecule
Nrp	Neuropilin
O.C.T.	Optimum cutting temperature (freezing medium)
OCNC1	Cyclic nucleotide gated channel alpha 2
OMP	Olfactory marker protein
ONL	Olfactory nerve layer
OR	Odorant receptor
PCR	Polymerase chain reaction
PD(number)	Post natal day ()
PFA	Paraformaldehyde
RFP	Red fluorescent protein
RNA	Ribonucleic acid

Abbreviation	Full name
Robo	Round about
Sema	Semaphorin
SO	Septal organ
TAAR	Trace amine-associated receptor
TGV	Total glomerular volume
V1R	VR class 1
V2R	VR class 2
VNO	Vomeronasal organ
VR	Vomeronasal receptor
YFP	Yelllow fluorescent protein
z-stack	Optical sections in the z direction
β2AR	β2-adrenergic receptor

1 Summary

Odorant receptor (OR) genes were discovered by Buck and Axel (1991). Around 1,100 ORs are expressed in mouse olfactory sensory neurons (OSNs) in a monoallelic and monogenic manner (Chess et al., 1994). These OSNs are located in the main olfactory epithelium and project their axons to the olfactory bulb (OB) where they form homogeneous glomeruli. The glomeruli are formed at conserved positions in the OB. Several laboratories have studied the mechanisms that guide the OSN axons to their target where they form synapses with the mitral cells that convey the olfactory signal to other brain regions. Several theories have emerged to explain these mechanisms, but none has yet achieved full explanation for the precise axonal wiring in the mouse olfactory system.

This thesis describes three approaches for gaining further insight into the mechanisms that govern axonal wiring. In the first approach a gene-targeting vector was designed to target the M71 locus and knock in the constitutively active $G_{\alpha s}$ subunit (caGs) in M71-expressing OSNs. It has been reported that OSNs expressing caGs shift their glomerular position to a posterior position in the OB. However this shift was shown only with transgenic mice. A gene-targeted expression from the M71 locus would have provided a better understanding, because it is closer to the native mechanism. Unfortunately the assembly of the targeting vector was more difficult than anticipated and the project was suspended after a year.

The second approach was an empirical study of the fundamental components of the olfactory system. Green-fluorescent OSNs in 11 gene-targeted strains coexpressing GFP with a specific OR gene were evaluated quantitatively. It was shown that their OSN number is proportional to the respective total glomerular volume (TGV). These data enable new methods of quantifying and qualifying the properties of the OSN population and allow an estimate of the OSN numbers from the easier to measure TGV, which is much easier to measure than counting cells. With the first broad collection of

complete datasets of the number of OSNs, several other results could be extrapolated. The full datasets allowed an in-depth analysis of the sampling error for the 11 strains and established a well-grounded threshold for sampling of the main olfactory epithelium from every fifth section. I also demonstrated that these 11 strains have different stabilities of expression in terms of numbers of labeled OSNs, measured by the coefficient of variation (CV), with the strain MOR23-IRES-tauGFP being the most stable. It was also shown that most of the strains tested have a unique expression pattern along the anterior-posterior axis, except for OR-expressing OSNs in the classical zone 1, which displayed a similar expression pattern. For this study several reporter genes were expressed from the M71 locus, in addition gene replacements and downregulation of M71 were measured as well. These strains showed differences in the OSN numbers compared to M71-IRS-taulacZ expressing OSNs. The latter being expressed three times more than in the strains expressing fluorescent marker proteins. However each strain maintained the characteristic expression pattern for M71.

The final approach discussed in this thesis is the influence of a conditional Neuropilin-1 (Nrp1) knockout on axonal wiring of the mouse olfactory system. It has been reported that the position of a glomerulus in the OB along the anterior-posterior axis is determined by a gradient of Nrp1. However this finding was in mice expressing a transgene. Here an approach was chosen to generate a better test of this hypothesis. Conditional knockouts of Nrp1 in M71-expressing OSNs were generated, exploiting the unusual feature of monoallelic expression of ORs to provide a control in the same individual mouse. The results show not a gradual shift of glomeruli to the anterior OB as reported previously (Imai et al., 2009), but the formation of ectopic glomeruli in the anterior bulb, resembling the effect an adenylyl cyclase 3 (AC3) knockout has on M71-expressing OSNs. This phenotype is established directly at the onset of glomerular formation and is maintained during adulthood. These finding leads to the conclusion that the signal transduction cascade of OSNs is indeed linked to the expression of Nrp1, but a simple Nrp1-gradient hypothesis cannot explain the phenotype M71-expressing OSNs.

2 Introduction

Of the five senses the sense of smell is probably the most complex one to investigate. While for example the sense of taste has five different receptor types to coordinate, the sense of smell has to coordinate hundreds of different olfactory sensory neurons (OSNs) each expressing a single odorant receptor (OR) gene (Chess et al., 1994). The discovery of the OR genes 24 years ago has triggered a substantial amount of research on the mechanism that determines and regulates axonal wiring in the mouse olfactory system.

2.1 Anatomy of the mouse olfactory system

The olfactory system of mice consists of several organs, which express many types of molecular chemosensory receptors (Figure 2.1). The first of these organs is the Grüneberg ganglion (GG), located at the tip of the nose of the mouse. The chemosensory neurons there probably express receptors for early warning signals (Brechbühl et al., 2008). The vomeronasal organ (VNO) is situated on the septum in the nasal cavity and receives mostly information from pheromones and kairomones (Døving and Trotier, 1998). The most prominent chemosensory receptors in the VNO are the vomeronasal receptors (VR) and will be further described in Chapter 2.4. Another sensory organ is also situated on the septum, the septal organ (SO). In the SO a subset of olfactory sensory neurons (OSNs) can be found (Ma et al., 2003b, Tian and Ma, 2004). Most OSNs reside within the main olfactory epithelium (MOE). OSNs in SO and MOE send their axons through the cribriform plate to the main olfactory bulb (MOB), where they form glomeruli that are homogeneous for a single OSNs type.

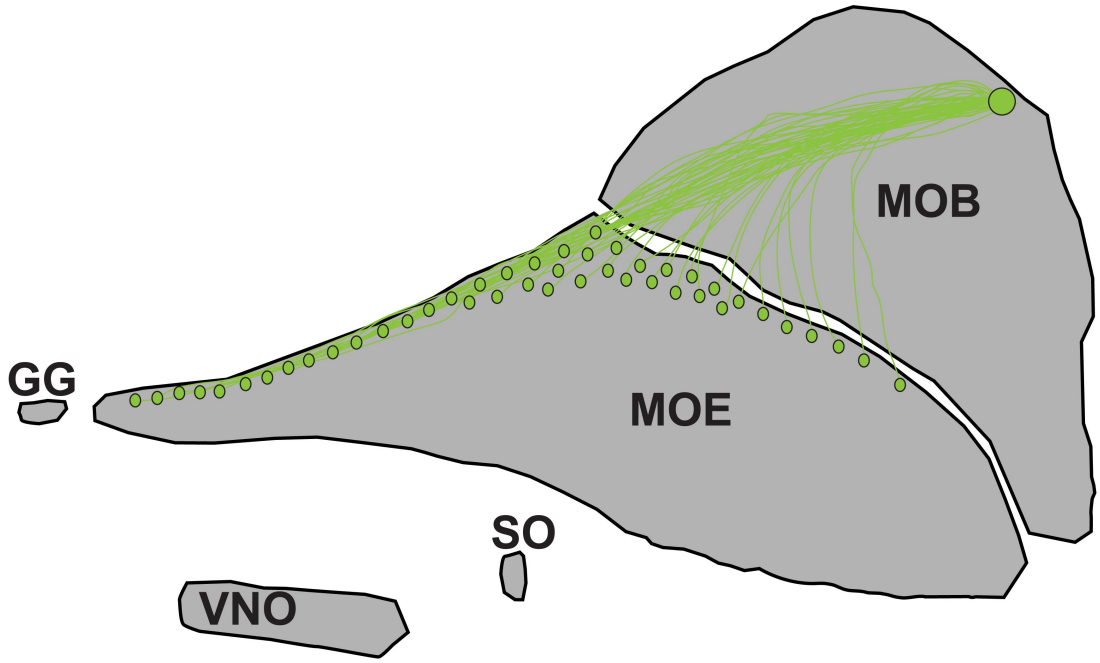

Figure 2.1 Mouse olfactory system
Representative sagittal map of the mouse olfactory system showing the different sensory organs: Grüneberg ganglion (GG), vomeronasal organ (VNO), septal organ (SO) and main olfactory epithelium (MOE). OSNs (small green dots) located in MOE project their axons to the mouse olfactory bulb (MOB) to form homogeneous glomeruli (large green circle).

2.2 Olfactory receptors (ORs) and olfactory sensory neurons (OSNs)

The OR gene family is the largest gene family in the mammalian genome. It was discovered by Linda Buck and Richard Axel in 1991 (Buck and Axel, 1991) and recognized with the 2004 Nobel Prize in Physiology or Medicine. The OR genes are expressed in OSNs monogenically and monoallelically (Chess et al., 1994), which makes them an interesting model for the study of gene choice. Recent studies estimate that approximately 10 million mature OSNs are present in an eight-week old mouse (Kawagishi et al., 2014).

Most OSN cell bodies reside within the middle layer of the main olfactory epithelium (Strotmann et al., 1996). The MOE is layered from basal to apical along the maturation of OSNs (Nickell et al., 2012). The basal layer provides the progenitor OSNs, which develop to immature OSNs (iOSNs), determined by the expression of GAP43. Mature OSNs are detected by their expression

of the olfactory marker protein (OMP) and they are situated in the apical half of the epithelium (Figure 2.2).

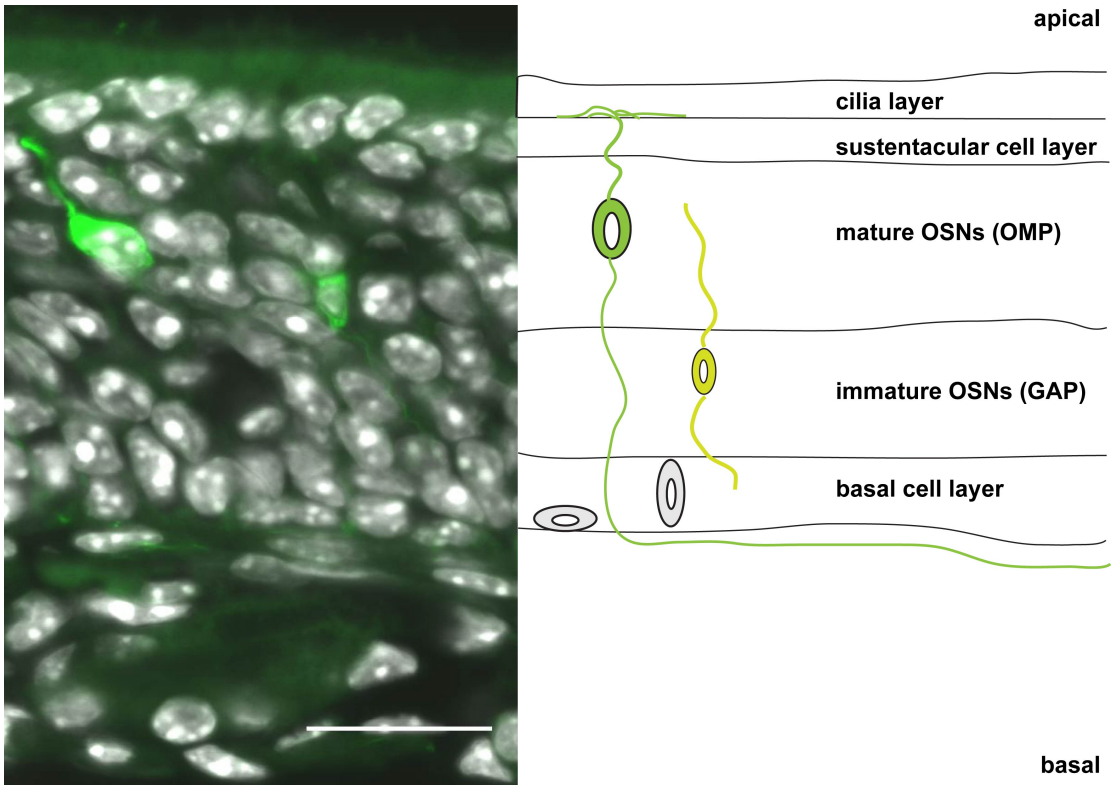

Figure 2.2 Olfactory epithelium layers
Schematic overview of the layers in the main olfactory epithelium from apical to basal along a coronal section of aPD21 M71-IRES-tauGFP mouse taken with a confocal microscope. OSN progenitor cells are formed from the basal cells (grey). While maturing the immature OSNs (light green) express GAP and move in apical direction. Dendrite and axon begin to form. Cell bodies of mature OSNs (green) are in the apical half of the epithelium. They have fully formed dendrites crossing the sustentacular cell layer and cilia spreading on the apical side. Mature OSN axons project to the olfactory bulb. The mature OSN layer is characterized by OMP expression. Scale bar: 20 µm

It has been established that OSNs expressing a specific OR are not spread homogeneously across the whole surface of the MOE. The first studies identify four discrete zones of expression, arranged roughly from dorsal to ventral MOE (Ressler et al., 1993). Later studies gave rise to the idea that each OR-expressing OSN population is expressed in a unique gradient across the epithelium (Miyamichi et al., 2005). Recent unpublished studies in our lab suggest an intermediate scenario. The OR gene family can be divided into two classes. Class I ORs are expressed exclusively in the dorsal area and project to anterior-dorsal region of the bulb (Tsuboi et al., 2006), while class II ORs are expressed in all zones of the MOE (Figure 2.3).

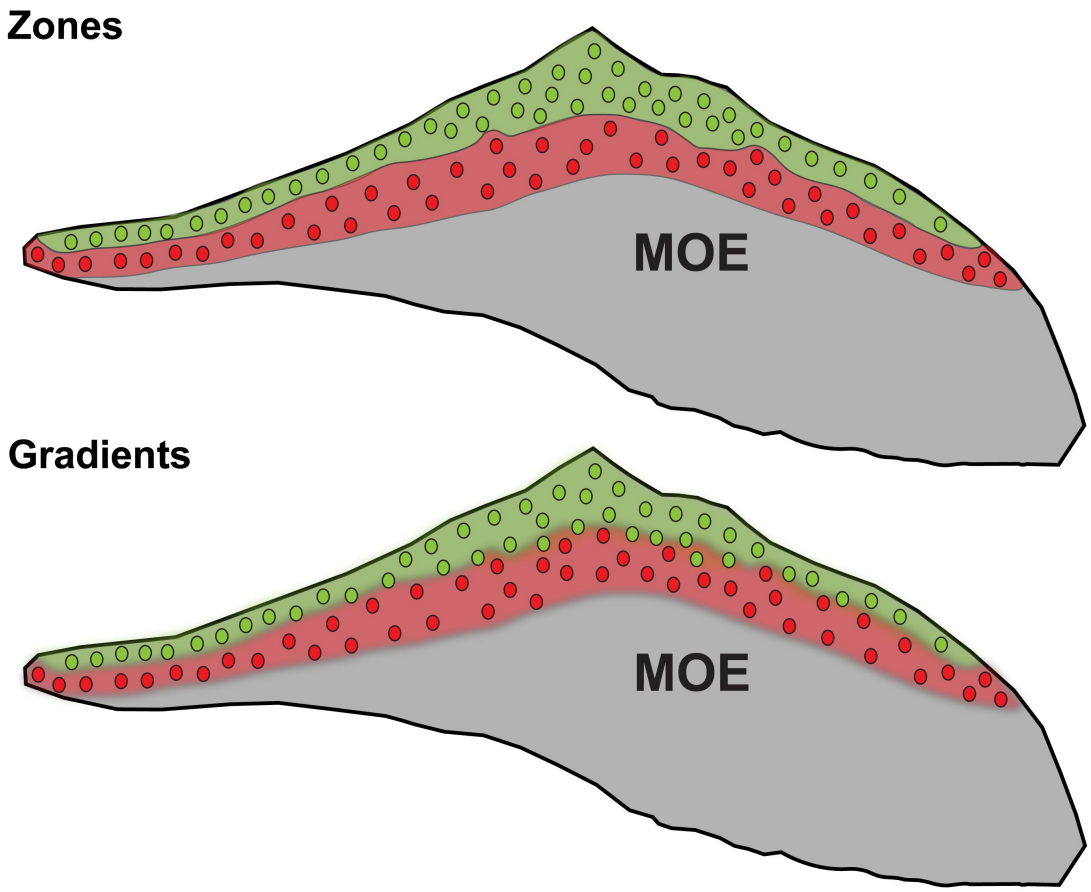

Figure 2.3 Illustration of zones and gradients
This sketch illustrates the difference between the theory of OSN expression in zones and in gradients. For zonal expression each OSN population (green & red) is confined to a specific zone (historical four with the green are representing zone 1 and the red area zone 2). Each OSN population would fall in one of these zones. In the gradient theory each OSN population would be expressed preferentially also in its own zone, however, also in a stripe overlapping with the zones of one or more other OSN population.

Since 1991, approximately 1,100 OR genes have been identified in mouse (Zhang and Firestein, 2002), located on most chromosomes. The structure of these ORs contains seven-transmembrane spanning regions, similar to other G-protein coupled receptors such as the β2 adrenergic receptor, but there is a substantial variance in sequence (Liu et al., 2003). ORs are expressed already very early in development and can be detected by antibody staining as early as embryonic age 12 (E12) in cilia of OSNs (Schwarzenbacher et al., 2005). These receptors are not only expressed in the cilia of the OSNs but can also be detected in their axon terminal (Barnea et al., 2004 , Strotmann, 2004). Ca^{2+} influx and cyclic adenosine monophosphate (cAMP) as second messenger in the signaling cascade (Maritan et al., 2009) were also observed in early OSNs.

The zonal expression of a population of OSNs as well as the regulation of monogenic expression of the ORs in OSNs is still not fully understood. Several groups have been working on the issue of gene choice and the regulation of OR expression and suppression. Once an OR is chosen and successfully expressed, the OSN never changes this chosen OR. However there are no genetic alterations of the OR locus accompanying gene choice (Li et al., 2004). Expression of a functional receptor is important for a stable expression of this OR through the OSNs life. If the OR is not functional another OR gene is chosen for expression (Shykind et al., 2004). However the alternate choice does not have to originate from the same gene clusters, as shown with the highly related mOR37 gene cluster (Bader et al., 2010). The OR sequence is sufficient for silencing expression other OR genes (Nguyen et al., 2007) even from transgenic ORs. The sequence of untranslatable OR mRNA is sufficient for an effective silencing of other ORs (Lewcock and Reed, 2004). There is a hierarchy in the choice of an OR (Hirota et al., 2007) where the class is determined before the specific OR.

Recently several factors regulating the gene choice haven been discovered. The regulatory element called the P element was reported in 2011 in this lab (Khan et al., 2011). The structure of OR promoters has been revealed a year later (Plessy et al., 2012). The first initiator for OR expression has been discovered, with downregulation of LSD1 associated with stabilization of OR gene choice (Lyons et al., 2013).

2.3 Oddities of OSN populations

Of the ~1,100 ORs in mouse only a few percent have been characterized in some detail. But already several OSN populations are reported to have remarkable and so far unique expression patterns. For example OSNs expressing the receptor SR1, which represent one of the largest OSN populations, constitute half of all OSNs situated in the septal organ (Tian and Ma, 2004, Figure 2.4). This broad expression is even more interesting since SR1 has a very broad response profile for an OR (Grosmaitre et al., 2009).

Another interesting gene family is the mOR37 gene family, with an unusual expression pattern in a patch in the middle of the MOE on one turbinate. However a transgene expression of the mOR37C leads to expression of the OR outside of this patch (Strotmann et al., 2009, Bader et al., 2010).

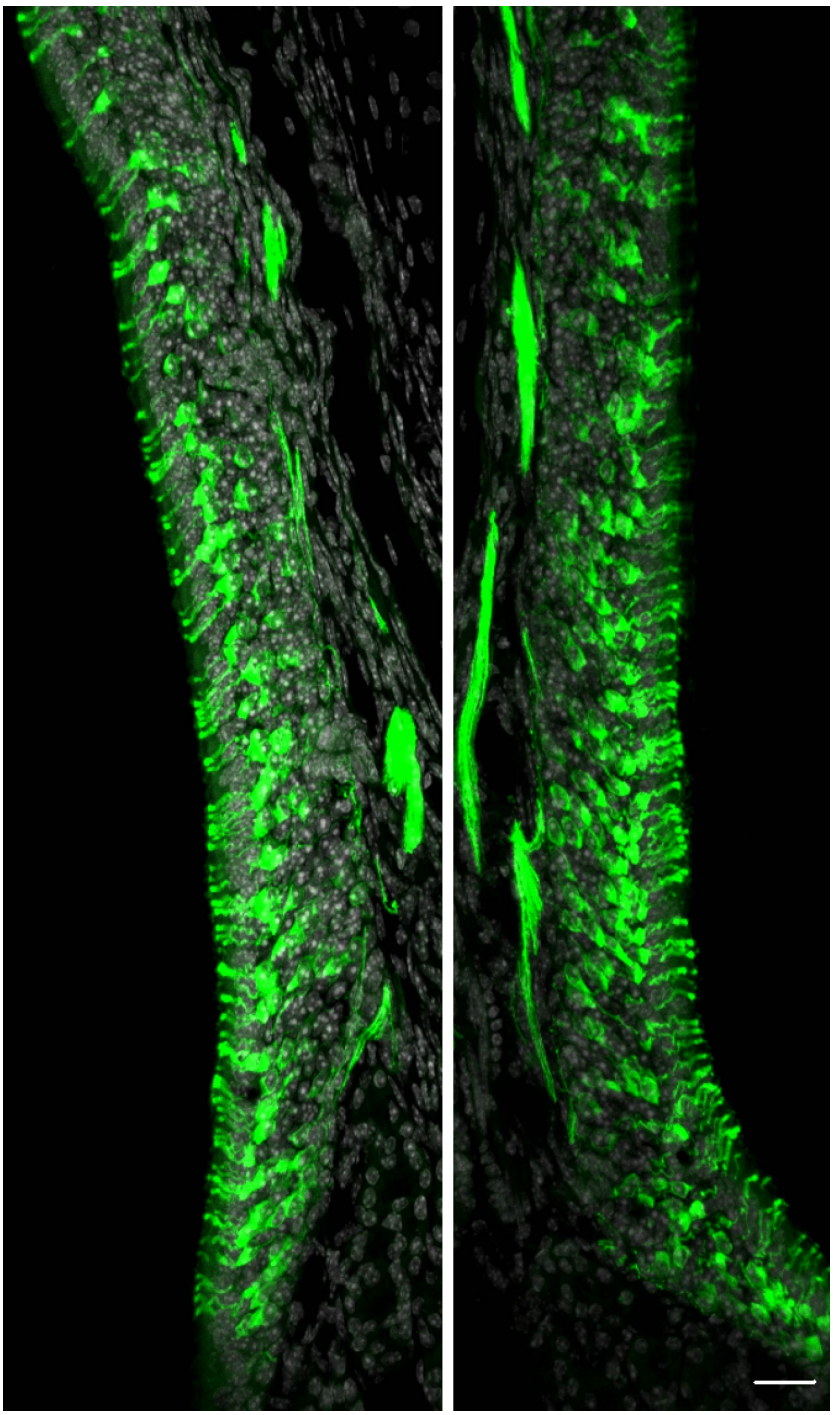

Figure 2.4 Example of SR1 expression in the septal organ
Confocal image of coronal 12 µm section of the septal organ of a PD21 SR1-IRES-tauGFP mouse. Both images are from the same coronal section; the septum was removed. Green intrinsic fluorescence shows OSNs expressing SR1. The strong green fluorescent lines close to the septum are the axon bundles heading towards to the olfactory bulb. DAPI staining in grey. Scale bar: 20 µm.

2.4 TAARs & VRs

Olfactory receptors are not the only chemosensory receptor families expressed in the olfactory system. Another family is the vomeronasal receptors (VRs), which are expressed in the vomeronasal organ (VNO) that is situated on the septum and senses pheromones. VR genes are the largest receptor gene family expressed in VNO, constituting almost all of the sensory neurons. VRs can be divided into two subfamilies (called V1R and V2R). V1Rs are expressed in the apical VNO epithelium while V2Rs are expressed in the basal VNO epithelium. Their axons project to the accessory olfactory bulb (AOB) situated dorsally and posterior of the MOB (Figure 2.5). The separation between V1R and V2R is still maintained in the AOB, the V1R glomeruli occupying the dorsal half of AOB while the V2R glomeruli occupy the ventral half of the AOB. But compared to the OSNs, only V1Rs are expressed similarly in a monogenic fashion, while V2Rs are not (Roppolo et al., 2007). It is also interesting to note that in mouse subspecies the VR repertoire differs in terms of the functional VR genes (Wynn et al., 2012).

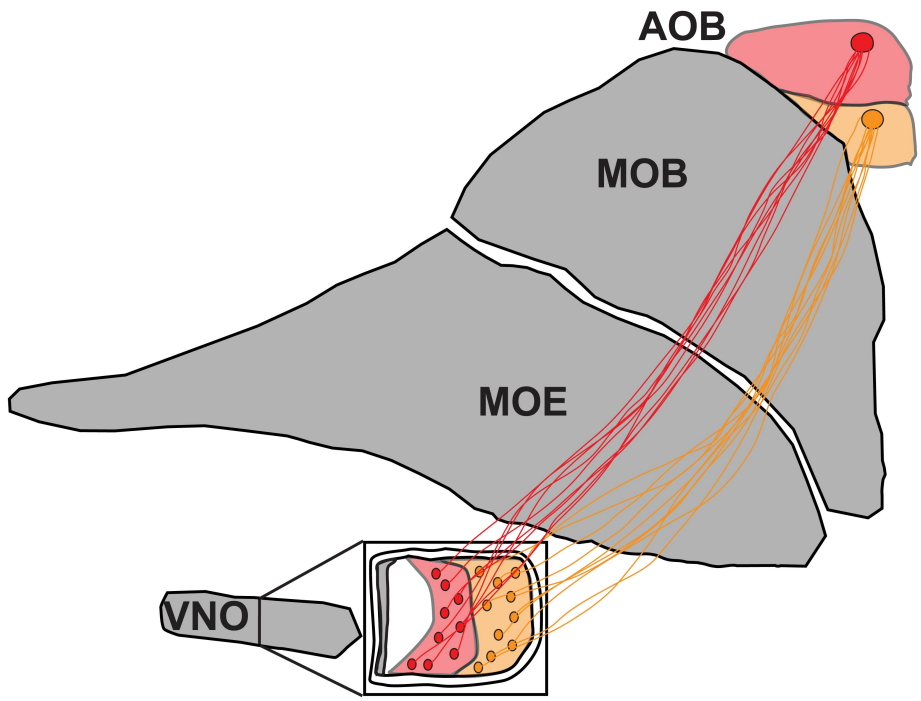

Figure 2.5 Axonal wiring of the vomeronasal system
Schematic overview of the axonal wiring of the VNO to the AOB in sagittal view. The VNO in coronal view (box) consists of cavernous tissue (grey), basal epithelium with V2Rs (orange) and apical epithelium with V1Rs (red). Both chemosensory neuron types send their axons to representative zones in the AOB. V1R to the dorsal half and V2R to the ventral half of the AOB.

Another recently discovered gene family is expressed in the MOE, the trace amine-associated receptors (TAARs). They are coexpressed with ORs but have the same signal transduction cascade, the G_{α} olfactory subunit ($G_{\alpha olf}$), as mature OSNs (Liberles and Buck, 2006). They are closely related to OR genes, explaining this similarity (Pacifico et al., 2012). It has been shown that TAAR-expressing sensory neurons respond to the odors of predators and other odors that trigger aversive reactions (Dewan et al., 2013). If a TAAR gene is deleted, TAAR expressing sensory neurons tend to express other TAARs rather than ORs. TAAR-expressing neurons project to a dorsal area in MOB, in between the areas D1 and D2. It seems that TAAR-expressing cells do not maintain such a strict homogeneity in their glomeruli as OSNs do (Pacifico et al., 2012).

2.5 Signaling

The primary task of a functional OR is the detection of odorants. Since ORs are G-protein coupled receptors (GPCRs) the molecular events following binding of an odorant by the OR are similar to other GPCRs and were established shortly after the discovery of the ORs themselves (Levy et al., 1991). The ORs are expressed early in development at E12. Other important factors such as NCAM and Big2 are expressed at E11 and E14, respectively (Saito et al., 1998).

If an odorant is bound to an OR, the the G_{α} subunit is activated by binding a GTP (guanosine tri-phosphate). In immature OSNs the activation is by the $G_{\alpha s}$ subunit, while after E14 (Saito et al., 1998) the $G_{\alpha olf}$ subunit is used for signal transduction (**Figure 2.6**).

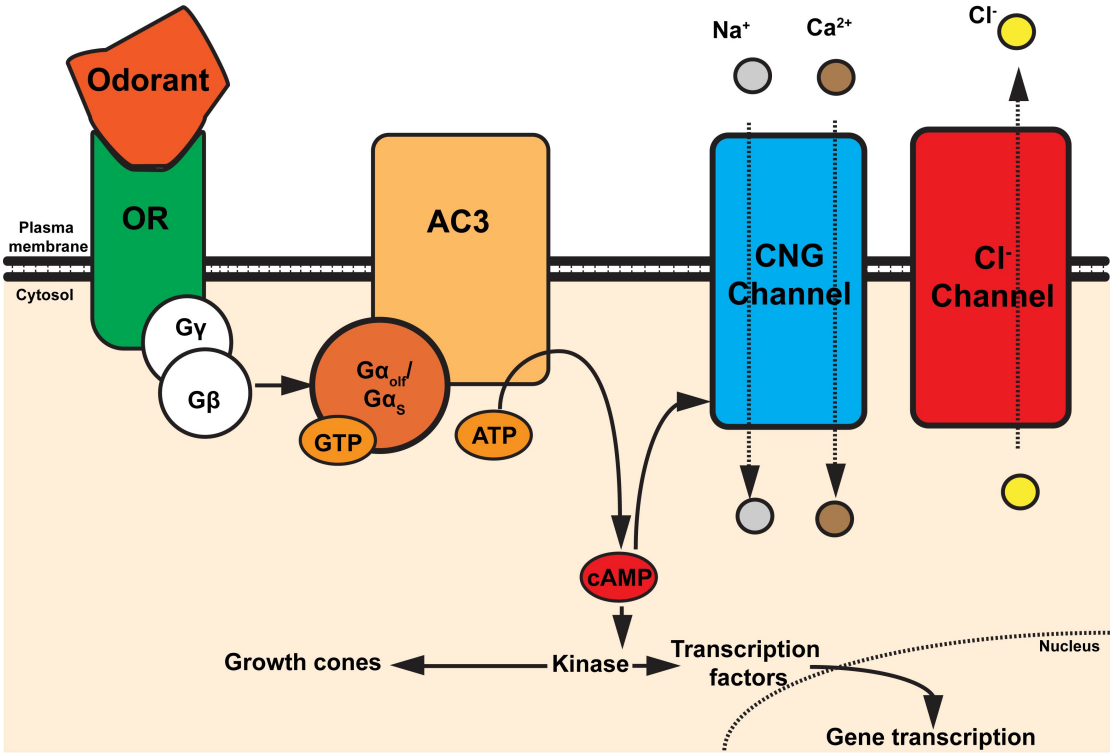

Figure 2.6 Signal transduction in OSNs
Schematic overview of the signaling transduction cascade in OSNs. Odorant is bound by OR. The G_α subunit (either $G_{\alpha s}$ in inmature or $G_{\alpha olf}$ in mature OSNs) is activated and in turn activates AC3. AC3 will transform ATP into the second messenger cAMP, which will then activate kinase towards the growth cone and/or transcription factors. cAMP will also open CNG channels, where the Na^+ and Ca^{2+} influx causes a depolarization of the cell membrane which will ultimately lead to an action potential.

The activated $G_{\alpha olf}$ subunit is binding the adenylyl cyclase 3 (AC3), which transforms adenosine triphosphate (ATP) to cAMP. The second messenger cAMP is the critical signaling molecule in OSNs (Firestein et al., 1991). Mice with a knockout of the AC3 gene have viable OSNs but multiple ectopic glomeruli are formed and wiring defects are seen (Zou et al., 2007). AC3 and $G_{\alpha olf}$ are also the first steps in the signal transduction cascade in the septal organ, supporting further the close relationship between the SO and MOE (Ma et al., 2003a). However, the same cascade does not apply to the VNO. For instance, $G_{\alpha olf}$ could not be detected in the VNO, but low traces of AC3 were found (Berghard et al., 1996). Consequently, the VNO can still detect odors and pheromones even after a deletion of AC3 (Trinh and Storm, 2003).

The primary targets for the second messenger cAMP in the signaling cascade are the cyclic nucleotide gated (CNG) channels. When cAMP binds to the CNG channels, they open and allow the influx of sodium (Na^+) and

calcium ($Ca2^+$) ions. This influx of cations leads to a depolarization of the membrane and ultimately to the formation of action potentials. The depolarization is further supported by the opening of chloride ion (Cl^-) channels. The critical role of CNG channels is emphasized by a deletion of CNG channels in mice, resulting in profound anosmia (Brunet et al., 1996).

Three studies report other interesting observations concerning the modulation of the signal transduction cascade in OSNs. The first study shows that a complex of ORs with other GPCRs strengthens the localization of all GPCRs in the plasma membrane (Bush et al., 2007). The second study identifies Pl3k as a mediator of inhibitory signaling in OSNs (Ukhanov et al., 2010). Pl3k is enforcing G-protein signaling and thus Pl3k expression leads to a faster rise time of the signaling cascade and stronger negative feedback to suppress expression of other ORs. The third study shows that OR expression increases AC3 expression, which then makes OR choice permanent (Dalton et al., 2013).

2.6 Development

Since the sense of smell is one of the most important senses for mice after birth and later in life, it is not surprising that ORs are expressed early in development and that OSNs mature quickly. The first expression of ORs (for example MOR256-17) can be detected by E12 in the dendritic knob (Schwarzenbacher et al., 2005). By E13 most ORs are expressed, but in unique, adult-like patterns and with an unique timing (Rodriguez-Gil et al., 2010). At the same time (E11-14) OSNs can also be detected in the cribriform mesenchyme, where they are thought to support the projecting axons from the epithelium to the olfactory bulb (Schwarzenbacher et al., 2004). About two days later in development, at E15.5, the first axons (shown for P2-IRES-taulacZ) can be detected in the OB (Royal and Key, 1999). OSNs are fully responsive by E16.5 (shown for S1 and MOR23) and glomeruli start forming directly after birth (Lam and Mombaerts, 2013). The OB interneurons move to the bulb at E14.5 and differentiate by PD21. Their identity is autonomously

defined in the lateral ganglionic eminence (LGE) and is irreversible (Tucker et al., 2006).

Even with the onset of OR expression in early development, the development still continuess to mature age at 10-12 weeks (Pomeroy et al., 1990). The population of M72-expressing OSNs is maintained and stable and their glomerular number is consistent even after 24 months after birth (Richard et al., 2010).

The maturation is dependent on the activity of the OSNs, especially in glomerular formation. The M71 and M72 glomeruli were reported to become more homogeneous with development, from PD10 to PD60 (Zou et al., 2004). Glomerular development can be accelerated by odor training and exposure (Kerr and Belluscio, 2006).

OSNs maintain their plasticity even at old age (Jones et al., 2008). After naris closure, the OSN number and glomerular volume for P2-expressing OSNs do recover (Cummings and Belluscio, 2010).

2.7 Axonal wiring

One of the most impressive feats in the mouse olfactory system is the precise projection of OSN axons to the olfactory bulb to form glomeruli (Ressler et al., 1994). These glomeruli are formed homogeneously by axons of OSNs expressing the same OR (Treloar et al., 2002), illustrated as an example in **Figure 2.7**). All OSN populations project their axons to conserved positions in the olfactory bulb (Figure 2.8). Before reaching the position of their glomeruli the axons travel across the outer olfactory nerve layer until they are close to the glomerular position (Au et al., 2002), branching only within the glomerular position (Klenoff and Greer, 1998). Other axons expressing the same OR are needed for glomerular stability (Ebrahimi and Chess, 2000). Glomeruli start forming after birth and their number increases until more than 12 weeks after birth (LaMantia et al., 1992, Pomeroy et al., 1990). The general position of the glomeruli for a given OSN population is

consistent but the number of glomeruli varies in some populations, for example in P2-expressing OSNs (Schaefer et al., 2001).

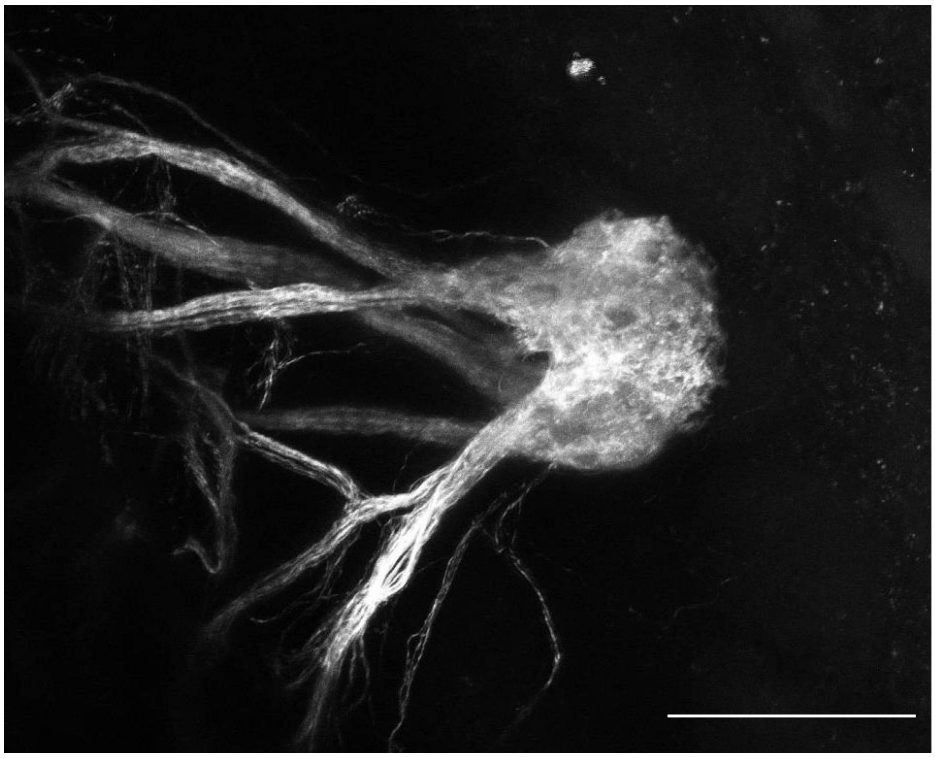

Figure 2.7 SR1-IRES-tauGFP glomerulus
Two-photon microscope image of SR1-IRES-tauGFP PD21 mouse shows a lateral glomerulus. This image shows how the axon bundles project and form the characteristic homogeneous, round structure of a glomerulus. This image was reconstructed from z-stacks images with intrinsic fluorescence of GFP-expressing OSNs. Scale bar: 250 µm.

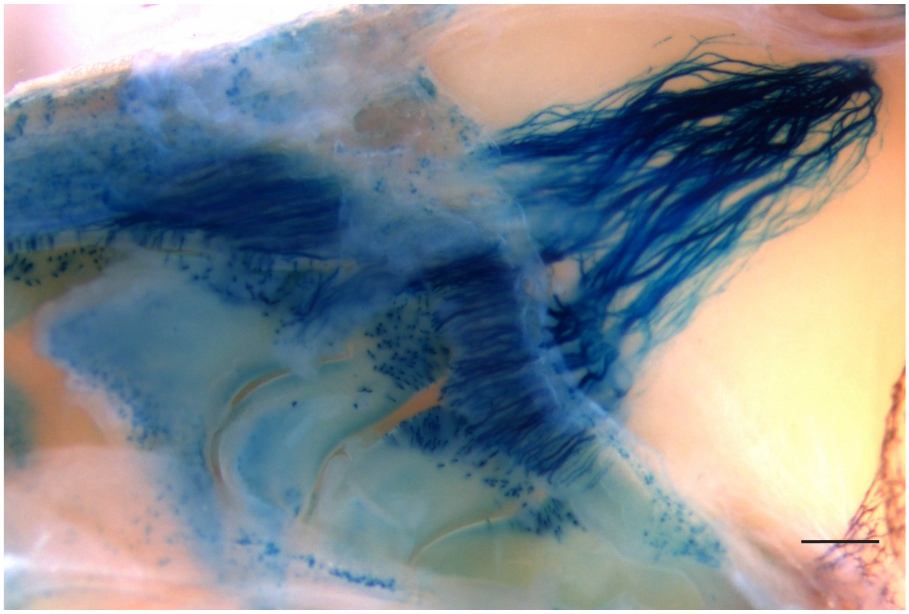

Figure 2.8 Axonal projection of M71
Sagittal whole mount of M71-IRES-taulacZ PD21 shows the projection of M71-expressing OSNs to the olfactory bulb where they form one glomerulus per half-bulb. OSNs and axons were visualized by x-gal staining. Scale bar: 500 µm.

Nearly quarter of a century after the discovery of the ORs the mechanisms that govern this precise axonal wiring are not fully understood. In recent years several factors that modify the glomerular position or axonal wiring in general have been discovered. For instance several knockouts in parts of the signal transduction cascade in mice have interesting effects on axonal wiring. Silencing of an OR by mutating the N terminal G protein binding site with a RDY mutant abolishes glomerular formation in rat I7-expressing OSNs in transgenic mice (Imai et al., 2006). This phenotype can be rescued with the expression of a constitutively active $G_{\alpha s}$ subunit (caGs). CaGs does not need to bind to the GPCR to initiate a signal transduction event and thus can maintain cAMP level even with a silent OR. The most prominent effects are reported for a knockout of AC3, resulting in a disturbed axon wiring. For all OSNs tested in an AC3-deficient background, the axonal wiring was found to be perturbed leading to the formation of ectopic glomeruli or abolishing the formation of glomeruli even when the axons project to the correct position (Zou et al., 2007). An AC3 deletion also perturbs the fine axon sorting in the glomerular layer (Chesler et al., 2007). The same article also shows that even the ectopic expression of $G_{\alpha olf}$ can be sufficient to establish a unique glomerular position. A knockout of β3GnT2, which modifies AC3, leads to defects in axonal wiring (Henion et al., 2011). Surprisingly a knockout of CNG still leads to fairly normal axonal wiring in the OB even though the depolarization as a result of the signal transduction cascade is abolished (Lin et al., 2000). However a conditional knockout of OCNC1 (a subunit of the CNG, now known as Cnga2) leads to miswiring and multiple, ectopic glomeruli for M72 neurons (Zheng et al., 2000). In the OCNC1 knockout strain these nonfunctional OSNs die due to the lack of function, however if combined with naris closure the non functional OSNs are not replaced (Zhao and Reed, 2001).

Another important factor for axonal wiring is the OR sequence itself. Several articles have reported on the effect of replacing the OR genetic sequence with another and the consequences for axonal wiring. The first study in that regard was published in 1996 and showed that by replacing the P2 sequence with M71, labeled axons form glomeruli but at a different

position (Mombaerts et al., 1996). This gene replacement experiment was performed next with P3, M71 or M50 into the P2 locus: in each case, the axons still form glomeruli but at a different position (Wang et al. 1998). These positions are different from the P2 position and the normal position of the replacing OR, mostly somewhere in between the two positions (Mombaerts et al., 1996; Wang et al., 1998). Only when the OR sequence is closely related to the native OR sequence, for example in the case of M71 and M72, it is possible to shift the glomerular position completely to the position characteristic for the replacing OR (Feinstein and Mombaerts, 2004). But in most cases the OSNs with a replaced OR form glomeruli at novel position in the OB, as shown for the rat I7 in M71 (Bozza et al., 2002) and M72 in S50 (Bozza et al., 2009; Zhang et al., 2012). Even a single nucleotide substitution can shift glomerular position (Feinstein and Mombaerts, 2004). A non–olfactory GPCRs can substitute as an OR when put in an OR locus: the β2 adrenergic receptor (β2AR) expressed from the M71 locus can support the formation of glomeruli (Feinstein et al., 2004, Omura et al., 2014). Another interesting effect was shown with an intricate downregulation of M71 expression. In this gene-targeted strain the M71 sequence was flanked by fluorescent marker proteins and behind an IRES site. Genes downstream of an IRES site are expressed less well. This so-called hypomorph shows an anterior shift in glomerular position (Feinstein et al., 2004) even though the OR sequence is identical. All gene replacements described have the functional responsiveness of the replacing OR (Bozza et al., 2002) but the hypomorph has a reduced responsiveness compared to M71-expressing OSNs (Zhang et al., 2012). Several transgenic strains expressing ORs have been established, either forming glomeruli in the same position as the OSN populations that normally express these ORs (Vassalli et al., 2002, Rothman et al., 2005) or not (Nakatani et al., 2003, Miyamichi et al., 2005). Modification of the homeodomains upstream of M71 show that axonal wiring can be shifted or perturbed even if the OR is still expressed (Rothman et al., 2005). Accordingly the O/E proteins, which bind Olf1 sites found in promoter regions of genes in OSN development such as OMP, are important for correct axonal wiring (Wang, 2004).

Surprisingly mitral cells, which form the first synapse with the axons of OSNs in the glomerular layer, are not important for glomerular formation (Royal et al., 2002). Even with an aberrant organization of the postsynaptic mitral cells in the olfactory bulb, P2-IRES-taulacZ-expressing OSNs project to their typical position. Likewise the GABAergic interneurons are not necessary for glomerular formation (Bulfone et al., 1998). However it is important to note that the glomeruli of a single OSNs population are functionally connected within the OB. The activity in a glomerulus does not only inhibit their neighboring glomeruli via lateral inhibition fine tuning their postsynaptic mitral/tufted cells (Tan et al., 2010) but also inhibit their corresponding glomerulus in the same bulb (Lodovichi et al., 2003). It has been shown for M71-expressing OSNs that their glomerulus is bilaterally connected via the anterior olfactory nucleus pars externa (Yan et al., 2008).

One further explanation for the precise and homogeneous axonal wiring is found in the diverse expression of cell adhesion molecules, marker proteins for regions of the epithelium and cell surface molecules. Similarly, the olfactory cell adhesion molecule (OCAM) expressed in OSNs in the ventral region of the MOE, which project to the ventral region of the OB. OCAM is however not needed for axonal wiring per se, but for establishing a fine axonal sorting and subcompartments within a glomerulus (Walz et al., 2006). Other molecules, like neurotropin-3 (NT-3) and transient receptor potential M 5 (TrpM5), are also differentially expressed by OSNs, but the role of these molecules is not resolved (Rolen et al., 2014). The protein Big-2 is differentially expressed in the OB and is reported to mediate olfactory axon convergence (Kaneko-Goto et al., 2008). Another cell adhesion molecule called Gicerin is differentially expressed in the OB at E17.5 (Williams et al., 2007). Again its role remains to be determined.

Several prominent cell adhesion molecule systems are also expressed in the olfactory system and play an important role in axonal wiring. For example the roundabout (Robo)/Slit complex is important in early axonal wiring. If Robo 1, which is expressed in ensheathing cells, is deleted, the axons are stopped from reaching the dorsal OB and axonal wiring is perturbed. However this

effect was only shown in transgenic mice, expressing β2AR from the MOR23 promoter (Aoki et al., 2013). In Robo-2 or Slit-1 knockout mice, OSNs residing in zone 1 do not project their axons to the dorsal bulb but form glomeruli in the ventral region of the bulb (Cho et al., 2007). In Robo-1 and Robo-2 double knockout embryos (E16-18) most OMP positive axons fail to reach the OB. However MOR256-17-expressing OSNs still form ectopic homogeneous glomeruli in Slit-1 and Slit-2 double knockout as well as in Robo-1 and Robo-2 double knock out mice at E18 (Nguyen-Ba-Charvet et al., 2008). These results show that Robo/Slit is an important but broadly applied factor in the dorsal/ventral axonal wiring in mouse.

Another factor in the dorsal/ventral patterning is the cell adhesion molecule Neuropilin 2 (Nrp2) and its repulsive ligand Semaphorin 3F (Sema3F). Nrp2 has been reported to be expressed in a gradient increasing in ventral direction and a knockout of Nrp2 will shift glomerular position dorsally (Takeuchi et al., 2010). Another study shows that a knockout of Nrp2 mostly influences OSNs expressed in the classical zone 4 of the MOE. In Nrp2 knockout mice, OSNs expressing MOR28 and I7 start forming multiple and partly ectopic glomeruli but this result was shown with two mice (Takahashi et al., 2010).

As stated before, intact activity of OSNs is an important factor for the formation of homogeneous glomeruli. For example, an overexpression of the inward rectifying potassium channel Kir2.1 diminishes the excitability of OSNs and severely disrupt glomerular formation (Yu et al., 2004). Two pairs of cell adhesion molecules play a crucial role in the fine sorting of the axons and maintaining homogeneity: Kirrel2/Kirrel3 (self adhesive) and Eph-A5/Ephrin-A5 (repulsive effect) are activity dependently expressed and support fine axonal sorting in glomerulus (Serizawa et al., 2006). A knockout of Ephrin-A3 and Ephrin-A5 shifts glomeruli of OSNs expressing SR1 and P2 to a more posterior position in the OB (Cutforth et al., 2003).

The last group of differentially expressed molecules, and least studied, is cell surface carbohydrates (glycans). For example, the cell surface carbohydrates UEA and DBA are expressed in conserved patterns in the

MOB. However these patterns are not correlated with glomeruli of OSNs expressing M71 or P2 (Lipscomb et al., 2003). UEA is expressed in subset of cells in MOE forming several small microglomeruli, which appear to be a different population to AOE glomeruli and OR glomeruli (Lipscomb et al., 2002b). The lectin DBA is differentially expressed in glomeruli and can be detected with different intensities in the glomerular layer of the bulb. But there are OMP-negative and DBA-positive axons contributing to these glomeruli (Lipscomb et al., 2002a). Finally a knockout of the β3GnT1, which regulates extension of lactoseamines in glycans, results in cell death of OSNs and impaired wiring (Henion et al., 2005).

2.8 Neuropilin-1

The cell adhesion molecule Neuropilin 1 (Nrp1) is for one of the most promising contenders for establishing the anterior/posterior glomerular position of glomeruli in the MOB. Nrp1 is differentially expressed in the MOE and MOB (Pasterkamp et al., 1998). OCAM and Neuropilin-1 form distinct and different patterns in the MOB (Nagao et al., 2010). Nrp1 is also expressed in sensory neurons in the Grüneberg ganglion. It has been shown that it is needed for axonal wiring (Matsuo et al., 2012). Nrp1 forms a complex with Plexin A1 and detects the repulsive ligand Semaphorin 3A (Sema3A). This complex is sufficient for Sema3A detection, but the expression level of Nrp1 is increased in the presence of Plexin A1 (Takahashi et al., 1999). The soluble Sema3A has been shown to be important for axon sorting. It is expressed in a spiral pattern around the rostro-caudal axis in the MOB. Nrp1 is expressed in a contrary pattern (Schwarting et al., 2000). A knockout of Sema3A perturbs axonal wiring of P2-expressing OSNs. Lack of Sema3A results in formation of multiple glomeruli and their characteristic position is not maintained (Schwarting et al., 2004). Expression of Sem3A is involved in reducing cAMP levels in vitro, giving a clue about the relation between the signal transduction cascade and the expression of cell adhesion molecules, but these results have yet to be confirmed in OSNs (Shelly et al., 2011). A popular theory has emerged in the last years that a gradient of Nrp1 is the sole determinant of the

glomerular position along the anterior-posterior axis, while the finer sorting is activity-dependent mediated by fine sorting through Kirrel2/EphA5 and Kirrel3/ephrin-A5 (Imai and Sakano, 2008). A conditional knockout of Nrp1 initiated from a transgene expressed rat I7 OR from mouse MOR23 promoter shifts glomerular position more anteriorly, whereas expression of caGs in these OSNs shifts the glomeruli more posteriorly (Imai et al., 2009). The proposed model is that the basal activity of an OR in development mediated by the $G_{\alpha s}$ subunit is involved in regulating cAMP levels in a gradient manner (Nakashima et al., 2013). However this explanation cannot explain all the results of the AC3 knockout (Zou et al., 2007), which has a distinct phenotype of ectopic glomerular formation for the M71- or M72-expressing OSNs. In addition, recent studies showed that OSNs expressing M71 and MOR23 have similar spontaneous activity (Connelly et al., 2013) although the glomerular position is very different in the MOB (Col et al., 2007).

3 Materials

3.1 Animals

Most strains used in this thesis were generated by the lab of Dr. Peter Mombaerts using the method of gene targeting described in (Mombaerts et al., 1996), where a target sequence in the genome is replaced with a modified sequence by homologous recombination in mouse embryonic stem cells. Most strains contain an internal ribosomal entry site (IRES). This sequence originates from the encephalomyocarditis virus and enables coexpression of two genes from a single mRNA transcript (Kaminski et al., 1990). This IRES is used to coexpress a reporter gene, such as GFP, under the same promoter simultaneously with the gene of interest, such as an OR.

Mice were maintained in specified pathogen-free conditions in individually ventilated cages of the Tecniplast green line (Tecniplast, Italy). Mice received *ad libitum* gamma-irradiated ssniff V1124-727 (ssniff, Soest, Germany). Nesting, bedding, and enrichment were provided as nestpak, Datesand Grade 6 (Datesand, Manchester, United Kingdom). Mouse experiments were carried out in accordance with the German Animal Welfare Act, European Communities Council Directive 2010/63/EU, and the institutional ethical and animal welfare guidelines of the Max Planck Institute of Biophysics and the Max Planck Research Unit for Neurogenetics. Approval came from the Regierungspräsidium Darmstadt, and the Veterinäramt of the city of Frankfurt.

Table 3.1 List of strains

Strain name	Reference	Availability
P3-IRES-tauGFP	Feinstein and Mombaerts, 2004,	http://jaxmice.jax.org/strain/006684
M71-IRES-tauGFP	Bozza et al., 2002, Feinstein et al., 2004;	http://jaxmice.jax.org/strain/006676
mOR37C-IRES-tauGFP	Strotmann et al., 2000,	http://jaxmice.jax.org/strain/006641
S50-IRES-tauGFP	Bozza et al., 2009,	http://jaxmice.jax.org/strain/006712
MOR23-IRES-tauGFP	Vassalli et al., 2002,	http://jaxmice.jax.org/strain/006643
M72-IRES-tauGFP	Potter et al., 2001,	http://jaxmice.jax.org/strain/006678
M50-IRES-GFP-IRES-taulacZ	Feinstein and Mombaerts, 2004,	http://jaxmice.jax.org/strain/006686
mI7-IRES-tauGFP	Bozza et al., 2002,	http://jaxmice.jax.org/strain/006664
P2-IRES-tauGFP	Feinstein and Mombaerts, 2004,	http://jaxmice.jax.org/strain/006669
SR1-IRES-tauGFP	Fuss et al., 2013,	http://jaxmice.jax.org/strain/006711
MOR256-17-IRES-tauGFP	Khan et al., 2011,	http://jaxmice.jax.org/strain/007762
β2AR→M71-IRES-tauGFP	Omura et al., 2014,	http://jaxmice.jax.org/strain/006734
RFP→M71iM71iGFP	Feinstein et al., 2004,	http://jaxmice.jax.org/strain/006689
M71-IRES-tauYFP	unpublished	http://jaxmice.jax.org/strain/006746
M71-IRES-tauRFP2	Li et al., 2004,	http://jaxmice.jax.org/strain/006679
M71-IRES-Cre	Li et al., 2004,	http://jaxmice.jax.org/strain/006677
Z/EG	Novak et al., 2000,	http://jaxmice.jax.org/strain/00417
Nrp-1-flox/J		http://jaxmice.jax.org/strain/005247
Npn1-5247	Gu et al., 2003,	same as Nrp-1^{flox} but directly obtained from Jackson Lab JR#5247
I7(WT)-Cre	Imai et al., 2006,	RBRC02932
ROSA-STOP-tauLacZ		unpublished
OMP-Cre	Li et al., 2004,	http://jaxmice.jax.org/strain/006668.html
OMP-tauSTOPlacZ		unpublished
R26-tauGFP		Unpublished, Uli Boehm, Hamburg

3.2 Chemicals

3.2.1 Molecular Biology

Chemicals	Provider
Plates	Mombaerts lab
Carbenicilin	Sigma-Aldrich, St. Louis MO, USA
Primers	ThermoFisher Scientific, Waltham, MA, USA & eurofins MWG, Ebersberg
Restriction enzymes & Buffers (EcoRI, NcoI, PacI, AscI, HindIII, KpnI, PmeI, NotI, XhoI, KapnI, SacI, SacI-HF, SacII, XbaI, EagI)	NEB, Ipswich, MA, USA
Vectors pBluescript K+ pGEMT easy vector	Vectors Agilent Technologies, Waghaeusel-Wiesental Promega, Madison, WI, USA
T4 Ligase & Buffer	Promega, Madison, WI, USA
Sequencing service	QIAGEN, Hilden
QIAprep Spin Mini Prep	QIAGEN, Hilden
QIAfilter Plasmid Midi Kit	QIAGEN, Hilden
QIAGEN Large-construct Kit	QIAGEN, Hilden
QIAquick Gel extraction Kit	QIAGEN, Hilden
Competent cells dH5α XL2-Blue Ultracompetent cells MAX efficiency DH5a	Competend cells Life Technologies GmbH, Darmstadt Agilent Technologies, Waghaeusel-Wiesental Life Technologies GmbH, Darmstadt
SOC Medium	Life Technologies GmbH, Darmstadt
Hyperladder II	Bioline, Luckerwalde
Phusion Polymerase	Finnzyme, Finnland and ThermoFisher Scientific, Waltham, MA, USA
Gel extraction kit QIEX	Gel extraction kit QIEX
2-log DNA ladder	NEB, Ipswich MA, USA
Ligation kit long	Takara Bio Inc, Shiga, Japan
Isopropanol	Sigma-Aldrich, St. Louis, MO, USA
Ethanol	Sigma-Aldrich, St. Louis, MO, USA
CIP	NEB, Ipswich MA, USA

LB media and plates were provided by the institute. They were made according to the following recipe (Table 3.2).

Table 3.2 MPI recipes

LB Medium	Agar Plates
10 g Tryptone (Fluka, 95039-1KG-F) 5 g Yeast Extact (Fluka, 70161-500G) 10 g NaCl (Roth, 3957.5) In 1L H_20	LB Broth with agar (SIGMA L7025-500TAB) 1Tablet per 50 ml 1 ml Carbenicillin (25 mg/ml) per 500 ml

3.2.2 Genotyping

Material	Provider
Taq Hot Start	Takara Bio Inc, Shiga, Japan
Primer	Sigma-Aldrich, St. Louis MO, USA
dNTPS	Takara Bio Inc, Shiga, Japan
10x Reaction Buffer	Takara Bio Inc, Shiga, Japan
Proteinase K	Bioline, Luckerwalde
Digestion buffer	Peqlab, Erlangen
Agarose	Carl Roth + Co. KG, Karlsruhe
Ethidium Bromide (EtBR)	Carl Roth + Co. KG, Karlsruhe
Standard	NEB, Ipswich, MA, USA
Tris Borate EDTA (TBE) 10x Stock	Carl Roth + Co. KG, Karlsruhe
Tris Acetate EDTA (TAE) 50x Stock	Carl Roth + Co. KG, Karlsruhe
Loading dye	Life Technologies GmbH, Darmstadt

3.2.3 Antibody staining

Material	Provider
Normal Donkey Serum	Jackson Immuno Research, Newmarket Suffolk, UK
Normal Goat Serum	Jackson Immuno Research, Newmarket Suffolk, UK
Bovine Serum Albumin	Sigma-Aldrich, St. Louis, MO, USA
Triton	Sigma-Aldrich, St. Louis, MO, USA
Parafilm	Parafilm, Oshkosh, WI, USA
Citrate Buffer	Sigma-Aldrich, St. Louis MO, USA
DAPI	Life Technologies GmbH, Darmstadt
Moviol	Calbiochem, EMD Chemicals, San Diego, CA, USA

3.2.4 Antibodies

Primary Antibody	Recommended concentration	Provider (serial number)
Chicken anti GFP	1:500	Abcam (ab13970)
Chicken anti β-gal	1:1000	Abcam (ab9361)
Chicken anti M71	1:500-1:3000	Abcam (ab65573)
Rabbit anti dsRED	1:250	Clontech (632496)
Rabbit anti Neuropilin1	1:200	Abcam (ab25998)
Goat anti Neuropilin1	1:100	R&D Systems (AF566)

Secondary Antibody	Recommended concentration	Provider (serial number)
ALEXA 488 Goat anti Chicken	1:500	Invitrogen (A11039)
ALEXA 546 Donkey anti Chicken	1:500	Invitrogen
Rhodamin Red-X (RRX) Donkey anti Rabbit	1:500	Jackson (711-295-152)
Fluorescein (FITC) Donkey anti Chicken	1:500	Jackson (703-545-155)
Cy5 Donkey anti Goat	1:500/1:200	Jackson (705-175-147)
ALEXA 546 Donkey anti Goat	1:500	Invitrogen (A11056)
ALEXA 488 Goat anti Chicken	1:500	Invitrogen (A11039)
ALEXA 488 Goat anti Rabbit	1:500	Invitrogen (A11034)
ALEXA 546 Goat anti Rabbit	1:500	Invitrogen (A11010)
DyLight 488 Goat anti Chicken	1:500	Bethyl Laboratories (A30-206D2)
ALEXA 555 Donkey anti Rabbit	1:500	Invitrogen (A31572)

3.2.5 X-gal staining

Material	Provider
5-bromo-4-chloro-3-indolyl-β-D-galactopyranoside (x-gal)	Roche Diagnostics Corporation, Indianapolis, IN, USA
Dimethylformamide (DMF)	Sigma-Aldrich, St. Louis, MO, USA
Magnesium Chloride ($MgCl_2$)	Sigma-Aldrich, St. Louis, MO, USA
ethylene glycol tetraacetic acid (EGTA)	Sigma-Aldrich, St. Louis, MO, USA
Na deoxychalate	Sigma-Aldrich, St. Louis, MO, USA
Kalium hexacyanoferrate II &III	Sigma-Aldrich, St. Louis, MO, USA
Igelpal CA-630	Sigma-Aldrich, St. Louis, MO, USA

3.2.6 X-gal staining buffer

Buffer A	Buffer B	Buffer C
100 mM PBS (pH 7.4) 2 mM $MgCl_2$ 5 mM EGTA	100 mM PBS (pH 7.4) 2 mM $MgCl_2$ 0.01% Na deoxycholate 0.02% IGEPAL CA-630	5 mM 5 mM 1 mg/ml X-gal in DMF In Buffer B

3.2.7 Perfusion

Material	Provider
Paraformaldehyde	Sigma-Aldrich, St. Louis, MO, USA & Merck, Darmstadt
Phosphate Buffered Saline	Sigma-Aldrich, St. Louis, MO, USA
Sucrose	Sigma-Aldrich, St. Louis, MO, USA
Ethylenediaminetetraacetic acid (EDTA)	Sigma-Aldrich, St. Louis, MO, USA
NaOH	Sigma-Aldrich, St. Louis, MO, USA
NaCL	B.Braun, Melsungen
10% Ketamin	Medistar Arzneimittelvertrieb GmBH, Ascheberg
Xylazin	bela-pharm, Vechta
Xylavet	cp-pharma, Burgdorf
Scissors	fine science tools, Heidelberg
Granulated dry ice	Linde AG, Muenchen

3.3 Consumables

Consumables	Provider
Falcon Tubes 15 & 50 ml	ThermoFisher Scientific, Waltham, MA, USA
Glass Ware	Simax, Sazava, Tschechische Republik &VWR, Darmstadt & Druan, Wertheim
Gloves blue & white	Ansell, Brüssel, Belgium & VWR, Darmstadt
Tissues	Kimberly-Clark, Mainz & VWR, Darmstadt
Pasteur Pipette	VWR, Darmstadt &
Big pipettes (5 ml, 10 ml, 25 & 50 ml)	Biosphere/SARSTEDT, Nuernbrecht
Pipette tips (2.5 µl, 20 µl, 200 µl & 1 ml)	Biosphere/SARSTEDT, Nuernbrecht
Needles	Henry Schein, Langen & B.Braun, Melsungen
Small petri dish	ThermoFisher Scientific, Waltham, MA, USA
Syringes	B.Braun, Melsungen
Filters	ThermoFisher Scientific, Waltham, MA, USA
Eppendorf tubes	Eppendorf, Hamburg
Tail tubes	Simport, Beloeil QC, Canada
PCR tubes+ caps	Brand, Wertheim
pH Standards	Merck, Darmstadt
Spatulas	VWR, Darmstadt
Gasburner	Fischer Scientific GmBH, Nidderau

Sectioning

Material	Provider
Coverslips	Menzel, Braunschweig
Slides	ThermoFisher Scientific, Waltham, MA, USA

3.4 Equipment

Equipment	Provider
Cryostat	Leica Biosystems, Wetzlar
ddH2O Filter Millipore Advantage	Millipore, Billerica MA, USA
PCR Machines/Thermocycler	Applied Biosystems, Darmstadt
Mac	
pH Meter	Eutech Instruments**,** Landsmeer, Netherlands
Windows PC	
-Pipett Boy Pipetus	Hirschmann Laborgeraete, Eberstadt
-Zetrifuge: Table Sorvall RC6 plus	Eppendorf, Hamburg), ThermoFisher Scientific, Waltham, MA, USA
Gel Doc	Peqlab, Erlangen
Gel Chambers	BioRad, Hercules CA
Incubator 37ºC	ThermoFisher Scientific, Waltham, MA, USA
Shaker 37ºC	Infors HT, Einsbach
Vacuum pump	Eppendorf, Hamburg
Autoclave	Systec, Wettenberg
Balances	Sartorius, Goettingen
Shaker	Stuart, Staffordshire, UK
Heater	Heidolph Instruments, Schwabach
Stirrer	Heidolph Instruments, Schwabach
Fridge	Liebherr, Biberach an der Riss
Freezer: -80˚C -20˚C	 ThermoFisher Scientific, Waltham, MA, USA, Gram, Sarstedt & Liebherr, Biberach an der Riss
Nanodrop	Peqlab, Erlangen
Waterbath	GFLN, Burgwedel
Quiacube	QIAGEN, Hilden

3.5 Microscopes

Microscope	Provider
LSM 510	Carl Zeiss, Wetzlar
LSM 710	Carl Zeiss, Wetzlar
Aperio Scanscope FI	Aperio (Leica), Wetzlar
NIKON SMZ25	Nikon GmbH, Duesseldorf
Two photon microscope Mai tai	Newport-Spectra-Physics, Darmstadt

3.6 Software

Software	Provider
Prism	Graphpad Software Inc., La Jolla, CA, USA
Excel	Microsoft
Word	Microsoft
ZEN	Carl Zeiss GmBH, Jena
Fiji	Open source software
Matlab	Mathworks, Ismaning
Scanscope Viewer	Leica Biosystems, Wetzlar
Papers	Mekentosj B.V., Dordrecht, Netherlands

3.7 Sequences

3.7.1 Primers for vector construction

Primer Name	Length (bp)	Sequence	Type	Annealing temp (ºC)	Target
OB1	35	TATATCCATGGATGGGCTGCCTCGGCAACAGTAAGA	f	67	NcoI site + caGS HA tag
OB2	39	GCGCTTAATTAATTAGAGCAGCTCGTATTGGCGGAGATG	r	67	caGs stop codon (TAA) + PacI site
OB3-F	26	CCATTGTGAAGCAGATGAGGATCCTG	f	60	Internal caGs site
OB4-R	22	CCCACAGAGCCTTGGCATGCTC	r	60	Internal caGs site
OB5-F	27	GCCCAGTACTTCCTGGACAAGATTGAT	f	60	Internal caGs site
OB6-R	26	CATCTCCACTAGCAGTGCTGATTCTC	r	60	Internal caGs site
OB7-F	42	CGGCGCGCCGAATTCCCATGGTTAATTAAGGCGCGCCGGTAC	f	N/A	pBSMK1-Forward: SacI-AscI-EcoRI-NcoI-PacI-AscI-KpnI
OB8-R	42	CGGCGCGCCTTAATTAACCATGGGAATTCGGCGCGCCGAGCT	r	N/A	pBSMK1-Forward: SacI-AscI-EcoRI-NcoI-PacI-AscI-KpnI
OB9-F	28	CTTAATTAAAGGCCTGGCGCGCCGGTAC	f	N/A	pBSMK2-Forward: SacI-PacI-StuI-AscI-KpnI
OB10-R	28	CGGCGCGCCAGGCCTTTAATTAAGAGCT	r	N/A	pBSMK2-Reverse: SacI-PacI-StuI-AscI-KpnI
mk146	20	GTCGTGAAGGAAGCAGTTCC	f	N/A	erxternal IRES caGs
mk147	20	CCTAAGCGTATTCAACAAGG	f	58	external Ires caGs
AscI-mk245r	39	TATATGGCGCGCCACATCAAAAGACTTTTCTCCTCAGTG	r	67	Reverse primer from stop codon TGA plus 3 nucleotides (TGT) at 3'UTR m71
PacI-mk246f	39	GCGTTAATTAAGATCTTCCAGAAGCAATGAGCTTCTCTG	f	64	Forward primer for left arm m71
AscI-MK248-F	44	GTATATGGCGCGCCAAATGCTGATCTTTCTTCATGTAAAAGTAAG	f	66	right arm forward primer m71
NotI-MK249-R	43	TATATATATGCGGCCGCTTCCCATCTCAATTCATGTCATCAAG	r	66	right arm reverse primer m71
MK254-F		CTGACAATGTGTAATAACACTCATGTG	f	55	Ia upstream junction
MK255-R	36	CTAGTCTCTAATATCTTCCTTACCATC	r	55	Ia upstream junction
MK256-R		CTTGCAGAGGTTATCATACAGGTGTGC	r	60	RA upstream junction
MK257-F		CTATCGTCACCTGGAAACAGACCTCT	f	60	RA downstream junction
MK258-R		ATGGATATACTCCATCATGGCAGGGAAG	r	60	RA downstream junction

Primer Name	Length (bp)	Sequence	Type	Annealing temp (ºC)	Target
MK259-F		GCTCTCGGCGCTTCTGAGGAG A	f	60	Internal ACNF primer
MK260-R		TATAAAGGGCGTCACTCAGCCA GTTC	r	60	Internal ACNF primer
MK261-F		CAGATTACGTATATCCTGGCAG CGATC	f	60	Internal ACNF primer
MK262-R		CCAGGTTCGTTCACTCATGGAA AATAGC	r	60	Internal ACNF primer
T7	20	TAA TAC GAC TCA CTA TAG GG		48	pBluescript cloning site
T3	20	ATT AAC CCT CAC TAA AGG GA		48	pBluescript cloning site
SP6	19	GAT TTA GGT GAC ACT ATA G		45	pBluescript cloning site
M13	18	TGT AAA ACG ACG GCC AGT	f	48	pBluescript cloning site
M13R	17	CAG GAA ACA GCT ATG AC	r	45	pBluescript cloning site
SPANPK-F	38	CTTAATTAAGGCGCGCCGCGG CCGCGTTTAAACGGTAC	f	71	linker LA RA construction: SacI-PacI-AscI-NotI-PmeI-KpnI
SPANPK-R	38	CGTTTAAACGCGGCCGCGGCG CGCCTTAATTAAGAGCT	r	71	linker LA RA construction: SacI-PacI-AscI-NotI-PmeI-KpnI
mk261 short		GATTACGTATATCCTGGCAG	f	50	Internal ACNF primer
pBSOB4 forward		CTTAATTAACGGCCGCCGCGGT CTAGAGGTAC	f	N/A	linker: SacI-PacI-EagI-SacII-XbaI-kpnI
pBSOB4 reverse		CTCTAGACCGCGGCGGCCGTT AATTAAGAGCT	r	N/A	linker: SacI-PacI-EagI-SacII-XbaI-kpnI
OB1-F	26	GCTGGAGTACAACTACATCAGC CACA	f	60	junction: CFP ACNF
OB2-R	26	AGGATGATCTGGACGAAGAGC ATCAG	r	60	junction: CFP ACNF
MK 91	27	GCA GCT GTG GGC TTG TTC TAT GGA TCC	f	63	M71 junction
MK 92	20	AT GGA GAG CAA TGA TTC CTG	r	50	M71 Junction
OB11F	26	CTCAAGCGTATTCAACAAGGGG CTGA	f	60	IRES 3' forward primer
OB12R	26	CTTGCTCACGATCTTCTGGTCC TCAT	r	60	gapCFP 5' reverse primer
OB13R	26	GTGCAGATGAACTTCAGGGTCA GCTT	r	60	gapCFP 5' reverse primer downsteam
MK249a-R		TATATATATGCGGCCGCGCTGG TAAAACTGGATGTCCACATGTA G	r	N/A	right arm reverse primer m71
MK249b-R		TATATATATGCGGCCGCCTGAA ACATGAGTTTAGCCATCTG	r	N/A	right arm reverse primer m71
MK249c-R		TATATATATGCGGCCGCCCATA TGGAACCATAAGAGACTAAGG	r	N/A	right arm reverse primer m71
AEPAa reverse		GGCGCGCCTTAATTAAGAATTC GGCGCGCCA	r	N/A	linker TOPO cloning reverse for pOB8 insert (AscI_EcoRI_PacI_AscI)
AEPAa		GGCGCGCCGAATTCTTAATTAA GGCGCGCCA	f	N/A	linker TOPO cloning forward for pOB8 insert (AscI_EcoRI_PacI_AscI)
NAEPAPme		CATCGGGCGCGCCGAATTCTTA ATTAAGGCGCGCCGTTT	f	N/A	linker TOPO vector for pOB8 insert (NcoI_AscI_EcoRI_PacI_AscI_PmeI)
NAEPAPme reverse		AAACGGCGCGCCTTAATTAAGA ATTCGGCGCGCCC	r	N/A	linker TOPO vector for pOB8 insert (NcoI_AscI_EcoRI_PacI_AscI_PmeI)

3.7.2 Genotyping primers

Primer Name	Internal number	Sequence	Length (bp)
720	35	GCC CAC TTG ATT CCC TGA	18
797	38	TGG AGC CCG TCA GTA TCG GC	20
803	39	GCA GGC CTT CTC CAC CTG TGC TTC	24
806	40	GCA GGC CTG ACA GAA AAA TAA AGG ATT C	28
819	41	GAG AAG CGC GAT CAC ATG GTC CT	23
824	42	ACA TAC TTC CGG CCA CGC TCA	21
950	45	CAG TAA TAA GAC CAC AAA TGC CT	23
1040	46	GCG AAT TCA AAG GCA AAG AAA TAT AGA AG	29
1243	50	AGC CAC TTG GAG AAT TCA TTG	21
1571	54	TTG CAG GGT GTA GTC CCC CTG AG	23
1992	55	CCC AAA TTT TAT TTT CTG CCA TCA C	25
1121B	47	GCA GCT GTG GGC TTG TTC TAT GGA TCC	27
1257A	52	GAA GAG TGC CCT CAG CAG GAC C	22
721A	36	AAA GGC CTC TAC AGT CTA TAG	21
900A	43	TCC AAT TTA CTG ACC GTA CA	20
901A	44	TCC TGG CAG CGA TCG CTA TT	20
A114A	56	ATG GAG AGC AAT GAT TCC TG	20
AW28	28	GCA TTG TAT GAG GTG GAC	18
AW29	29	GAA ACA GAG CAG CTT TCA CCA	21
Cat33	63	GAA CCC TGT TGT CTA CAG CCT CAG G	25
Cre-R	388	TGTCCCTGAACATGTCCATCAG	22
CZ40	64	GAA GCA GGA TGG TGA GAA GCT	21
CZ40A	65	CTG CAG TTC GAT CAC TGG AAC	21
G15A	68	TCC CGG GTG ATG GGT GAT GTT	21
G3A	67	AAG AAG GCC TTC TCC ACC TG	20
IRES-F	387	CGGTGCACATGCTTTACATGTG	22
LL1294	252	ATG GGG AGA GTG AAG CAG AA	20
LL1491	248	TTC CCA ACT GCC TGA GTC TT	20
LL1492	250	CAC CAC CCG TAC CCA CTA C	19
LL624	251	TAC GGG GTC ATT AGT TCA TAG	21
M168	80	TCA CTG GGG CTT CCT ATA TGG	24
M169	81	CAA GTT TTA TAT TAT CAA CTG CTC C	25
MK162	153	GTG ATG AAG ATC CGC TCT GTG GAG	24
MK163	154	CTG TTA CCT GTG GTC CAC AGT CGT A	25
MK564	221	AGG TTA GGC TTC AGG CCA AT	20
MK565	222	GGT ACC CTG GGT TTT CGA TT	20
MK99	151	GAG AAG CGC GAT CAC ATG GTC CT	23
olMR0042	385	CTAGGCCACAGAATTGAAAGATCT	24
olMR0043	386	GTAGGTGGAAATTCTAGCATCATCC	25
SF1	123	CTT GGT GCC TCT CAG CCT CAT CCT G	25
SF2	124	CAG TCT TGC TGC AGC TCA AGC ATC C	25
SF3	125	GAG AAG CGC GAT CAC ATG GTC CT	23
SF7	129	CTC ATT GGT CTG TCA GTG G	19
T334	91	TGA CGG CAG TTA TCT GGA AG	20
T335	92	TAA CGC CTC GAA TCA GCA AC	23

Primer Name	Internal number	Sequence	Length (bp)
T524	95	ACC TGG TAA GGT CAT TCC TGA GTG	24
T525	96	ACA TCT CAG TAG CTT TAC CAC GAT	24

3.7.3 Restriction enzyme sites

Enzyme	Restriction Site	NEB Buffer
AscI	5'…GG/CGCGCC…3' 3'…CCGCGC/GG…5'	CutSmart
EagI	5'…C/GGCCG…3' 3'…GCCGG/C…5'	3.1
EcoRI	5'…G/AATTC…3' 3'…CTTAA/G…5'	Unique
HindIII	5'…A/AGCTT…3' 3'…TTCGA/A…5'	2.1
KpnI	5'…GGTAC/C…3' 3'…C/CATGG…5'	1.1
NcoI	5'…C/CATGG…3' 3'…GGTAC/C…5'	3.1
NotI	5'…GC/GGCCGC…3' 3'…CGCCGG/CG…5'	3.1
PacI	5'…TTAAT/TAA…3' 3'…AAT/TAATT…5'	CutSmart
PmeI	5'…GTTT/AAAC…3' 3'…CAAA/TTTG…5'	CutSmart
SacI	5'…GAGCT/C…3' 3'…C/TCGAG…5'	1.1
SacI-HF	5'…GAGCT/C…3' 3'…C/TCGAG…5'	CutSmart
SacII	5'…CCGC/GG…3' 3'…GG/CGCC…5'	CutSmart
XbaI	5'…T/CTAGA…3' 3'…AGATC/T…5'	CutSmart
XhoI	5'…C/TCGAG…3' 3'…GAGCT/C…5'	CutSmart

4 Methods

4.1 Molecular work

This chapter describes the methods used for molecular work, the modification of the deoxyribonucleic acid (DNA), the generation of new plasmids and the amplification of DNA regions of interest.

4.1.1 Polymerase chain reaction (PCR)

In the thermocycler the hydrogen bonds of the double-stranded DNA are broken, the primers anneal at the complementary position and Taq DNA polymerase uses these primers as starting points to complement the single DNA stands to double strands again. This process is repeated for several cycles while the original DNA and the new synthetized strands serve as template for DNA synthesis, doubling the DNA sequence defined by the primers in each cycle.

PCR was performed to genotype the strains using the protocols described in Chapter 4.8.2 using the standard protocols there. Also PCR was used to generate PCR fragments for targeting vector construction as described in Chapter 4.1.8.

4.1.2 Gel electrophoresis

Gel electrophoresis is a method to separate DNA molecules by their size. To that end, the DNA molecules, mostly from PCR reactions or restricted plasmids, are loaded with the loading dye onto agarose gels with 3 µl Ethidium Bromide (EtBr) per 100 ml gel. EtBr intercalates with double-stranded DNA and shows fluorescence in the UV spectrum (302 nm). The percentage of agarose varies for the different experiments and ranges from 1 to 1.5 % (w/v). After applying a voltage, normally between 80 to 120 V, the negatively charged DNA molecules migrate toward the positive pole. Due to the interconnections that the agarose forms after heating, larger molecules are traveling slower through the gel. A standard with known DNA sizes is loaded onto the gel for reference.

4.1.3 Restriction enzyme digestion

To generate the plasmids described in Chapter 5 and to arrange the DNA sequences restriction endonucleases were used. These enzymes recognize specific sequences of four to eight base pairs of DNA and cleave after a specific nucleotide of that sequence. All endonucleases and buffers were obtained from New England Biolabs (NEB). Occasionally the restricted DNA molecule is additionally treated with CIP to remove phosphate from restriction sites and prevent reannealing. The restriction reaction (Table 4.1) is incubated at 37ºC for 4 h or overnight. If necessary, the sample is incubated with 1 µl of CIP at 37ºC for 10 min afterwards. The mix is loaded on a 1% ultrapure agarose gel and run with 80 V. The DNA is cut from the gel and purified using Qiagen Gel Extraction Kit.

Table 4.1 Restriction mixture

	µl
DNA (5 µg or 10 µg)	X
Buffer	2
BSA (depending of enzyme)	0.2
H_2O	Fill up to 19 (18 if double digestion)
Enzyme(s)	1
Total	20

4.1.4 Ligation

To insert the restricted and cleaned DNA fragments into a plasmid vector a ligation reaction is set up. For each insert and vector several concentrations for the insert are tested. The mixture is incubated at 4ºC overnight or at 16ºC for 5 h. The ligated mixture is used for transformation. The ligation kits used were from TaKaRa (Shiga, Japan) for ligation of long fragments or from Promega (Madison, WI, USA) for assembling the insert cassette.

Table 4.2 Ligation mixture

	µl	µl	µl	µl
Vector	1	1	1	1
Insert	1.5	5	9	0
Buffer	2	2	2	2
Ligase	1	1	1	1
Water	14.5	11	7	16
Total volume	20	20	20	20

4.1.5 Transformation

This protocol was used to transform the bacteria with the plasmid generated for this thesis. Using bacteria culture is a fast way to amplify plasmids for further usage, using the antibiotic resistance provided by the plasmid to foster the growth of the transformed culture.

- Remove required number of LB-Carb plates from 4°C and warm in 37°C incubator.
- Leave open for 10-15 min to dry the plates (not too dry!)
- Thaw competent cells on ice slowly, over 5-10 min.
- Label Eppendorf tubes and place them on ice.
- Dispense 50 μl of competent cells to labelled Eppendorf tubes gently.
- Add 3 μl ligation reaction mixture (see Ligation protocol).
- Incubate the cells-ligation mixture on ice for 30 min.
- Heat shock cells for 45 sec at 42°C in the water bath.
- Place tubes immediately on ice.
- Leave the cells to rest for 10 min.
- Add 500 μl SOC medium to each tube (Always 10x of the competent cell volume) and leave for another 10 min on ice.
- Incubate on rotating platform for two hours at 37°C.
- Add 20 μl of X-Gal directly onto plate and spread evenly with plastic spreads. (Only necessary for first insert)
- Put plates back in 37°C incubator and leave the plates exposed to dry for 10-30 min.
- Remove the competent cells from rotating platform and begin spreading.
- Resuspend the cells gently by pipetting and transfer 300 μl directly onto plate.
- Spread gently and evenly with glass pipettes.
- Incubate plates at 37°C overnight. Remove the plates to RT or 4°C in the morning.

4.1.6 DNA extraction from colonies

This chapter describes the protocols used to seed a culture with the transformed bacteria and to extract the plasmid from it after growth. Two sizes of cultures were used: a 20 ml (mini) and a 200 ml (midi). The 20 ml culture is used to verify the correct sequence of the plasmid and the 200 ml is used to obtain larger volume of plasmid vector for further processing. To extract the plasmid from the cultures the Qiagen Kits for Mini and Midi Prep are used. For Mini Prep the extraction is done both manually as well as using the Qiacube.

Colonies are picked from agar plates with sterile pipette tips. The tip is then inserted in LB medium with Carbenicillin with final concentration of 50 µg/ml. The seeded culture is kept overnight (16-20 h) at 37ºC and 150 rpm. When the bacteria culture is grown overnight the plasmids are extracted using the protocols provided by the Qiagen kits.

Following either protocol the cultures are spun down in a centrifuge and the supernatant is removed leaving the bacteria pellet behind. Subsequently, buffers and filter syringes provided in the kit are used to break the cells open and filter out all other molecules and organelles. The plasmids are then cleaned with ethanol and suspended in TE buffer for storage.

4.1.7 Sequencing

To verify the success of a ligation after preliminary testing with PCR or restriction enzyme digestion, plasmids are sequenced with corresponding primers. Targeted sequences are amplified similar to a PCR. However a proportion of the nucleotides used for sequencing is labeled and terminates the annealing reaction. Each of the four nucleotides is labeled differently. By measuring the length of the terminated fragment and knowing the label for each nucleotide the sequence of the template can be determined. The sequencing service of Qiagen (Hilden) was used. Sequencing results were generated as digital files.

4.1.8 Generating gene-targeting vectors

To generate the gene-targeting vectors for Chapter 5 multiple restrictions and ligations were needed using the techniques described in this chapter. The flowcharts illustrate the steps taken for generation of the final targeting vector.

For the insertion cassette a polylinker of nucleotides was generated containing SacI, AscI, EcoRI, NcoI, PacI AscI and KpnI as restriction sites (ThermoFisher). This linker was inserted in pBluescript K+ Vector (Agilent Technologies). Afterwards the other sequences were ligated into the vector (Figure 4.1) step by step. The caGs (constitutively active G-protein subunit s) sequences were obtained from T. Imai (Imai et al., 2006) and amplified from the donated vector with primers designed to flank the gene by restriction sites for NcoI and PacI. All other sequences were taken from stock plasmids available in the lab. The sequences were cut from the vector with restriction endonucleases (see Chapter 3.7.3), cut from gel and ligated in the target vector restricted with the same enzymes. Afterwards bacteria were transformed (see Chapter 4.1.5) with the ligated vector. After testing the correct insertion and transformation with PCR and sequencing the bacteria were amplified in a midi approach (see Chapter 4.1.6) and the plasmid vector was extracted and the process was repeated for the next step.

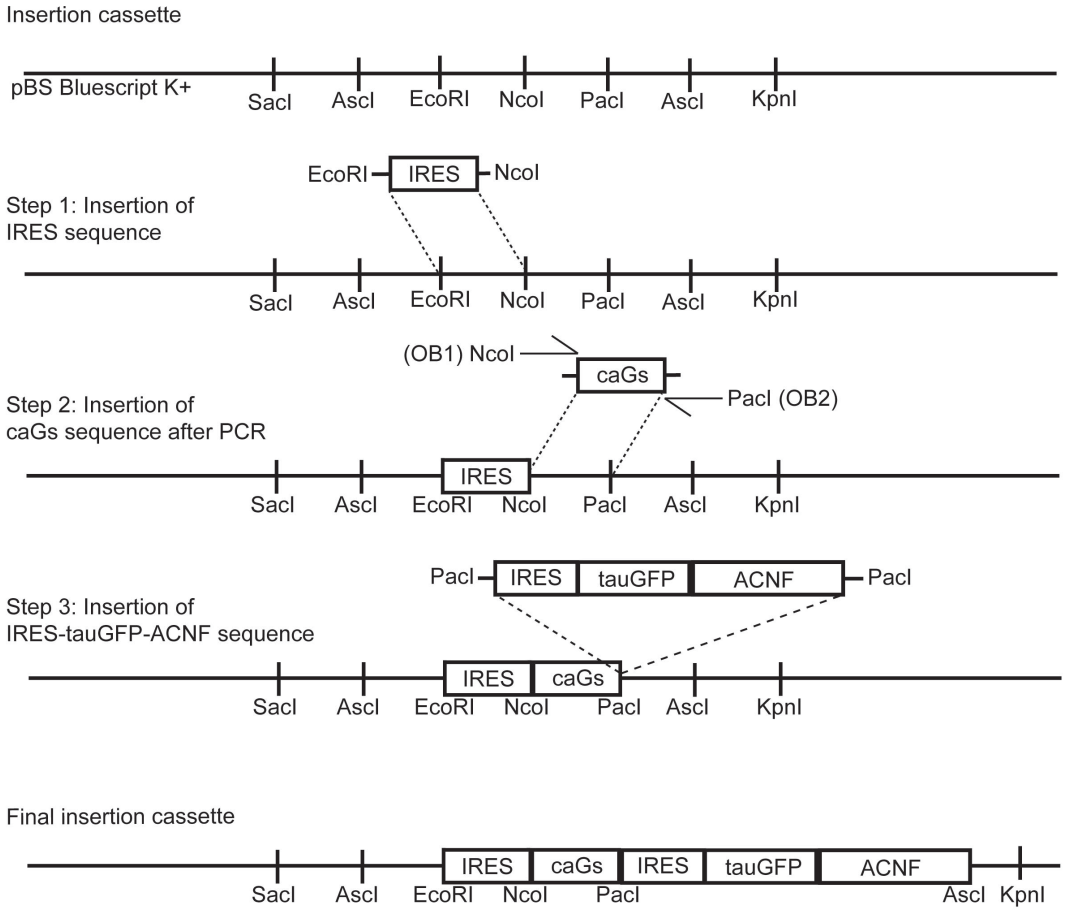

Figure 4.1 Generating the insertion cassette vector
In this figure the individual steps of restriction reactions and ligation constructing the insertion cassette vector are shown. The line represents the part of the plasmid vector containing the linker with all the restriction sites needed for the construction. Each insert was cut from the origin plasmid and ligated in the insertion cassette vector, except caGs, which was amplified from the original plasmid by PCR adding the necessary restriction sites (indicated by the arrow symbols in step 2).

At the same time the targeting vector on the basis of a pGEMT vector (Promega) was generated (Figure 4.2) by amplifying 4,532 base pairs (bp) in upstream direction from the end of M71 locus, called the left arm (la). Another arm was generated by amplifying 3,807 bp downstream of the M71 gene. Both PCRs used the Phusion Polymerase (Finnzyme through ThermoFisher) and were conducted with a M71 targeting available available in the lab. These two arms were inserted in the targeting vector and as a final step the insertion cassette generated in the other vector was cut and ligated in the targeting vector. The PmeI restriction site in the targeting vector is used for linearization of the vector prior to electroporation into ES cells.

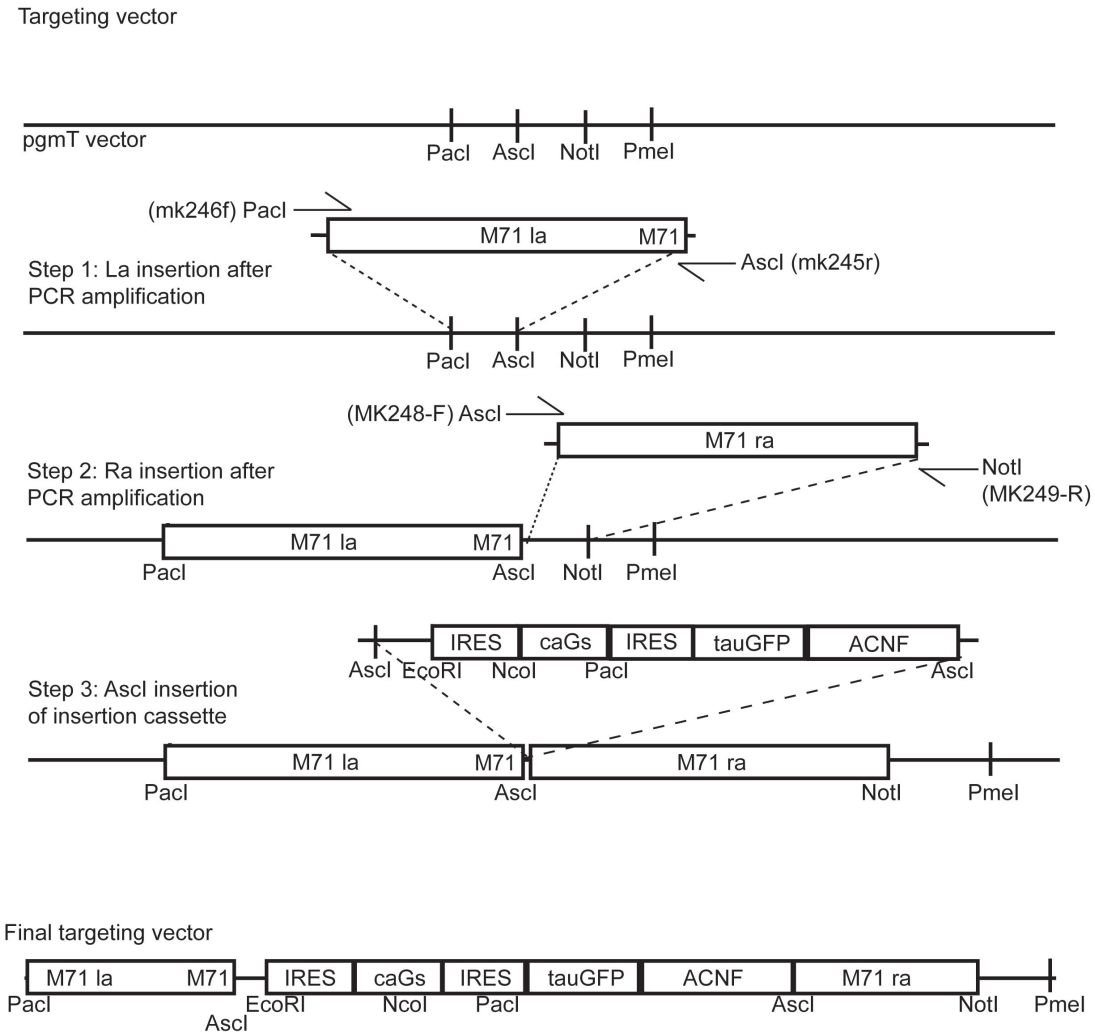

Figure 4.2 Generation of the gene-targeting vector
In this figure the individual steps of restriction reactions and ligation constructing the targeting vector are shown. The line represents the part of the plasmid vector containing the linker with all the restriction sites needed for the construction. The left and right arms of the targeting sequence were amplified for the M71 targeting vector with PCR adding the necessary restriction sites (indicated by the arrows). As a final step the insertion cassette was ligated into the targeting vector.

For a new construct the IRES-tauGFP sequences were replaced with IRES-tauCFP sequences but using the same method and concept.

4.2 Perfusion & Cryoprotection

Fixation of tissue is the first and most critical factor in microscopy. A strong fixation might prevent antibodies from reaching the intended targets and a weak fixation will not stop the degradation of the tissue post mortem. Likewise a good cryoprotection prevents tissue damage and preserves the anatomical structure of the tissue. The following protocol details the methods found most

suitable for the experiments in the mouse olfactory system reported in this thesis.

Mice were anesthetized with an intraperitoneal (i.p.) injection of 0.01ml/g anesthetic (0.25 ml 2% Rompun, 1.2 ml 10% Ketamin and 8.55 ml 0.9% NaCl) and after onset of narcosis fixed on a bench. Alcopads were used to mildly sterilize the fur and the skin was removed from the mouse abdomen. The ribcage was removed from sternum to throat. The left ventricle of the heart was pierced at the apex, parallel with the heart, with the syringe containing 1x PBS, then the right atrium was opened and the PBS was pumped into the ventricle. For PD21 or younger mice, 10 ml of PBS was used to wash out the blood. For PD70 mice 20 ml was used. Following the perfusion with PBS the mouse was perfused with the same volume of 4% PFA in 1x PBS (10 ml for PD21 mice).

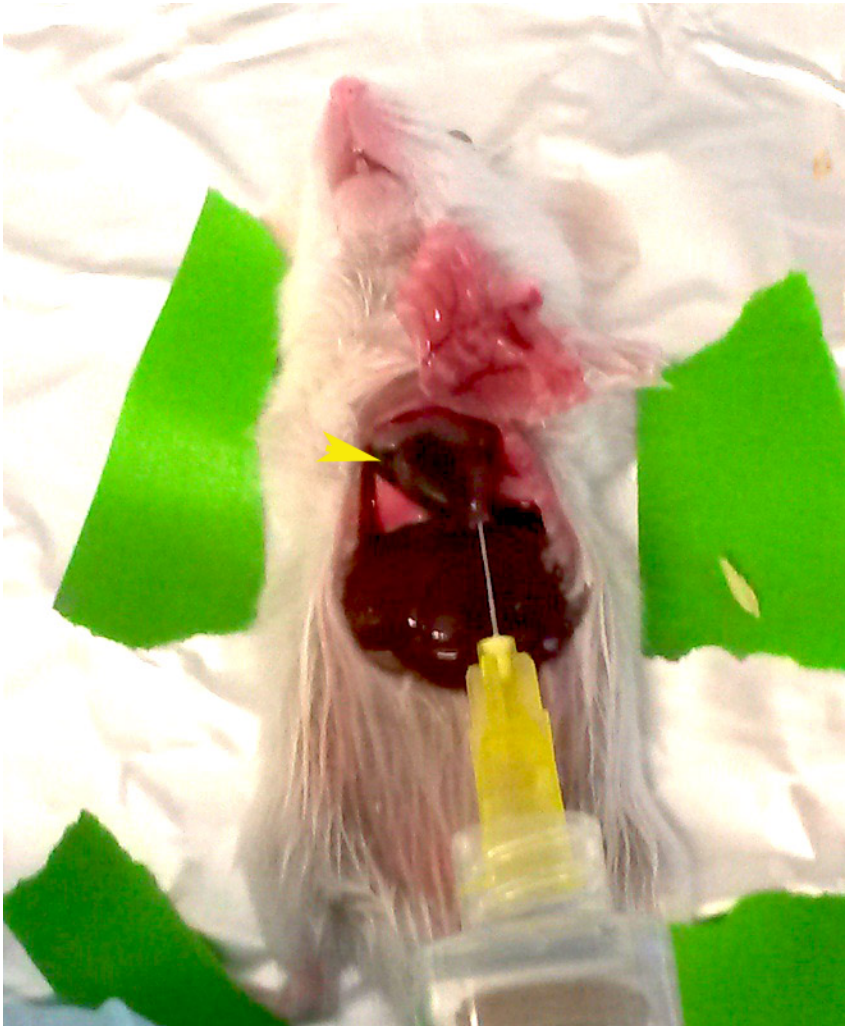

Figure 4.3 Perfusion
Image of perfusion of a PD21 mouse. A needle is inserted in the left ventricle. The arrowhead points to right atrium.

After perfusion the head was removed with scissors. The mouse was tailed for genotyping. The skin, as well as eyes, ears, lower jaw and the palatine bone were removed. The head was immersed in 4% PFA in 1x PBS for 5 min in a vacuum pump and then incubated at 4ºC for 2 h on a shaker. After the incubation PFA was exchanged for 0.45 M EDTA in 1x PBS and incubated over night on a shaker at 4ºC (two nights for PD70 mice). EDTA was exchanged for 15% sucrose in 1x PBS and consecutively 30% sucrose in 1x PBS, always incubated over night at 4ºC on a shaker (time doubled for PD70 mice).

After cryoprotection the head was trimmed and the teeth were removed. The caudal part of the head was cut in coronal direction (frontal plane) so it could be placed on the stage of the microtome for freezing. Afterwards the head was immersed in a cylinder of aluminum foil filled with O.C.T. The rostral tip was orientated to point to the center of the cylinder and the coronal base of the head was lowered to the bottom. Afterwards the cylinder was placed in granulated dry ice until O.C.T. was frozen. The cylinder with the frozen block was stored at -20ºC for sectioning.

4.3 Sectioning

A consistent and reproducible method for sectioning is crucial for cell counts and reconstructions of three-dimensional objects from sections. All sections were collected from the fixed and frozen mice heads gained with the previously detailed method. The frozen samples were sectioned with a Leica CM3050 S cryostat at 12 µm thickness and -20ºC. The sections were collected in sets of ten slides, alternating the slides for each section. In the end each slide contained 12 sections. The whole epithelium was sectioned in this manner and collected in sets of ten slides. The slides were stored at 4ºC up to 48 h or at -80ºC for longer storage.

4.4 Whole mount dissection (sagittal & dorsal)

While sections are ideal for the analysis of the cellular composition and quanititative estimates, whole mount preparations of the olfactory system are important for a general overview of the axon projections of the OB. Two different directions of the sections for the whole mounts were used: sagittal and dorsal. Each direction enables a different view on the OB and in concert they provide an overview of the axon projections for the strains reported in this thesis.

Mice were anesthetized with an i.p. injection of 0.01 ml/g anesthetic (0.25 ml 2% Rompun, 1.2 ml 10% Ketamin and 8.55 ml 0.9% NaCl). After onset of narcosis the mouse was decapitated with scissors. The mouse was tailed for genotyping. The skin, eyes, ears, lower jaw and the palatine bone were removed.

For the sagittal whole mount preparation the septum was cut from the ventral side with a scalpel and then the rest from the dorsal side. The halfs were separated and the rest of the septum was removed.

For the dorsal whole mount preparation the skull was cut along the midline of the axial plane from the cauda over the ear holes to the eye sockets. Then the dorsal part was carefully removed with a forceps.

The heads were stored in 1x PBS at 4ºC.

4.5 β-galactosidase staining

Some of the strains used express not a fluorescent reporter but β-galactosidase (β-gal). While fluorescent cells can be visualized directly with the microscope, β-gal tissue has to be stained and can only be observed afterwards with a bright field microscope. However, the reaction product is more stable. The protocol described in the following was used for visualization of OSNs expressing β-gal.

Sagittally or dorsally dissected samples were fixed with 4% PFA in 1x PBS for 10 min at 4ºC. The PFA was removed and the samples were washed once with Buffer A at 4ºC and then washed twice with Buffer A (Chapter 3.2.6) at

room temperature (RT) each for 5 min. Then the samples were incubated at RT in Buffer A on a shaker for 5 min. Afterwards the samples were incubated twice at RT in Buffer B for 5 min each. The samples were afterwards inserted into Buffer C and incubated for an hour or overnight at 37ºC in the dark until a strong blue staining was visible. The samples were then washed in Buffer B and stored in 4% PFA in 1x PBS.

4.6 Fluorescent antibody staining

For antibody staining two different protocols were used. One protocol is optimized for the Neuropilin-1 antibody and one for all other antibodies used.

4.6.1 Neuropilin-1 protocol

- Drying sample slides from -80ºC or 4°C with dryer (cold wind).
- Wash three times in 1x PBS at RT for 5 min each
- Blocking with 10% NDS in 1x PBS / 0.1 % Triton X 100 (PBS-T), 150µl per slide, cover with parafilm strip and incubation at RT for 1 h
- Remove excess blocking solution
- Primary antibody Goat α Nrp1 (1:100) (optional add Rabbit α dsRed 1:200 for double staining) and 3% BSA in PBS-T, 150 µl per slide, cover with parafilm strip and incubate over night (>16 h) at 4ºC
- Wash three times in PBS-T at RT for 10 min each
- Secondary antibody Donkey α Goat Cy5 (1:250) (optional add Donkey α Rabbit Alexa 555 1:250 for double staining) and 3% BSA in PBS-T, 150 µl per slide, cover with parafilm strip and incubate for 1.5 h at RT
- Wash three times in PBS-T at RT for 10 min each
- Wash once PBS for 1 min at RT
- DAPI staining with 5 µl of 5 mg/ml DAPI stock solution to 150 ml PBS for 10 min at RT
- Wash the slides with PBS
- Mount slides with 60 µl Moviol and coverslip
- Let slides dry over night at RT

4.6.2 β-galactosidase staining protocol

- Drying sample slides from -80ºC or 4°C with dryer (cold wind).
- Wash three times in 1x T-PBS at RT for 10 min each
- Blocking with 10% NDS in PBS-T, 150 µl per slide, cover with parafilm strip and incubation at RT for 1h
- Remove excess blocking solution
- Primary antibody Chicken α LacZ (1:500) and 2% NDS in PBS-T, 150 µl per slide, cover with parafilm strip and incubate over night (>16h) at 4ºC
- Wash three times in PBS-T at RT for 10 min
- Secondary antibody Donkey α Chicken FITC (1:250) and 2% NDS in PBS-T, 150 µl per slide, cover with parafilm strip and incubate for 1h at RT
- Wash three times in PBS at RT for 10 min
- DAPI staining with 5 µl of 5 mg/ml DAPI stock solution to 150 ml PBS for 10 min at RT
- Wash the slides with PBS
- Mount slides with 60 µl Moviol and coverslip
- Let slides dry over night at RT

4.7 Microscopy

Confocal imaging was performed using Zeiss LSM 510 and 710. For cell counting 25x water immersion lens and for glomerular volume measurements 40x water immersion lens was used. For confocal whole mount images 10x water immersion and 5x air lens were used. Whole slide scanning for overviews was performed with Aperio scanscope FL. Whole mount two photon images were taken with 40x water immersion lens using the Mai Tai system. Fluorescent whole mount images were also done using the NIKON SMZ25 stereomicroscope.

4.8 Genotyping

4.8.1 Genomic DNA extraction

This method was used to extract genomic DNA from tail biopsies. The tails were usually obtained while weaning the mice at PD21 and after perfusion for confirmation. Approximately 5 mm of tail was cut and placed in screw capped tail tubes. The tail biopsy was kept at -20ºC until lysis. Before genotyping the tail was incubated overnight at 55ºC in 200 µl of 1:100 Proteinase K (20 mg/ml) in digestion buffer. The next day Proteinase K was deactivated at 85ºC for 45 min. The tail lysate was stored at 4ºC until genotyping.

4.8.2 Genotyping protocols

For this thesis it was of great importance to determine unambiguously the genotype of the mice used. Especially for the complex breeding described in Chapter 7, reliable and accurate genotyping was essential. To achieve a high level of certainty, specific primers for each gene-targeted strain and crosses were used to amplify specific DNA sequences of known length using PCR. The table below details the primer pairs used and the PCR program chosen for each strain (Table 4.3). For most strains a primer pair for the wild type (WT) allele and the mutated (MUT) allele was tested. This was not possible for transgene (TG) strains since the locus in the genome is unknown. For each genotyping positive (B6), negative (water) were tested as well.

Table 4.3 List of primers for genotyping

Mutant name	Oligo wildtype	WT band size	Oligo MUT	MUT band size	PCR
M71-IRES-tauGFP	1121B/A114A	309 bp	819/ A114A	~250 bp	PCR 1
M71-IRES-taulacZ	1121B/ A114A	309 bp	797/ A114A	~250 bp	PCR 1
M71-IRES-tauRFP2	1121B/ A114A	309 bp	SF5/A114A	701/1397 bp	PCR 1
M71-IRES-tauYFP	1121B/ A114A	309 bp	819/ A114A	~250 bp	PCR 1
M71-IRES-Cre	1121B/ A114A	309 bp	900A/ 901A	~450 bp	PCR 1
RFP->M71-IRES-M71-IRES-tauGFP	1121B/ A114A	309 bp	819/ A114A	~300 bp	PCR 1
b2AR->M71-IRES-tauGFP	1121B/ A114A	309 bp	819/ A114A	~300 bp	PCR 1
b2AR->M71-IRES-taulacZ	1121B/ A114A	309 bp	797/ A114A	~250 bp	PCR 1
MOR23-IRES-tauGFP	Cat33/ 1992	243 bp	819/ 1992	~300 bp	PCR 1
MOR256-17-IRES-tauGFP	MK162/ MK163	455 bp	MK99/ MK163	401 bp	PCR 1

Mutant name	Oligo wildtype	WT band size	Oligo MUT	MUT band size	PCR
M50-IRES-GFP-IRES-taulacZ	803/ 806	404 bp	797/ 806	~300 bp	PCR 1
mOR37C-IRES-tauGFP	G3A/ G15A	~400 bp	819/ G15A	~300 bp	PCR 1
S50-IRES-tauGFP	T524/ T525	586b p	819/ T525	~750 bp	PCR 7
mI7-IRES-tauGFP	M168/ M169	361 bp	819/ M169	~250 bp	PCR 7
SR1-IRES-tauGFP	SF1/SF2	562 bp	SF3/ SF2	439 bp	PCR 1
P2-IRES-tauGFP	824/ 1243	220 bp	819/ 1243	~213 bp	PCR 1
P3-IRES-tauGFP	1257A/ 1040	198 bp	819/ 1040	~300 bp	PCR 1
M72-IRES-tauGFP	1121B/ 950	475 bp	819/950	~400 bp	PCR 1
Neuropilin-1-floxed		~200 bp	AW28/ AW29	~350 bp	PCR 1
npn1-5247/J		~ 550 bp	MK564 / MK565	660 bp, 710 bp	PCR 1
I7(WT)-Cre	oIMR0042/oIMR 0043	324 bp	IRES-F / Cre-R	260 bp	PCR 1
OMP-Cre	CZ40A/ 721A	542 bp	900A/ 901A	~450 bp	PCR 1
OMP-tau-STOP-lacZ	CZ40/ 721A	615 bp	1571/ 720	~200 bp	PCR 7
ROSA-STOP-taulacZ			T334/ T335	488 bp	PCR 1
Z/EG	LL1491/ LL1492	588 bp	LL624/ LL1294	~400 bp	PCR 1

For all genotyping reactions a standard reaction mix was used. For each reaction 0.40 ml of each primer at 20 µM concentration was used. Buffer, dNTPs and Taq were provided by Takara Bio Inc.

Table 4.4 Reaction mix

	µl
H_2O	18.08
10 x Puffer	2.50
dNTP	2.00
Each primer	0.40
Taq	0.12
Template	1.50
Total	25.00

For genotyping two protocols for PCR were used, internally called PCR 1 and PCR 7. Otherwise the PCR did not differ from the method described in 4.1.1.

Table 4.5 PCR protocols for genotyping

Steps	PCR1	Cycles (35x)	PCR 7	Cycles (40x)
Initial denaturation	95ºC	5 min	94ºC	5 min
DNA denaturation	95ºC	1 min	94ºC	45 sec
	60ºC	1 min	58ºC	30 sec
DNA polymerization	72ºC	2 min	72ºC	1 min
Final polymerization	72ºC	10 min	72ºC	10 min
Holding	4ºC		4ºC	

After PCR amplification the DNA fragments were stained with loading dye and loaded on a 1,5% agarose in TBE gel and the NEB standard was added. The gel was run at 120V in TBE buffer for approximately 30 min. Gel pictures were taken with PeqLab Geldoc.

4.9 Cell counting

Every fluorescent cell body profile with full nucleus in each section of PD21 or younger mice was counted using a Zeiss confocal microscope LSM 510. Each section was counted manually, by direct inspection with the microscope. Sampling methods (Geuna, 2000; Guillery, 2002; Schmitz and Hof, 2005) were not used due to the multitude of distinct spatial expression patterns attributed to zones for OR genes. The sparse and possibly non-homogeneous distribution of OSNs that express a given OR gene make most techniques not practical. Due to the inherently strong tissue shrinkage in cryosections combined with the sparse distribution of labeled cells an optical dissector correction for the z-axis was not used (Benes and Lange, 2001). Instead an empirical strategy was chosen. Counting of up to ~50,000 cells in a mouse is still practical. To get a closer approximation to the real cell numbers the Abercrombie correction (Abercrombie, 1948) was applied to the cell counts. For the correction the average nucleus diameter of 10 cells for each of the 11 core strains for Chapter 6 was measured (Figure 4.4). Subsequently for each strain the correction factor was calculated (section thickness of 12 µm) using the formula (Table 4.6):

$$cell\ number = cell\ count\ x \frac{Section\ thickness}{nucleus\ diameter + section\ thickness} (correction\ factor).$$

Table 4.6 Nucleus diameter and correction factor

Strain name	Abbreviation	Nuclear diameter (µm)	Standard deviation (±µm)	Correction
P3-IRES-tauGFP	P3	4.51	0.80	0.73
M71-IRES-tauGFP	M71	4.26	1.05	0.74
mOR37C-IRES-tauGFP	mOR37C	4.39	0.62	0.73
S50-IRES-tauGFP	S50	4.40	0.91	0.73
MOR23-IRES-tauGFP	MOR23	4.00	0.39	0.75
M72-IRES-tauGFP	M72	4.47	0.74	0.73
M50-IRES-GFP-IRES-taulacZ	M50	4.49	0.79	0.73
mI7-IRES-tauGFP	mI7	4.53	0.65	0.73
P2-IRES-tauGFP	P2	4.53	0.60	0.73
SR1-IRES-tauGFP	SR1	4.49	0.72	0.73
MOR256-17-IRES-tauGFP	MOR256-17	4.59	0.58	0.72
β2AR→M71-IRES-tauGFP		4.26	1.05	0.74
RFP→M71iM71iGFP		4.26	1.05	0.74
M71-IRES-tauYFP		4.26	1.05	0.74
M71-IRES-tauRFP2		4.26	1.05	0.74

A priori knowledge or assumptions of OSN distribution in the MOE are not needed, hence this strategy enables analysis and comparison of a relatively large number of strains.

For overview images of the MOE, a Leica Aperio Scanscope FL was used. For mice older than PD21, cells in every fifth coronal section were counted. For statistical analyses and graphs, Graphpad Prism 5 was used.

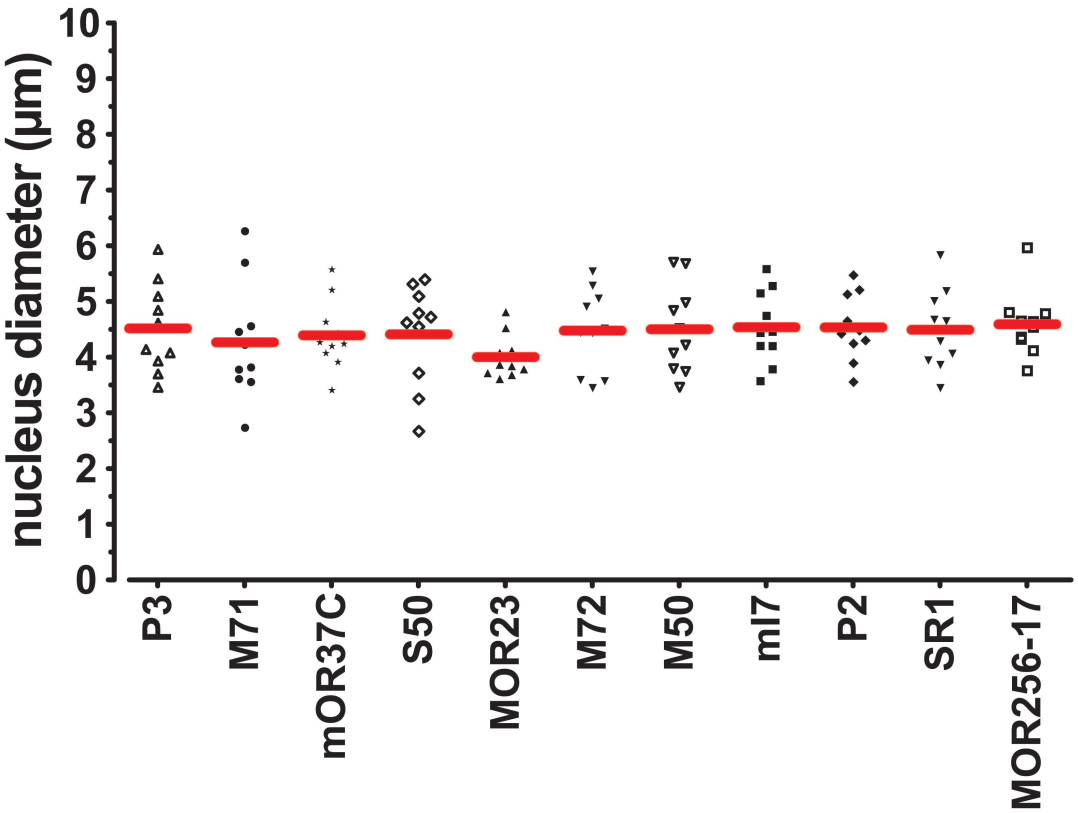

Figure 4.4 Average nucleus diameter
This figure shows the average nucleus diameter measured for 11 gene-targeted strains. Each symbol represents a single OSN measured. For each strain, 10 different OSNs were measured. There is no statistical significant difference between the diameters (One-way Annova, F=0.52, P=0.87).

4.10 Glomerular reconstruction

The same series of coronal sections used for estimating the OSN numbers were also used to determine the total glomerular volume (TGV) of fluorescent glomeruli in mice at PD21. Images of glomerular sections were taken with the LSM 510. Glomerular reconstruction and fluorescent pixel density measurements in glomeruli were performed using Microsoft Excel, Fiji V1.48u and Matlab V7.12. For statistical analyses and graphs, Graphpad Prism 5 was used.

Glomeruli are distributed on average over five physical sections but can span more than ten physical sections. Glomeruli were not always of elliptical shape so a simple estimation for glomerular volume was not feasible (Schaefer et al., 2001).

First, glomeruli were reconstructed by taking z-stack images with the LSM 510 in 1 µm intervals through all physical sections that contained labeled axons within the glomerular layer, similar to other methods reported (Cummings and Belluscio, 2010). In each optical section of the z-stack that contained a sharp and defined glomerular profile (Figure 4.5), the surface area of the glomerulus was measured. These areas were summed and multiplied with optical section thickness (1 µm) to get a close approximation of the glomerular volume.

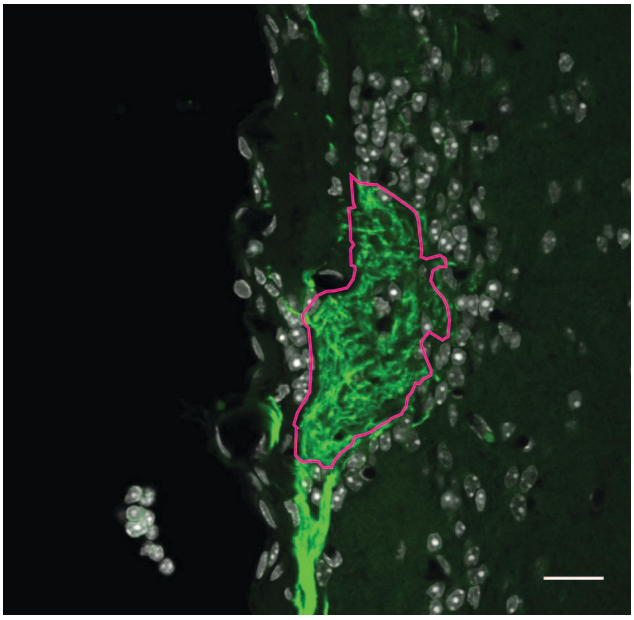

Figure 4.5 Measuring area in optical sections
Confocal image of an M71-IRES-tauGFP glomerulus. Green, intrinsic fluorescence, white: DAPI. Scale bar: 20 µm. The area framed in magenta is measured as the cross sectional area of the glomerulus in this section. Image taken with a 40x lens.

To reduce the labor of volume reconstruction, this thesis shows that a close approximation can be achieved by analyzing a single optical section per physical section. These optical section profiles from the middle of the physical section are summed and multiplied then with a factor of of 12 µm (the section thickness). The sum of all glomerular volumes of fluorescently labeled glomeruli per mouse is the TGV. This measure decreases the variance and corrects for differences in the numbers of glomeruli.

4.11 Measuring fluorescent pixel density

Fluorescent pixel density of a glomerulus was calculated by using the 40x confocal images of the optical sections used for TGV reconstruction. Images were loaded into a Matlab program. The background fluorescence was defined for each image in labeled regions of the glomerular layer close to the labeled glomeruli, and a threshold was set at mean background pixel intensity of the image plus three times the mean backgrounds standard deviation. The area of fluorescence was measured manually as for the glomerular volume. All pixels above threshold in the glomerular area were measured, and the ratio to the entire glomerular area was calculated as the fluorescent pixel density.

5 Generating a gene-targeting vector for the M71 locus

5.1 Results

Axonal wiring in the mouse olfactory system is a complex endeavor for the nascent OSN axon and still not fully understood. In 2006, Imai and colleagues (Imai et al., 2006) reported that a mutation in the G-protein binding site of the rat I7 OR (rI7) receptor abolishes axon wiring in OSNs expressing this receptor in transgenic mice. Axonal wiring can be recovered by expression of a constitutively active $G_{\alpha s}$ subunit (caGs). Expression of caGs in wild-type rI7 expressing OSNs shifts the glomerular position more posteriorly. The model that has emerged form these results is that the basal level of cyclic adenosine monophosphate (cAMP) plays a crucial role in glomerular positioning along anterior-posterior axis. In the present study I tried to generate gene-targeted strains with a knockin of caGs in M71-expressing OSNs as opposed to the transgenic random integration approach by Imai and colleagues (2006).

Unfortunately, the generation of a new gene-targeting vector needed to knockin caGs in the M71 locus failed despite of two approaches, which are described in the following paragraphs (5.1.1 and 5.1.2).

The process of generating the gene-targeted strains starts with the cloning of the targeting vector. In short, a sequence fragment consisting of the desired mutation is designed to be flanked by ~5,000 bp arms that are homologous to the genome. The completed targeting vector is then linearized and electroporated in E14 embryonic stem cell lines. The correct clone with the mutation is then screened by Southern blot. The positively identified clone is afterwards microinjected in C57BL/6J blastocysts which are then transferred to pseudopregnant CD1 mothers. Among the resulting mice are chimeras, and male chimeras are bred with C57BL/6J females to generate F1 offspring. Germline transmission is often confirmed by coat color identification, followed by Southern blot analysis of the tail biopsies.

5.1.1 First strategy

The cloning steps of the targeting vector for the M71 locus is described in Chapter 4.1.8. The cloning steps were based on modifying the existing targeting casettes for the M71 locus available in the lab. The task was to insert a new cassette “IRES-caGs” into an existing targeting vector, M71-IRES-tauGFP thereby creating a tricistronic vector, M71-IRES-caGs-IRES-tauGFP. Successful cloning steps were achieved resulting in the plasmid pOB08 (Figure 5.1A). Test restriction digest with three restriction endonuclease pairs (EcoRI/NcoI, NcoI/PacI & EcoRI/PacI, Figure 5.1B) showed the correct insertion and direction of the sequence (left example). Subsequently the correct plasmids were sent out to Qiagen for sequencing.

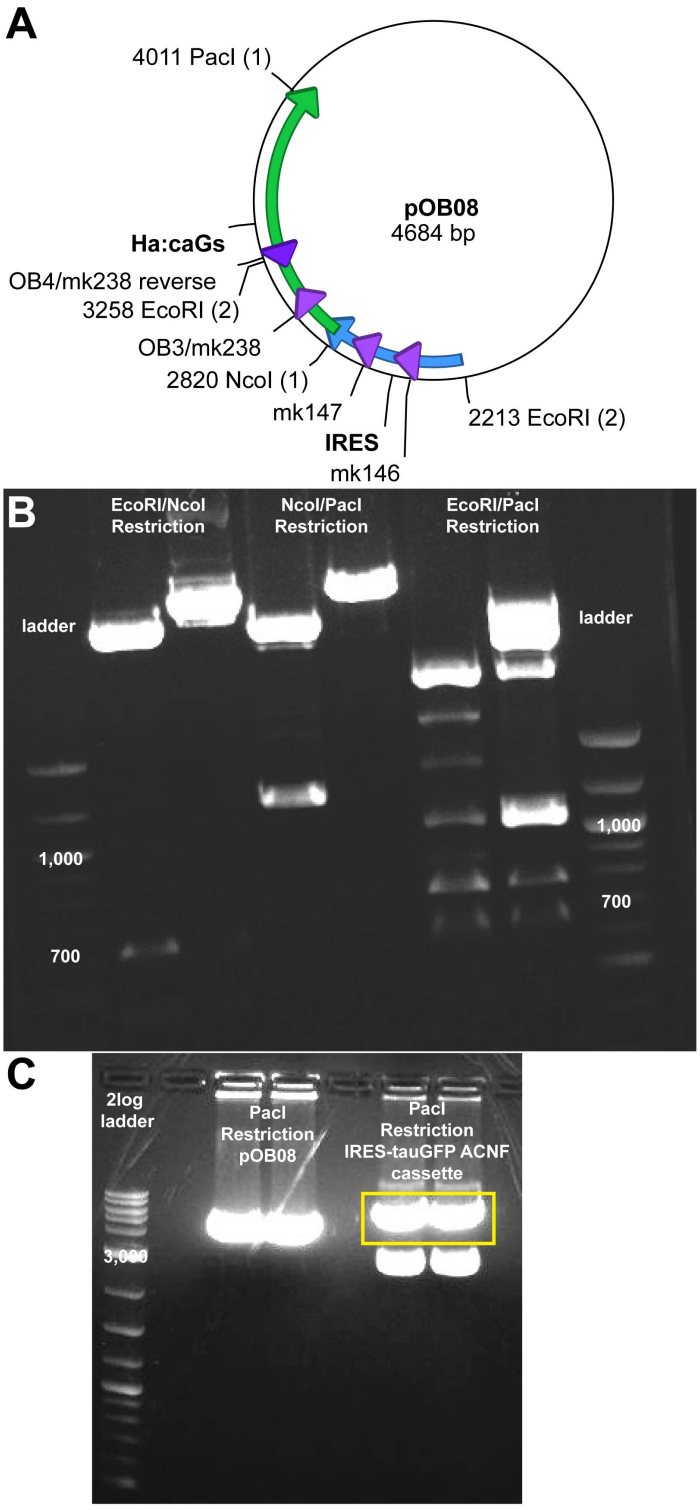

Figure 5.1 Generating gene-targeting vector 1

(A) Vector map of the pOB08 vector. This was the last step (step 2, Figure 4.1), which gave positive results. Purple arrowheads represent primer binding sites for genotyping and sequencing. The arrow tip shows the direction of primer. Long arrows represent the insert, indicating the direction. Also shown are the restriction sites used in confirmation of targeting and as further insertion sites. (B) Gel electrophoresis of test restriction with three restriction endonuclease pairs (EcoRI/NcoI, NcoI/PacI, EcoRI/PacI) for two pOB08 plasmids (left and right lane). Expected bands additional to vector band (2000 - 3000 bp) are: EcoRI/NcoI 486 bp & 473 bp, NcoI/PacI 1185 bp, EcoRI/PacI 1050 bp & 757 bp. (C) Gel electrophoresis of PacI restriction for two clones of pOB08 (left lanes) and two IRES-tauGFP ACNF plasmids. The yellow box highlights the band excised as insert for step 3.

After the confirmation by sequencing the final step involved cloning the IRES-tauGFP-ACNF cassette into pOB08 by PacI ligation (Figure 5.1C). However after several attempts using different clones of the IRES-tauGFP-ACNF plasmid and pOB08 forming the final plasmid pOB09 (Chapter 4.1.8) and despite intense screening and sequencing, a clone with the correct insert, which would have generated the full tricistronic construct, could not be identified. Different competent cell lines were used to facilitate correct plasmid amplification (dH5α, XL2-Blue Ultracompetent cells, MAX efficiency DH5a).

5.1.2 Second Strategy

Another approach was attempted; using another targeting vector donor available in the lab (IRES-gapCFP-ACNF) the fluorescent protein tauCFP was used as a reporter gene and with an additional linker the M71 targeting vector available in the lab was used (restriction endonuclease targeting site for PacI after M71 sequence). The assembly of the insert for the targeting vector worked and resulted in the plasmid pOB13 (IRES-caGS-IRES-gabCFP-ACNF, Figure 5.2A). Correct assembly was confirmed by PCR and restriction enzyme digest to identify correct clones (Figure 5.2B). However I encountered the same difficulty in the final ligation step to generate the tricistronic vector pOB13 (Figure 5.2C). After several attempts over months the project was finally suspended due to time constraints.

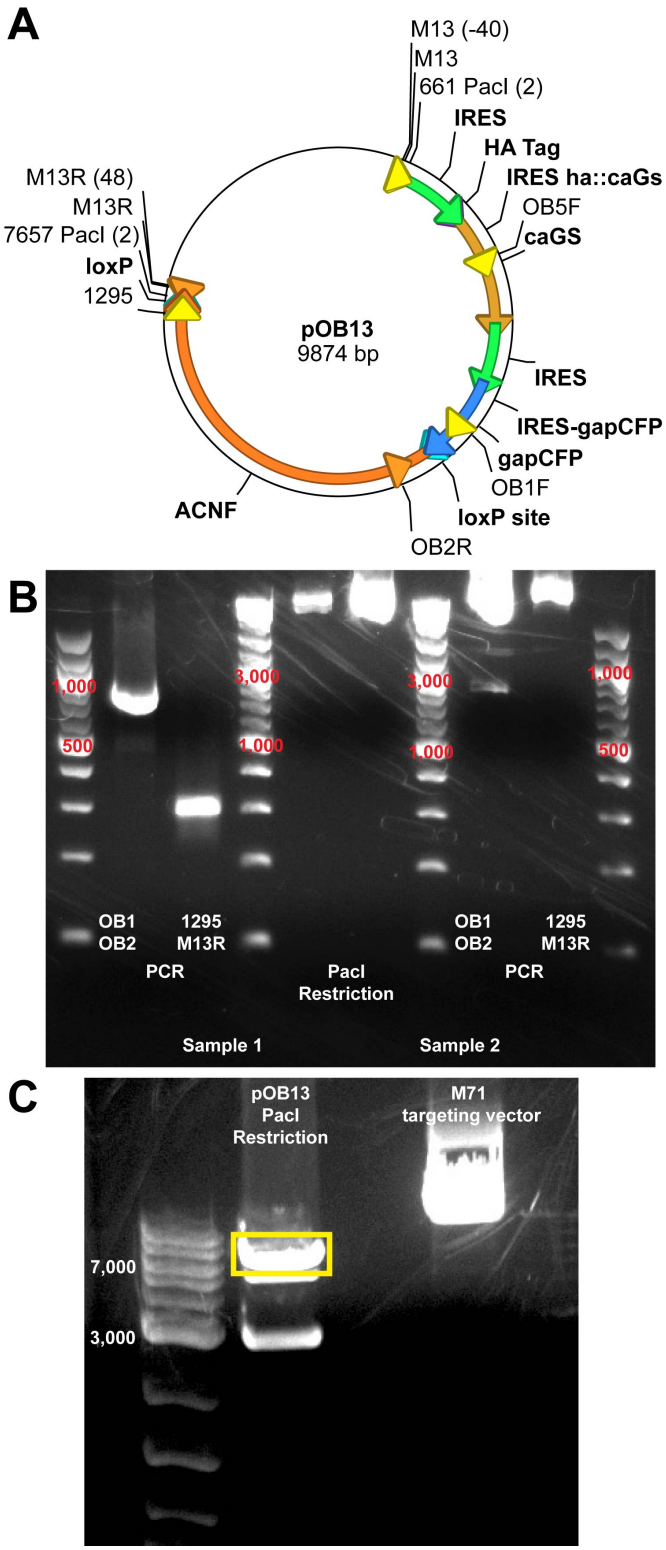

Figure 5.2 Generating gene-targeting vector 2
(A) Vector map of the pOB13 vector. This was the last step, which gave positive results. Yellow arrowheads represent primer binding sites for genotyping and sequencing. The arrow tip shows the direction of primer. Long arrows represent the insert, indicating the direction. Also shown are the restriction sites used in confirmation of targeting and as further insertion sites. (B) Gel electrophoresis for PCR for primer pairs OB1/OB2 (700 bp) and 1295/M13R (280 bp) and test for linearization with PacI restriction for two samples of pOB13 targeting vector. Sample two is negative for correct inserts. (C) Gel electrophoresis of PacI restriction of pOB13 and M71 targeting vector. Yellow box indicates 7000 bp band excised for insertion in M71 targeting vector after gel extraction.

5.2 Discussion

Unfortunately both strategies to generate a gene-targeting vector that expresses caGs and a fluorescent reporter gene from the M71 locus failed. There are several explanations why no correct and functional plasmid was obtained. One possibility is that the double IRES sites in the construct are toxic for the competent cells, or just very hard to correctly amplify due to the long GC rich sequence in IRES. It might be that the two IRES sequences interact because of the highly repetitive sequence homology and a recombination event occurs. In several sequencing results of the plasmids the sequence of the inserts seemed to be incorrect or not in the right orientation. Another problem might be the size of the vectors, which might influence the amplification of the plasmid.

I initiated this project to test the hypothesis of a prevailing model that cAMP determines the positional axis of glomeruli. Although the final cloning steps failed, I have gained a lot of insights and experience in targeting vector construction.

6 Quantitative analysis of gene-targeted strains

6.1 Results

The chemosensory system in mouse relies on the expression of ~1,200 OR genes across millions of OSNs for specificity. These millions of OSNs in the MOE project their axons to the OB and form ~3,600 glomeruli. In this chapter 17 gene-targeted strains are reported of the OR-IRES-marker design coexpressing a fluorescent protein or –taulacZ.

Representing a 1% sample of the OR gene repertoire, 11 strains were selected for detailed analysis. All serial coronal sections were evaluated quantitatively using confocal microscopy - a total of 685,673 cells in 56 mice at postnatal day 21 were counted. A strain-specific Abercrombie correction to these OSN counts was applied, in order to obtain a closer approximate of the true OSN numbers. In the same series of coronal sections, the total volume of the glomeruli (TGV) formed by coalescence of the fluorescent axons was measured, finding a strong linear correlation between OSN number and TGV. This leads to the conclusion that the glomerular volume is a possible estimate for cell numbers.

Most of these data have been published in Bressel et al. (2015).

6.1.1 Cell counts

The OSN numbers in the core set of 11 strains representing the 11 gene-targeted OR genes after Abercrombie correction at PD21 are, from low to high: P3 (2,236 ± 247 cells), M71 (2,419 ± 484), mOR37C (2,660 ± 175), S50 (3,289 ± 503), MOR23 (4,446 ± 327), M72 (5,265 ± 906), M50 (6,716 ± 648), mI7 (9,892 ± 1,852), P2 (13,975 ± 1,982), SR1 (23,846 ± 1,706), and MOR256-17 (37,023 ± 6,318) (Figure 6.1). The average OSN number has thus a range of 17-fold across these 11 OR-tagged strains. Importantly, the spread within a given OR-tagged strain is fairly small (see also below, coefficient of variation).

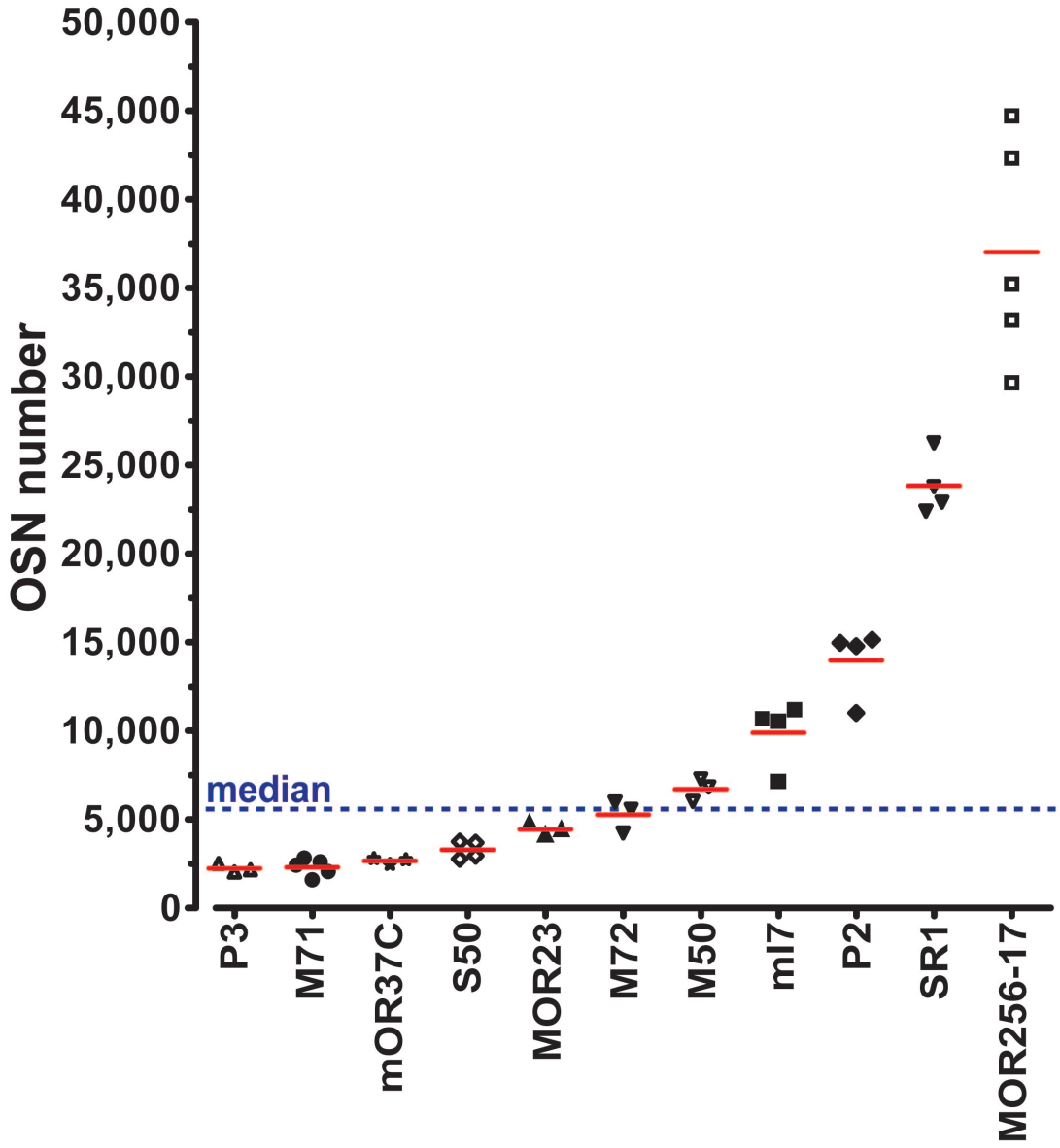

Figure 6.1 Numbers of fluorescent cells in OR-IRES-tauGFP strains
Average OSN number of the core set of 11 gene-targeted strains at PD21. A symbol represents a single mouse. The blue line indicates the median of 5,983.

The numbers of fluorescent cells in six other strains with mutations in the *M71* gene are-: β2AR→M71-IRES-tauGFP (460 ± 131), β2AR→M71-IRES-taulacZ (1475 ± 334), RFP→M71iM71iGFP (650 ± 77), M71-IRES-tauYFP (1,558 ± 156), M71-IRES-tauRFP2 (1,893 ± 14) (Figure 6.2) and M71-IRES-taulacZ (4610 ± 579). There is no significant difference (t-test, p = 0.21) in OSN numbers between M71-IRES-tauGFP and M71-IRES-tauRFP2 (red fluorescent protein), indicating a similar probability of OR gene choice and sensitivity of detection of intrinsic fluorescence. The OSN number in M71-IRES-tauYFP mice (yellow fluorescent protein) is lower than in M71-IRES-

tauGFP mice (t-test, p = 0.022) and M71-IRES-tauRFP2 mice (t-test, p = 0.015), reflecting a possible difference in probability of OR gene choice and/or in sensitivity of detection of intrinsic fluorescence. OSN number is significantly higher in the strain expressing taulacZ as a reporter gene (t-test, p = 0.0003). OSN numbers are decreased in mutations in which the *M71* coding region is replaced by that of the β2-adrenergic receptor (β2AR→M71-IRES-tauGFP) (t-test, p < 0.0001) and (β2AR→M71-IRES-taulacZ) (t-test, p = 0.02) or in which M71 translation is decreased by an *IRES*-mediated knockdown (hypomorph, RFP→M71iM71iGFP) (t-test, p = 0.0007).

There are 2,067 ± 441 OSNs in M71-IRES-tauGFP mice (n=3) at PD70, which is not significantly different (t-test, p = 0.52) from PD21. For the hypomorph there is no difference either between PD21 and three mice at PD70 (660 ± 248 cells) (t-test, p = 0.93).

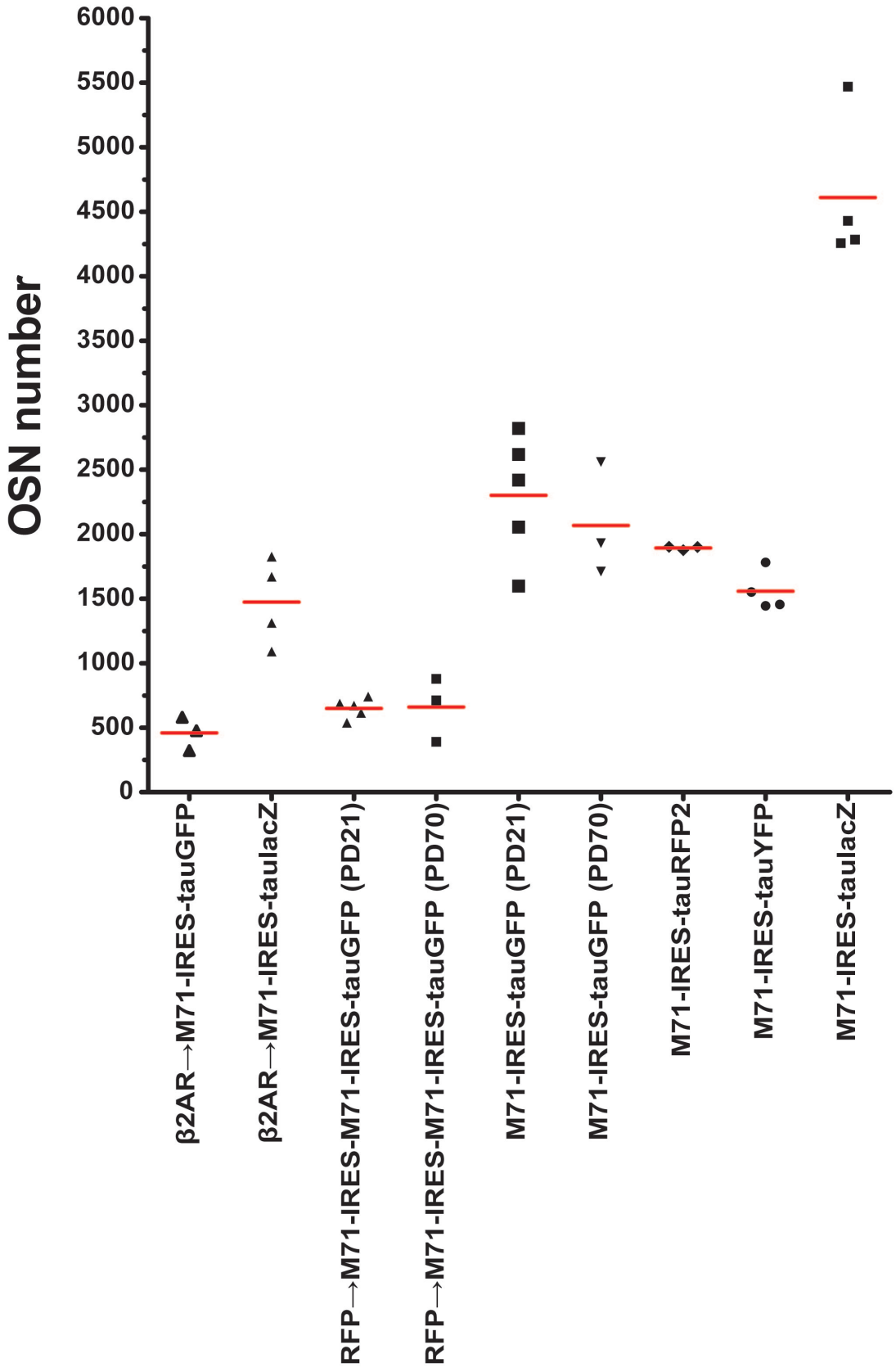

Figure 6.2 Numbers of fluorescent cells in M71-expressing strains
Average OSN number for strains with gene-targeted mutations in the *M71* locus at PD21 or PD70. The five mice of M71-IRES-tauGFP at PD21 in Figure 6.2 are the same as in Figure 6.1.

6.1.2 Sampling error

Partial cell counts from sampling are typically reported in the literature, because of the time and effort required to make full cell counts. The availability of full cell counts provides a unique opportunity to determine exactly the error that would have been introduced by interleaved sampling. Data sets of n size were generated for the full cell counts, corresponding to nth section sampling for the core set of 11 strains (Figure 6.3); for example, there would be 10 data sets consisting of cell counts in each 10th section. For each data set, the cell counts were summed and multiplied by the sampling interval; in this example, multiplied with 10.

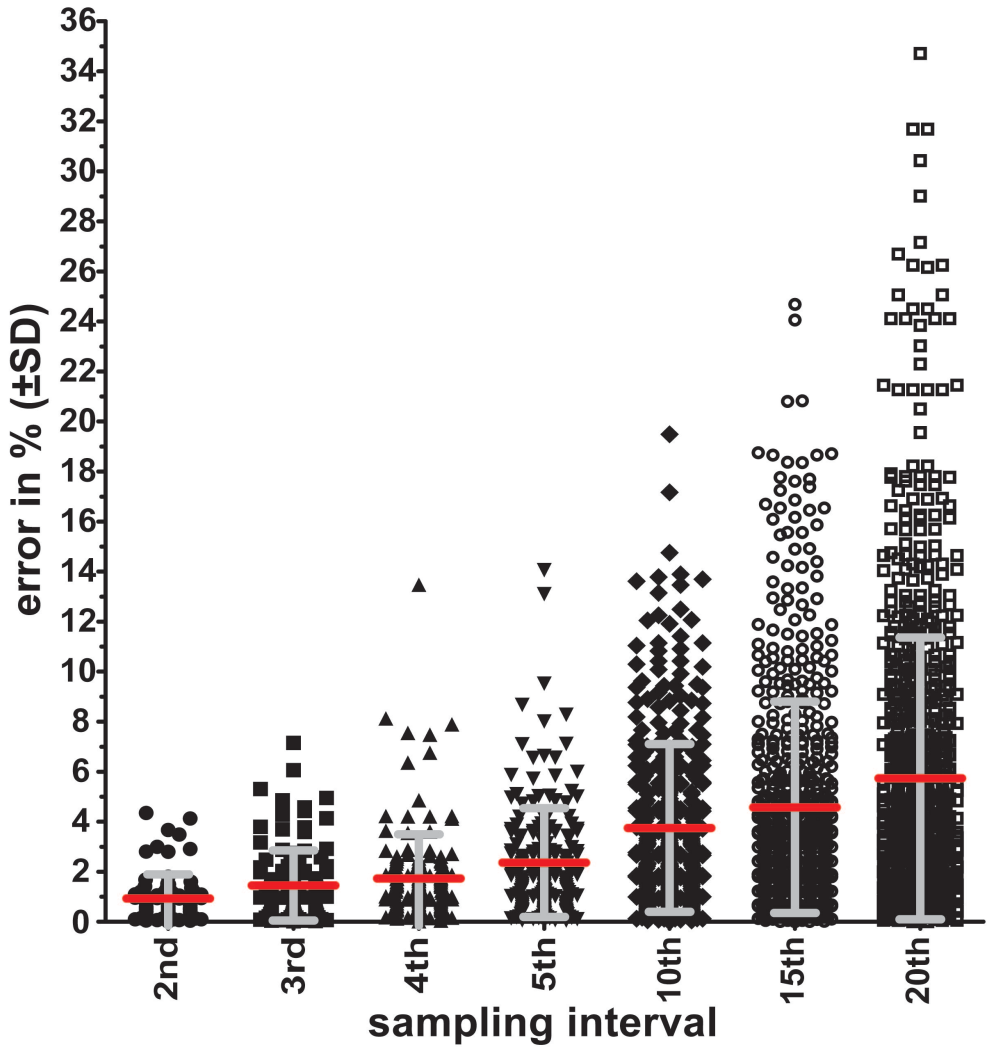

Figure 6.3 Effect of sampling interval
Average percentage of difference (error) in interleaved sampling compared to the "count every cell" approach (±SD). Errors for all tauGFP strains for each sampling interval were pooled to calculate the averages. A symbol represents a single virtual sampling set.

The error produced by interleaved sampling can then be calculated by comparing the summed counts of a virtual data set to the original full cell count. The error and standard deviation increase rapidly with decreased sampling interval, and are higher for strains with low OSN numbers such as P3-IRES-tauGFP than for strains with high OSN numbers such as MOR256-17-IRES-tauGFP (Figure 6.4).

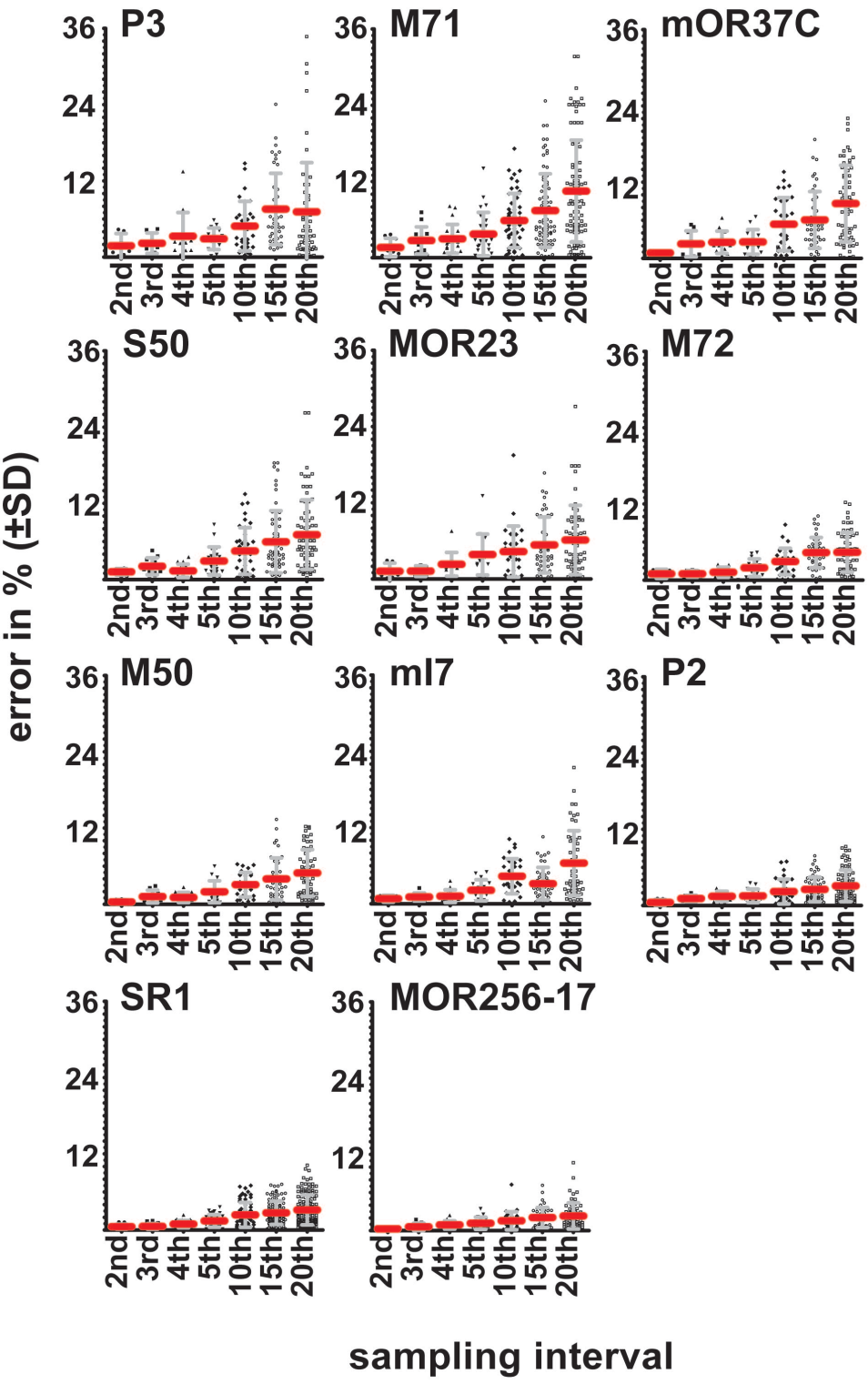

Figure 6.4 Sampling error per strain
Error of cell counts by sampling interval for GFP-expressing strains sorted by average OSN number, from P3, low, to MOR256-17, high. A symbol represents a single virtual sampling set.

6.1.3 Coefficient of Variation

The coefficient of variation (CV) is the ratio of standard deviation and average. Among the core set of 11 strains, the CV for the OSN number within a strain ranges over a factor of 3.2-fold, from 0.066 (mOR37C-IRES-tauGFP) to 0.21 (M71-IRES-tauGFP), but there is no correlation with average OSN number (Figure 6.5): MOR23-IRES-tauGFP has a similarly low CV (0.074) as SR1-IRES-tauGFP (0.072), but the number of OSNs is 5.5-fold lower. Conversely, M72-IRES-tauGFP has a CV (0.172) similar to that of MOR256-IRES-tauGFP (0.171), but the number of OSNs is 7-fold lower. Thus, the probability of OR gene choice appears to be more constant for certain OR genes than for others. From a practical experimental viewpoint, FP-tagged strains with a higher stability in OSN population size (a lower CV) such as MOR23-IRES-tauGFP are easier to study quantitatively.

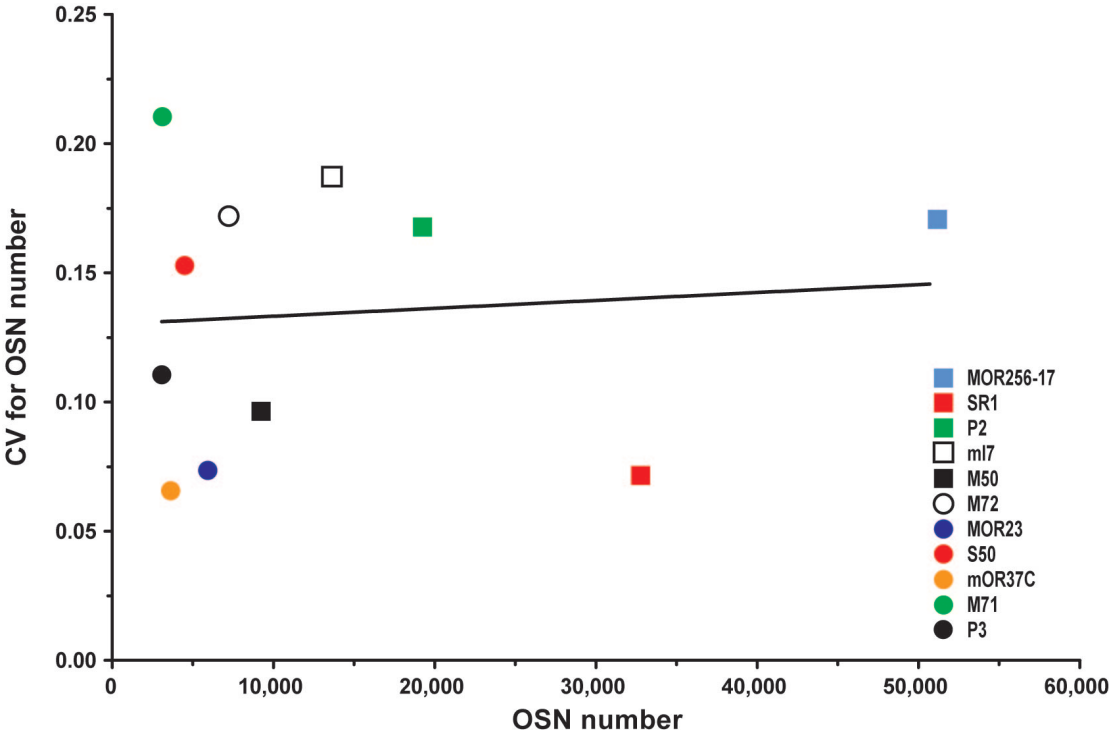

Figure 6.5 Coefficient of variation.
Coefficient of variation (CV) for average OSN number of the 11 tauGFP strains shows that there is no correlation between average OSN number and CV. The line is best modeled by $y = 3.1*10^{-7}x + 0.13$ ($r^2 = 0.008$, $p = 0.79$).

6.1.4 Cell counts along the anterior-posterior dimensions of the main olfactory epithelium

As described previously, OSNs expressing a given OR gene display a characteristic spatial pattern across the MOE (Ressler et al., 1993; Miyamichi et al., 2005). With the availability of full cell counts per 12 µm section, plotting the counts along the anterior-posterior dimension of the MOE became feasible. Figure 6.6 shows the diversity of these plots, reflecting the multitude of spatial expression patterns.

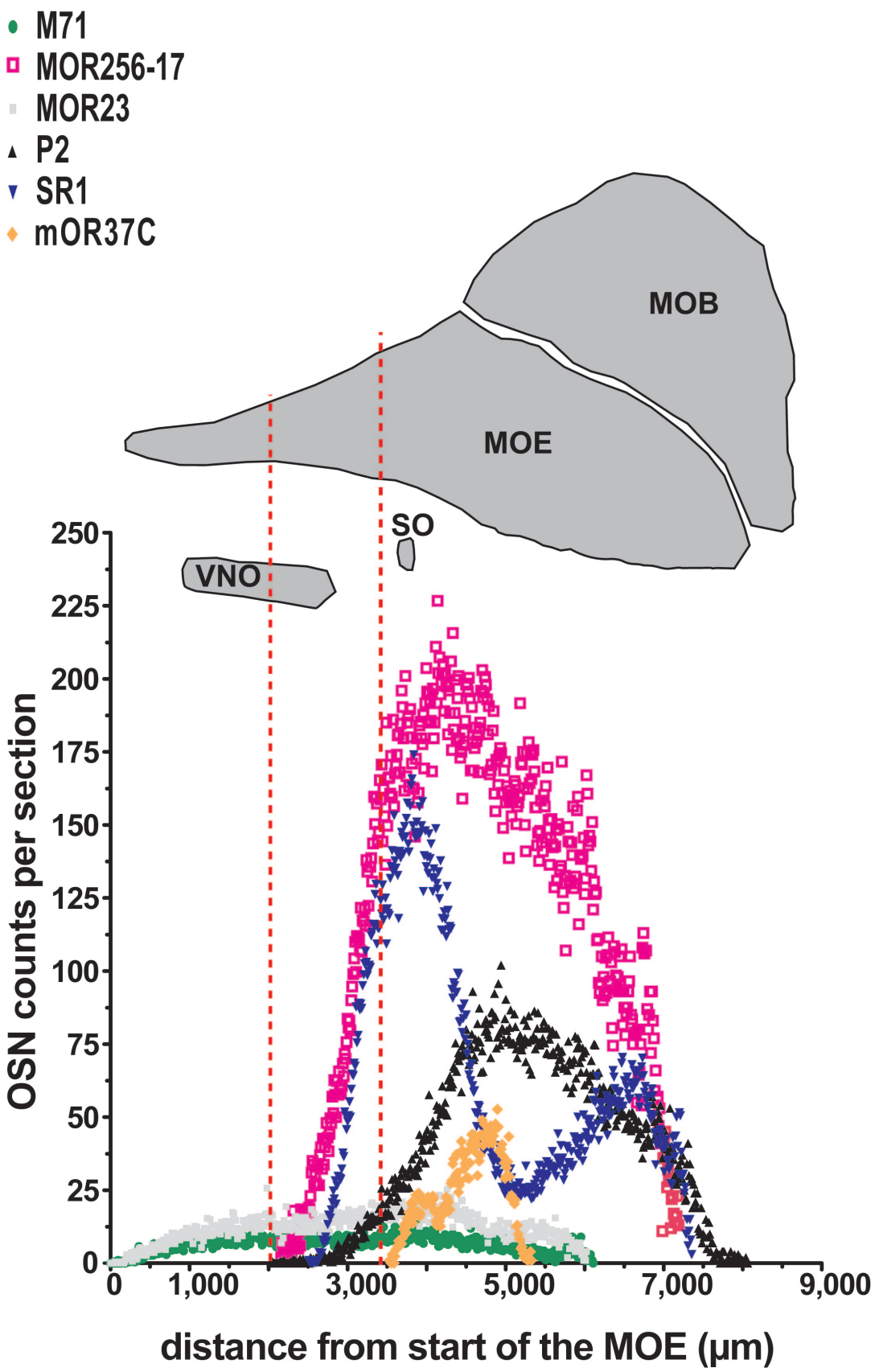

Figure 6.6 OSN counts across the anterior-posterior dimension of the main olfactory epithelium. Average OSN counts per section. The dotted red lines indicate two reference positions in a sagittal view of a mouse head. Strains were chosen for showing the diversity in expression per section. Cells in the septal organ are not included in these counts.

OR genes expressed dorsally such as *M71* and *MOR23* have a relatively even distribution, starting far anteriorly. The relatively even distribution of *M71* is maintained in mutations in which the *M71* coding region is replaced by that of the β2-adrenergic receptor (β2AR→M71-IRES-tauGFP) or in which M71 translation is decreased by an *IRES*-mediated knockdown (RFP→M71iM71iGFP) (Figure 6.7).

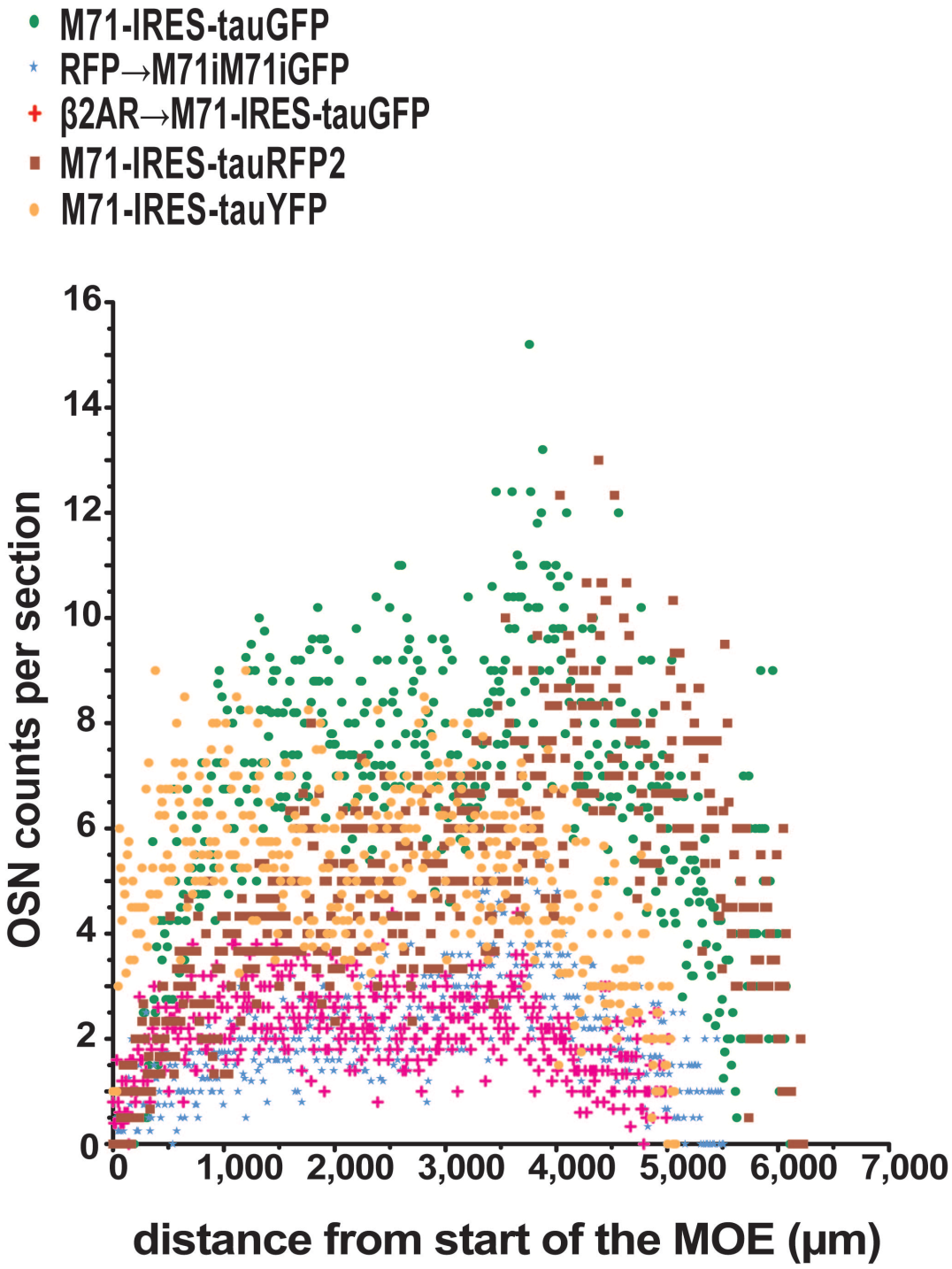

Figure 6.7 Average OSN counts along AP dimensions for strain expressing M71
Average OSN counts per section for strains with mutations in the *M71* gene along the anterior-posterior dimension showing a similar expression pattern even though the OSN numbers vary.

In contrast OR genes show a single peak (*MOR256-17*) or two peaks (*SR1*) along the anterior-posterior dimension (Figure 6.8). These peaks compromise the accuracy of comparing partial cell counts among individual mice, due to the lack of fiduciary points.

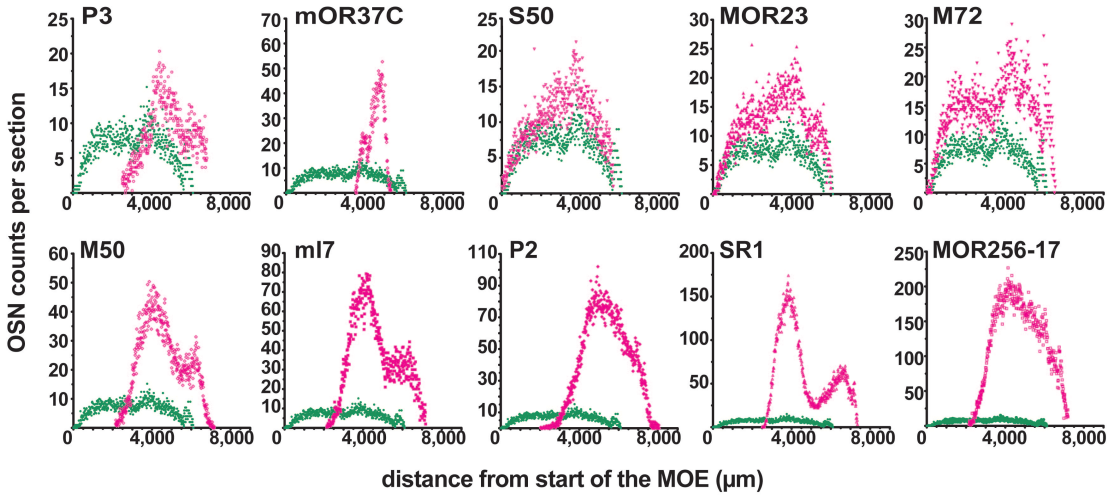

Figure 6.8 OSN counts per section for strains compared to M71
Average OSN counts per section of (tau)GFP-expressing strains (magenta) compared to M71-IRES-tauGFP (green), sorted by average OSN number from P3, low, to MOR256-17, high. The strains display a multitude of spatial expression patterns/zones.

6.1.5 Glomerular volume and cell counts

The same series of coronal sections as for counting OSNs in the MOE was used to study the glomeruli that correspond to a fluorescent protein-tagged OSN population. The area of a glomerulus displaying intrinsic fluorescence can be calculated by confocal imaging in z-stacks, but this procedure for determining glomerular volume is very time-consuming. Therefore the glomerular volume was computed by reconstruction. The sum of the reconstructed volumes of all fluorescently labeled glomeruli in a mouse is the total glomerular volume (TGV).

There is a strong linear correlation between OSN number and TGV among the 56 mice of the core set of 11 gene-targeted strains analyzed at PD21 (Figure 6.9): r^2=0.97 at $p \leq 0.0001$ with an intercept of the Y axis at 168,700 μm^3 and a slope of 81.55. The practical implication of this linear correlation is that TGV, which is relatively easy to compute, can be used to estimate accurately OSN number, which is far more time-consuming to determine.

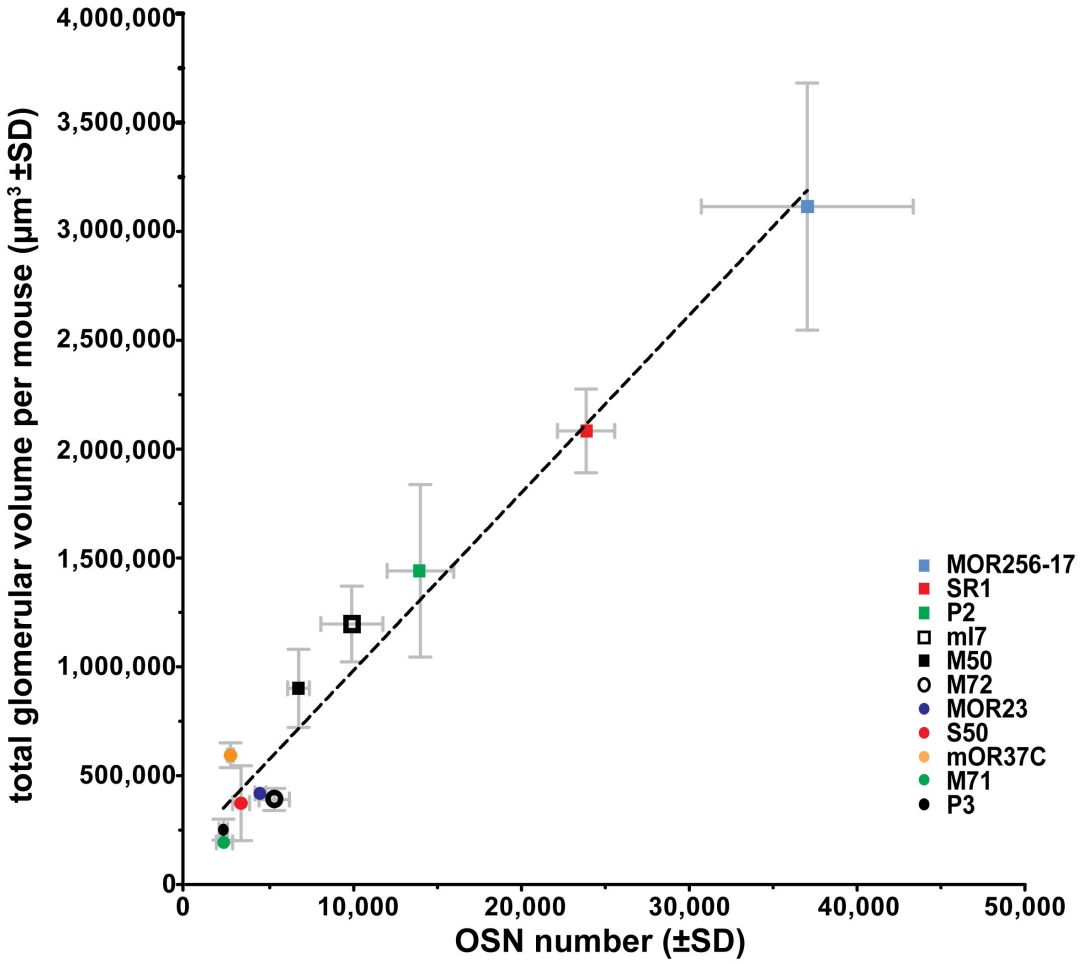

Figure 6.9 Glomerular volume and correlation with OSN numbers for strains coexpressing tauGFP .
TGV per strain at PD21 correlates strongly and linearly to the OSN number (r^2 = 0.97, p-value ≤ 0.0001) in the core set of 11 strains. The curve is best modeled by y = 81.55x + 168,700. A symbol represents a single strain.

A strong linear correlation exists as well when considering the strains with different marker genes for M71 (Figure 6.10): r^2=0.97 at p = 0.0018 with an intercept of the Y axis at -55,627 µm^3 and a slope of 121.1. However it was not possible to get a reliable glomerular volume measurement for the two β2AR→M71 strains.

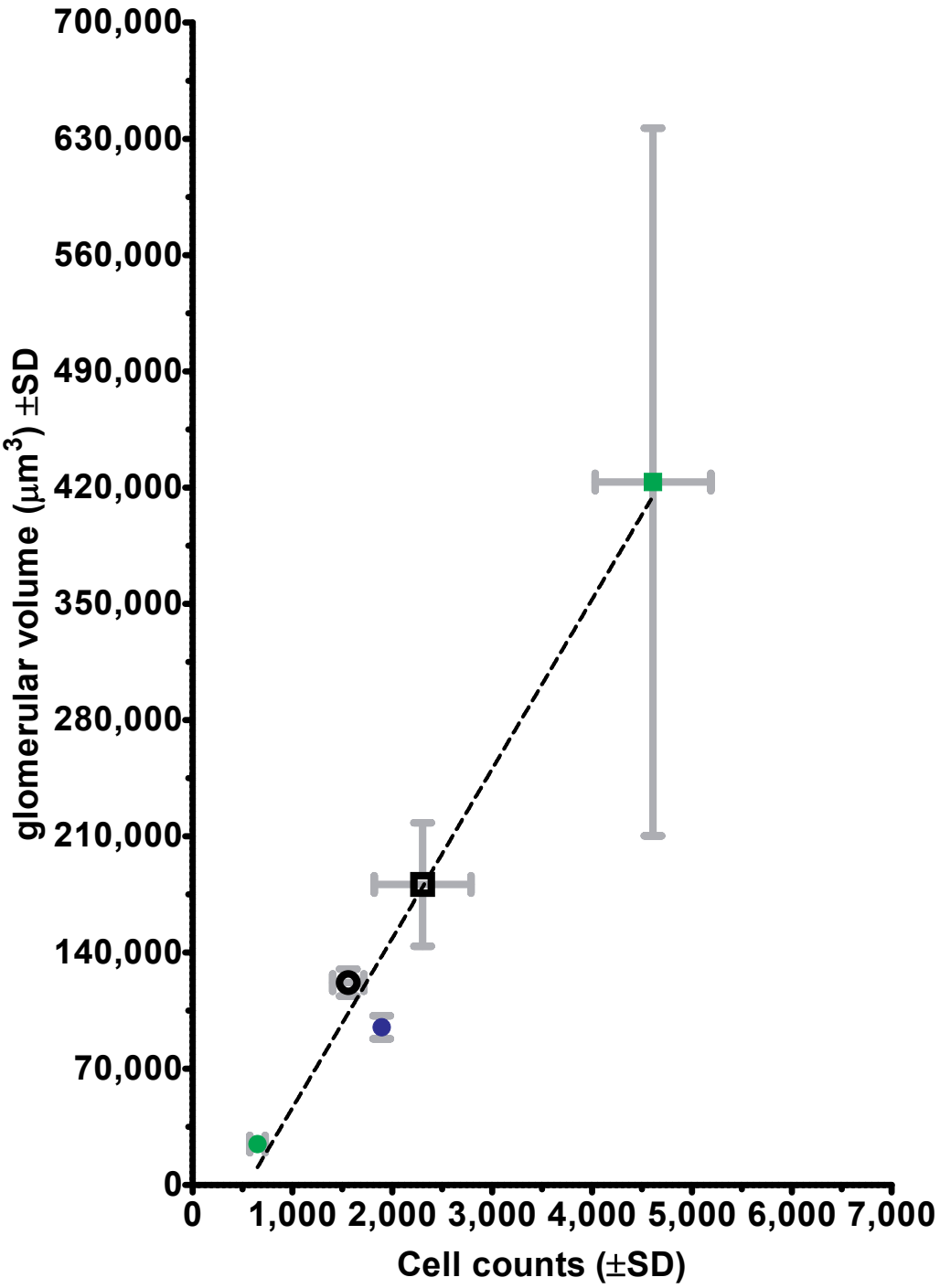

Figure 6.10 Glomerular volume and correlation with OSN numbers for M71-expressing strains
TGV per M71-expressing strain at PD21 correlates strongly and linearly to the OSN number (r^2 = 0.97, p-value = 0.0018) in the core set of 11 strains. The curve is best modeled by y = 121.1x - -55,627. A symbol represents a single strain.

6.1.6 Glomerular density

Finally, fluorescent pixel density of labeled glomeruli was determined in the confocal images used for the reconstruction of glomerular volume. Fluorescent pixel density is an estimate for the density of OSN axon branches and axon terminals within a glomerulus. We find a relatively constant density of ~0.80 across the strains; a density of 0.80 means that 80% of the pixels in the glomerulus display fluorescence above background (**Figure 6.11**).

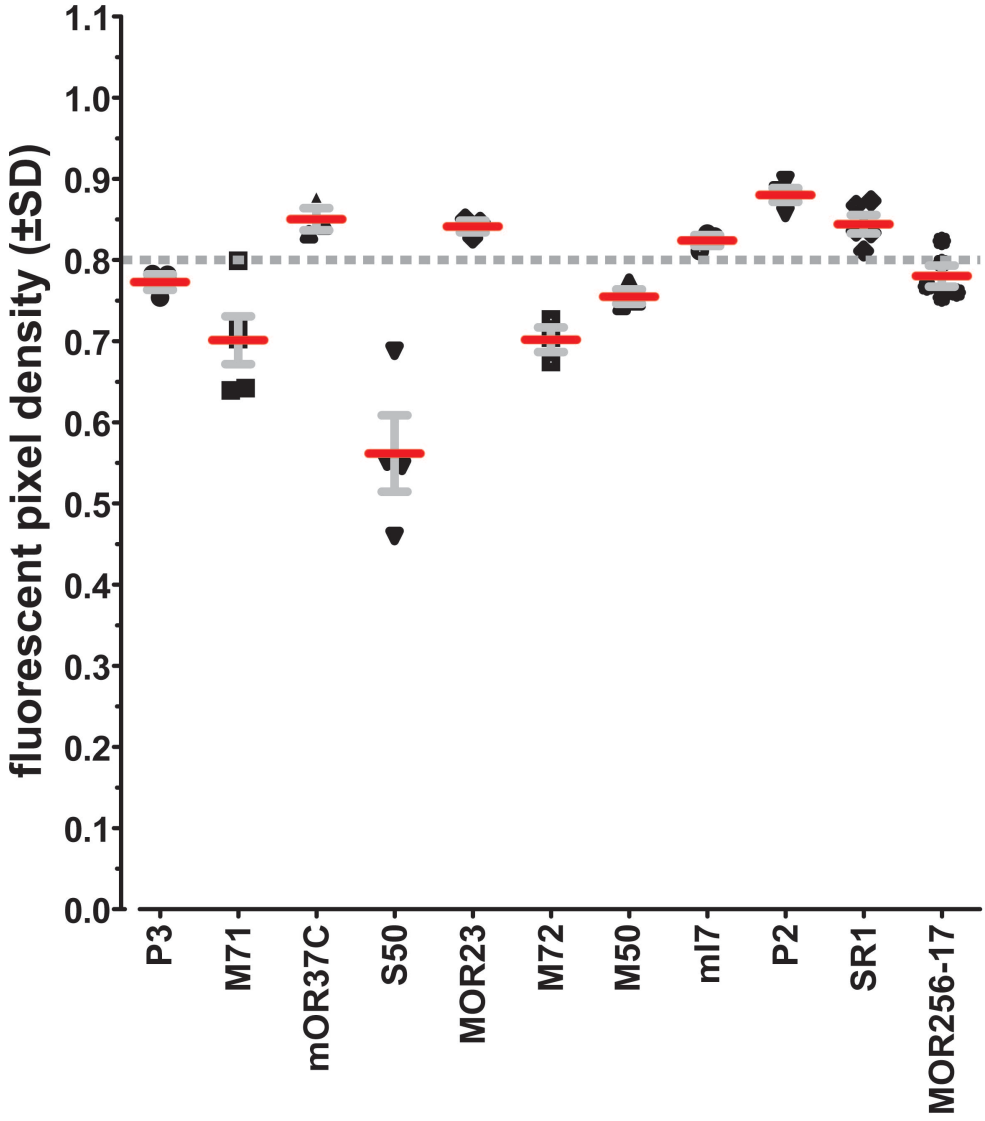

Figure 6.11 Fluorescent pixel density in glomeruli per strains
The ratio of fluorescent pixels to all pixels in the glomerular area is ~0.8 in all strains (ANOVA, F=21.50, $p < 0.0001$), except for S50-IRES-tauGFP. A symbol represents a single mouse. Strains are sorted by average OSN number from P3, low, to MOR256-17, high.

The S50 glomeruli have a value of 0.56. It turns out that the lateral S50 glomeruli have a value of 0.40 (Figure 6.12). However the medial S50 glomeruli have a normal value of 0.79 (Figure 6.13).

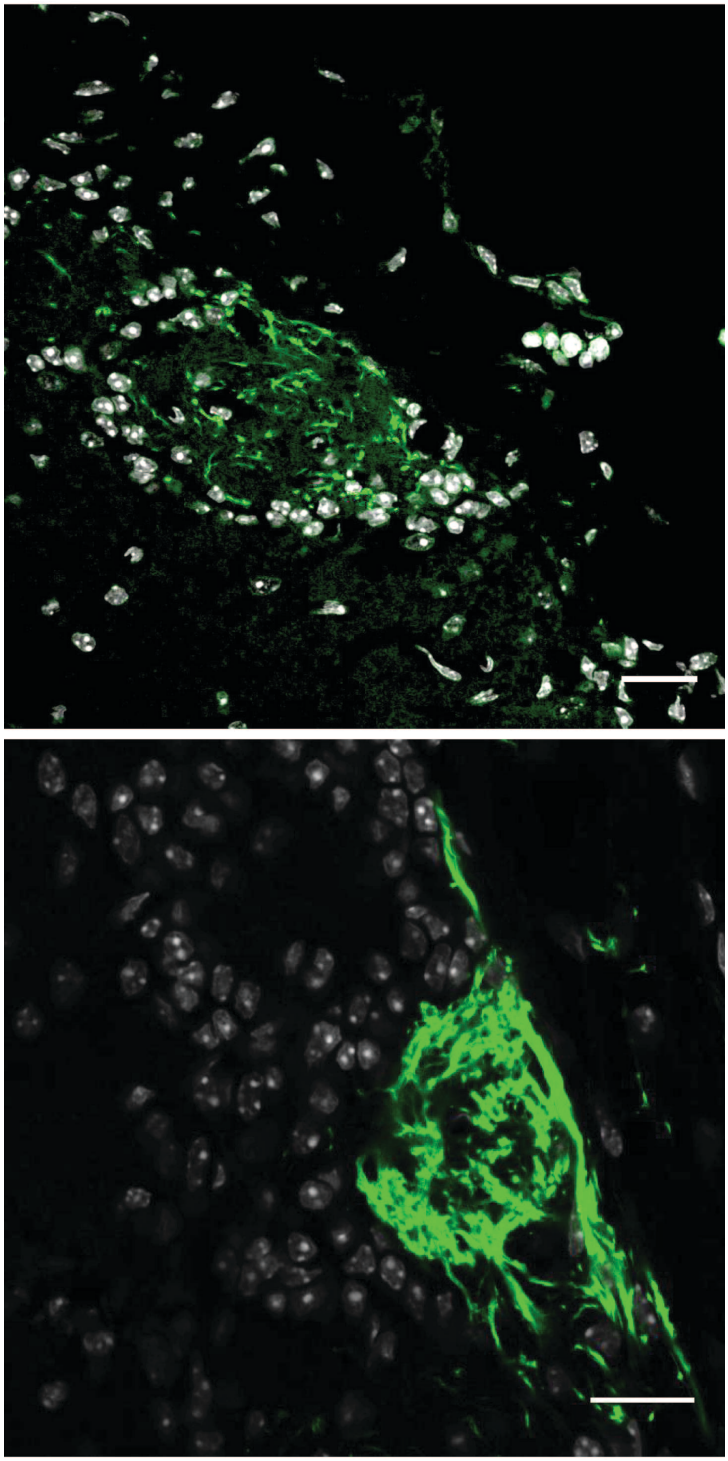

Figure 6.12 Example of a lateral S50-IRES-tauGFP glomerulus
The upper image illustrates the lower fluorescent pixel density in lateral S50 glomeruli, the lower image a medial S50 glomerulus. Green, intrinsic fluorescence; white, DAPI. Scale bar, 20 µm.

Explanations could be that lateral S50 glomeruli are not yet fully mature by PD21, that they have indeed a lower density of OSN axon branches and terminals, or that they are coinnervated by axons from OSNs expressing another OR.

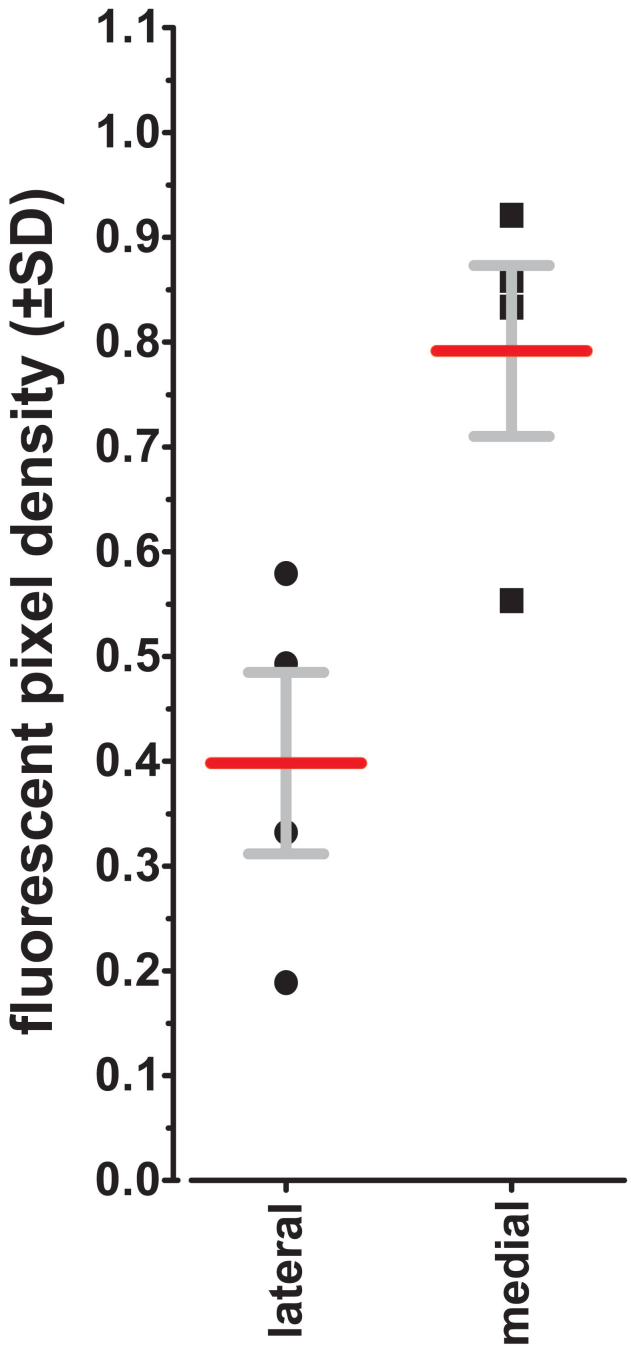

Figure 6.13 Ratios of axonal density for lateral versus medial S50-IRES-tauGFP glomeruli (±SD)
This figure shows that only the lateral glomeruli have a lower fluorescent pixel density. A symbol represents the average of glomeruli in both bulbs of an individual mouse.

6.2 Discussion

The introduction of a genetic strategy based on an IRES and the axonal marker tauβ-galactosidase in 1996 (Mombaerts et al., 1996) and the later addition of fluorescent marker proteins (tauGFP and variants tauYFP and tauRFP2) became essential for multiple studies in the olfactory system: they facilitate imaging of glomeruli by confocal microscopy and two-photon microscopy (Potter et al., 2001), they enable physiological studies (Bozza et al., 2002; Grosmaitre et al., 2006; Grosmaitre et al., 2009; Omura and Mombaerts, 2015), they allow for flow-cytometric cell sorting (Khan et al., 2011) and the manual picking of single cells expressing a given OR gene (Li et al., 2004; Fuss et al., 2010). Therefore this chapter is focused on mice of strains with a gene-targeted mutation in an OR gene that generates a fluorescent protein.

A lingering belief is that each of the ~1,100 OR genes is expressed in a similar number of OSNs. This chapter shows a factor of 17-fold between the smallest OSN population (P3-IRES-tauGFP) and the largest OSN population (MOR256-17-IRES-tauGFP) at PD21, in the 1% sample of the ~1,100 OR genes. Provisionally the median of 5,983 as the OSN number for the average OR gene at PD21 is the prudent estimate. In turn, this number of 5,983 results in an estimate of ~6.6 million OSNs expressing any of the 1,100 OR genes in a mouse at PD21 in this mixed 129 x B6 background. This estimate is lower than the estimate of ~9,400 OSNs expressing on average a given OR gene in the ~10 million mature, OMP-expressing OSNs in 8-week-old C57BL/6J mice (Kawagishi et al., 2014). But the age difference of 3 versus 8 weeks is substantial, and the fraction of OMP-expressing OSNs that does not express an OR gene is not known.

A broad range of NanoString counts for OR mRNAs in wild-type C57BL/6 mice was reported (Khan et al., 2011, 2013): 92% of OR genes have NanoString counts within a 32-fold range. These NanoString counts are not directly translatable into OSN numbers, for several reasons (Khan et al., 2013). The probabilities of OR gene choice appear to differ widely across the OR gene repertoire, and the mechanistic basis of these differences remains to

be clarified. OSN survival and turnover are likely dependent on the odorant composition of the inhaled air which in turn may contribute to the innervation and activity of the OSNs. Therefore Chapter 3.1 contains information about the type of caging, food, and bedding being used. It is conceivable that OSN counts may be different in mice that are housed in other types of caging (such as open cages versus individually ventilated cages) or given other food and bedding.

The empirical strategy generates total cell counts, which appear rarely in the literature presumably due to the amount of effort that is required. A rare example of total cell counts can be found in Royal and Key (1999). Counting cells expressing the OR gene P2 by X-gal histochemistry in P2-IRES-tauLacZ mice but without Abercrombie correction, Royal and Key reported 8,286 labeled cells at PD14.5 and 13,729 at 12 weeks, whereas here 13,975 ± 1,982 labeled cells at PD21 in P2-IRES-tauGFP mice are reported.

It appears that the choice of marker proteins has a significant effect on the cell number for the M71 strain. A downregulation of the expression of M71 in the strain RFP→M71iM71iGFP results not only in 68% less expression of the protein in the axon terminus (Zhang et al., 2012) but also in a 73% decrease in OSN number compared to M71-IRES-tauGFP at PD21. The decrease in OSN number in RFP→M71iM71iGFP is also correlated with TGV. The significant higher OSN numbers for the strain M71-IRES-taulacZ compared to M71-IRES-tauGFP could be further verified by performing RNA in situ hybridization of M71 specific probe on C57BL/6J tissue section. However, generation of M71 specific probe proved to be challenging since *M71* and *M72* genes are highly homologous to each other.

From the complete data sets n virtual data sets were generated, as if cells on every nth section had been counted, in n successive data sets, calculating the exact error that is produced by interleaved sampling. This chapter reports that, as expected, the standard deviation increases rapidly with increasing interval, reaching ±5.63 for every 20th section (average error 5.75%). The information provided about the 11 strains enables now to define *a priori* the acceptable error for studies in which cell counts are compared between experimental conditions.

Counting OSNs expressing a given OR gene or fluorescent protein remains a manual enterprise, no reliable automated methods have been developed thus far. This chapter reports a surrogate for cell counting, computing TGV, which takes far less effort. Reconstruction of these volumes can be done easily by measuring the glomerular area in the middle optical section of physical sections under a confocal microscope, reducing the number of sections analyzed drastically (see Chapter 6.1.2). The very strong linearity of the correlation between OSN number and TGV, over a range of 17-fold, implies that estimates of OSN numbers can be read out from the provided dataset. These findings are consistent with the linear correlation that has been described between partial cell counts in the MOE of M71-IRES-taulacZ mice and the average largest cross-sectional area of an M71 glomerulus (Jones et al., 2008).

OSN number estimates derived from TGV may be sufficiently accurate depending on the goals of the study and the number of mice that need to be analyzed. The linearity of this correlation is not entirely surprising but also not obvious. One could have expected that at low and high OSN numbers the curve would flatten out - in particular at lower OSN numbers, as conceivably a fixed minimum volume of a glomerulus could be occupied by non-axonal structures.

Another limitation of our studies is that they are based on mice in the conventional mixed 129 x B6 background, which is currently the best practice. Backcrossing of the targeted mutations to C57BL/6 may help in reducing some of the variability. But as most of OR gene regulation takes place in *cis*, at the promoter level, the regions around the targeted OR locus will always be of 129 origin - in fact, they will continue to be the nucleotide sequences that were present in the genome of the original embryonic stem cell in which the targeted mutation was introduced. New genetic manipulation technologies like CRISPR/Cas9 might generate FP-tagged mutations in a C57BL/6 background. It will then also be possible to compare cell numbers between counting fluorescent cells in FP-tagged strains with counting cells expressing the corresponding unmanipulated OR gene in wild-type C57BL/6 mice by RNA in situ hybridization.

In conclusion, the practical outcome of this empirical study is that TGV is a highly reliable indicator of OSN number.

7 Conditional knockout of Neuropilin-1 in M71-expressing OSNs

7.1 Results

Neuropilin-1 (Nrp1) is expressed in several different types neurons (Gu et al., 2003). As described in Chapter 2.8, Nrp1 is one of the major factors in axonal wiring in the mouse olfactory system. A conditional knockout of Nrp1 (Imai et al., 2009) moves the glomerular position of OSNs, expressing a transgene rat I7 from the MOR23 promoter, to a more anterior position in the bulb. In heterozygous conditional Nrp1 knockout mice, an intermediate position was observed. However Imai and colleagues (2009) used a transgene approach, by random integration of a rat OR (rI7) under the MOR23 promoter somewhere in the genome.

This chapter describes the phenotype of gene-targeted conditional knockout of Nrp1 in M71 OSNs. I found that M71-expressing OSNs that are devoid of Nrp1 form ectopic glomeruli at the anterior tip of the OB but also maintain glomerular coalescence in their typical position in the bulb, comparable to M71-IRES-tauGFP.

7.1.1 Breeding strategy

To study the effects of a conditional knockout of Nrp1 in OSNs, a genetic approach was chosen. The idea is to study axons expressing a certain OR and deficient for Nrp1 and compare them, in the same mouse, to axons expressing the same OR but not deficient for Nrp1. The unusual feature of monoallelic and monogenic expression of an OR gene enabled this strategy. To generate the crosses described in this chapter, gene-targeted strains expressing M71 were chosen because these are some of the most described and characterized strains available. Two Nrp1 conditional knockout alleles were used, resulting in two different strains which both were the result of a triple cross (Figure 7.1). The two conditional Nrp1 alleles are: Nrp1-flox/J was

generated in our lab (unpublished) and npn1-5247 (JR#5247), the same allele as used by Imai and colleagues (2009).

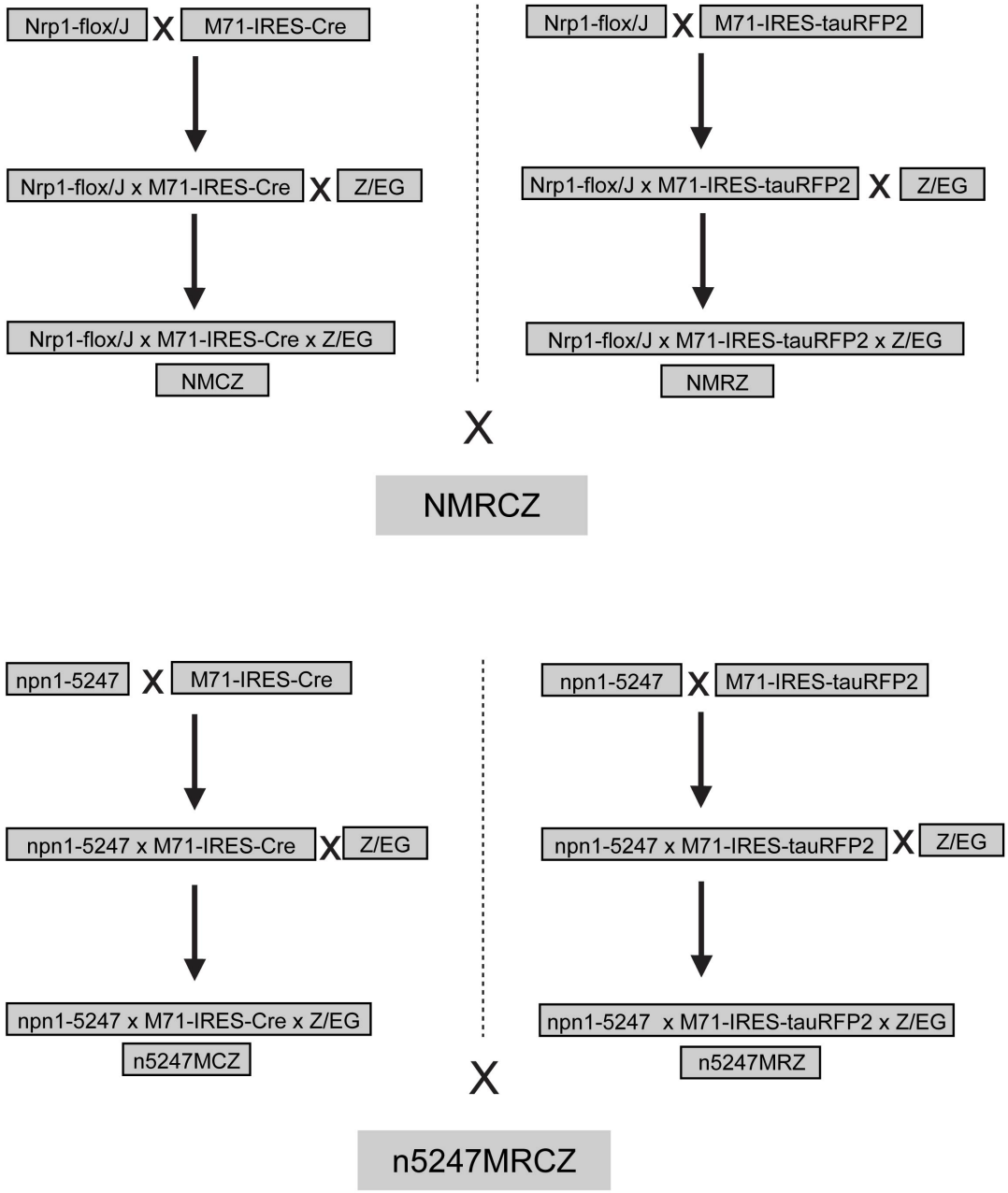

Figure 7.1 Breeding scheme for conditional Nrp1 knock out strain
This figure illustrates the crosses set up for the Nrp1 knockout strain. After crossing each strain, the offspring was intercrossed until the cross was homozygous for all genes of interest. Then the next strain was crossed to the previous cross and the process was repeated. The end result was four strains (NMCZ, n5247MCZ) with a conditional knockout of Nrp1 in M71-expressing neurons (with one of two different conditional alleles for Nrp1) and two strains that express normal levels of Nrp1 (NMRZ, n5247MRZ) where M71 coexpresses RFP2. Mating these crosses results in the desired compound heterozygous strains (NMRCZ, n5247MRCZ) where M71-expressing OSNs expressing Nrp1 coexist with M71-expressing OSNs not expressing Nrp1.

Each of the two crosses contains Nrp1 mutated with loxP sites for conditional knockout and the Z/EG transgene as a reporter for the expression of the Cre recombinase. The difference is the M71-expressing strain crossed to Nrp1-flox and Z/EG:

- crossing to M71-IRES-tauRFP2 should have no effect and should have the same phenotype as M71-IRES-tauRFP2 on its own.
- crossing to M71-IRES-Cre should knockout Nrp1 the loxP-flanked site in Z/EG resulting in conditional Nrp1 knockout phenotype and the expression of GFP.

Crossing the two homozygous triple crosses results in the desired compound heterozygous quadruple mutant strain (Figure 7.2).

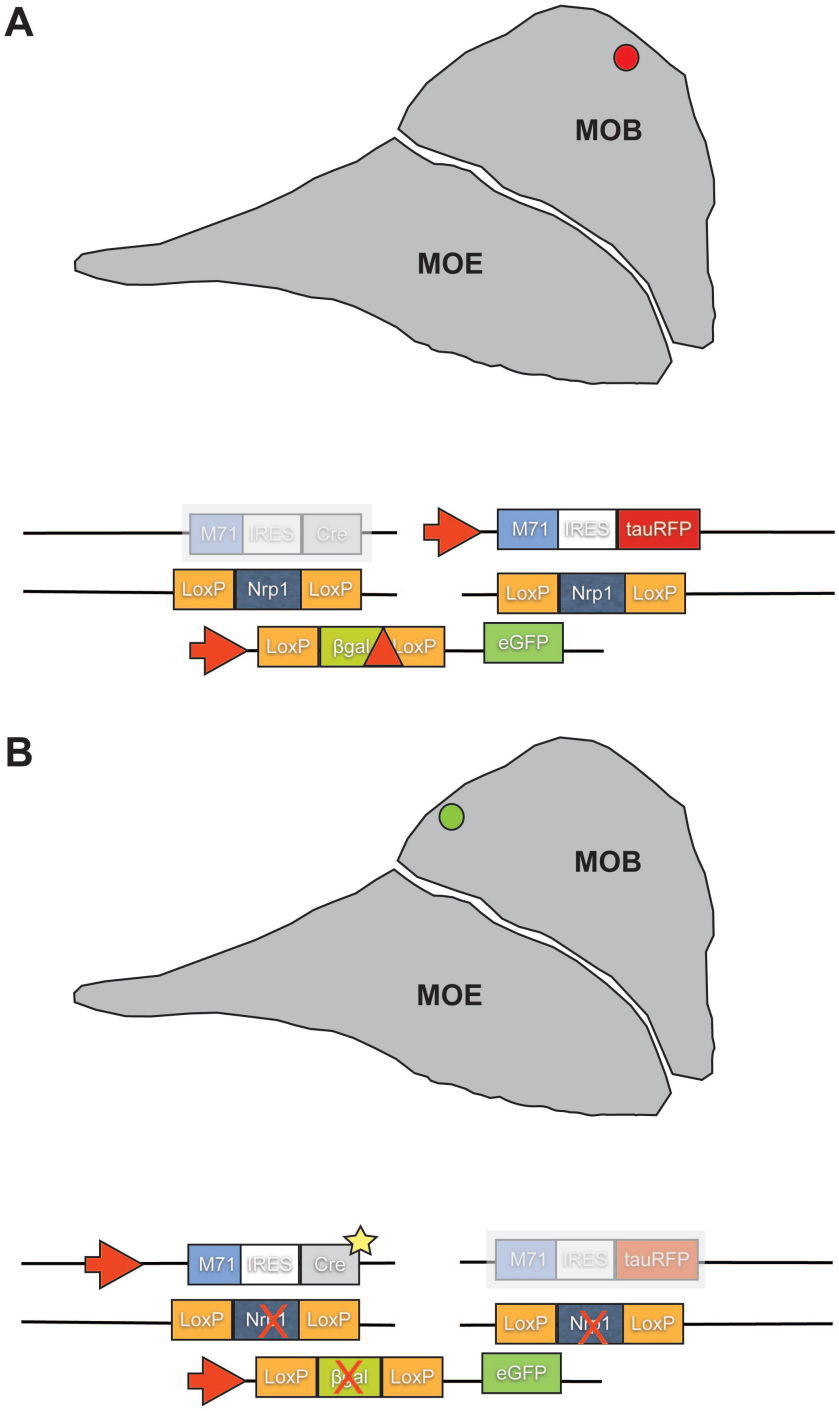

Figure 7.2 Conditional knockout in gene-targeted quadruple mutants
(A) All OSNs expressing the allele M71-IRES-tauRFP2 have normal levels of endogenous Nrp1 expression and coalesce into glomeruli at a position that is typical for M71 glomeruli (red dot). (B) In OSNs expressing the allele M71-IRES-Cre the Cre recombinase is expressed (yellow star) excising Nrp1 and the loxP-flanked β-galactosidase including the stop codon from the Z/EG transgene, enabling GFP expression. These axons coalesce into an ectopic, anterior position (green dot).

7.1.2 Nrp1 knockout

Another cross was created to examine the global effect of Nrp1 on axonal wiring in the mouse olfactory system. The Nrp1-flox strains were crossed to the Z/EG reporter transgene and the OMP-Cre strain. OMP, the olfactory marker protein, is expressed in all mature OSNs. In the OMP-Cre strain, the OMP coding sequence is replaced with the Cre recombinase. The knockout of Nrp1 in all mature OSNs has no discernible overall effect on axonal wiring. The glomeruli are formed apparently normally, and the glomerular layer lacks Nrp1 staining for Nrp1 antibody (Figure 7.3).

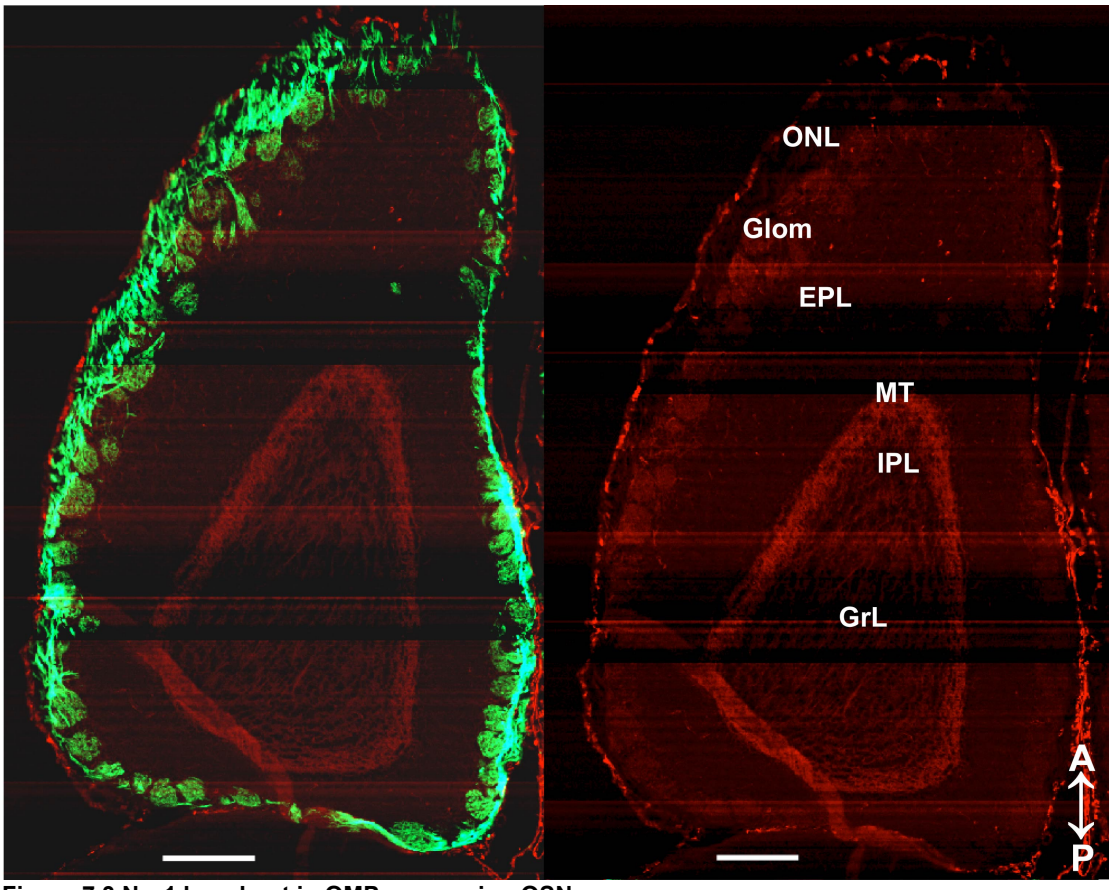

Figure 7.3 Nrp1 knockout in OMP-expressing OSNs
Horizontal section of PD21 olfactory bulb taken with the Aperio Scanscope shows intrinsic fluorescence of OMP-Cre x Z/EG expressing neurons (green) and antibody staining for Nrp1 (red). The distribution, size and form are similar to glomeruli expressing Nrp1. The right image illustrates the different layers of the olfactory bulb: Olfactory nerve layer (PNL), glomerular layer (Glom), external plexiform layer (EPL), mitral cell layer (MT), internal plexiform layer (IPL) and granule layer (GrL). Only background Nrp1 staining is detected in the glomerular layer of knockout strain (Scale bar: 250 µm).

Although the axonal wiring seems to be not affected by a knockout of Nrp1 in OMP-expressing neurons, antibody staining shows a lack of staining for Nrp1 in the glomerular layer of the OB compared to strains with normal expression of Nrp1 (Figure 7.4). The antibody staining for Nrp1 in NOCZ mice confirms the effectiveness of the conditional Nrp1 knock out using Nrp1-flox/J.

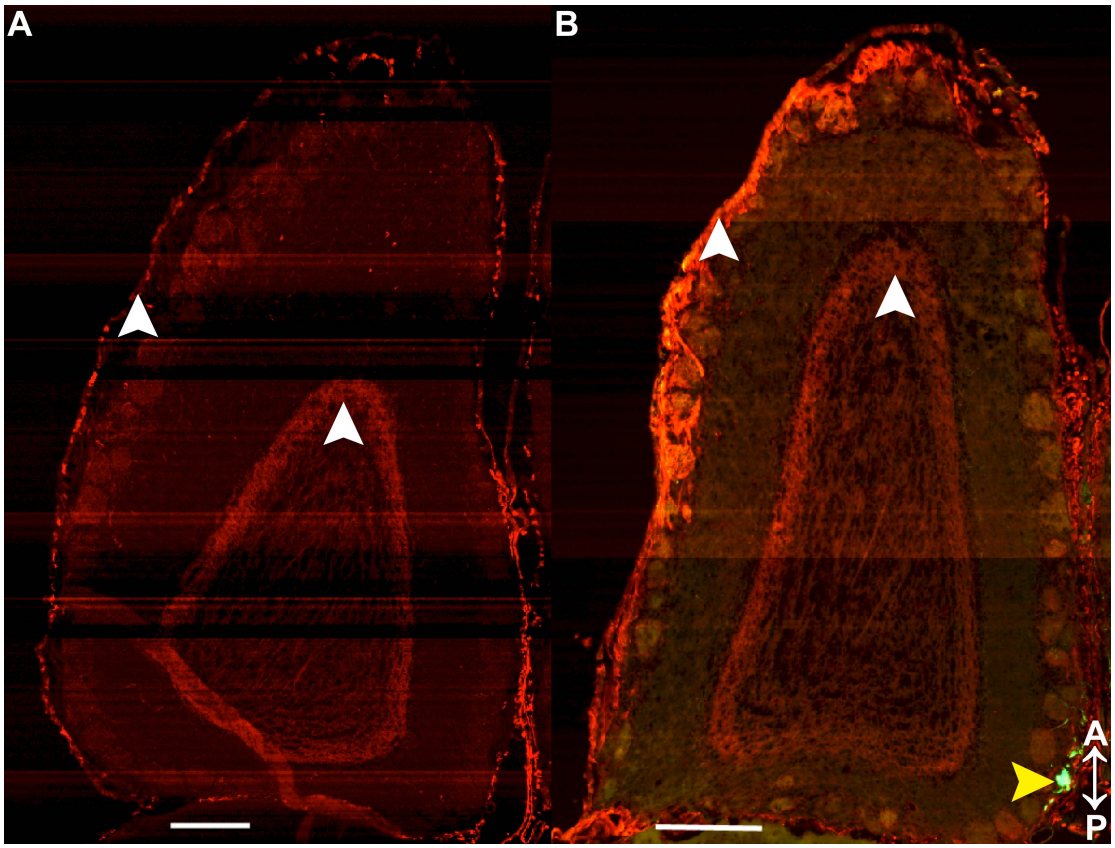

Figure 7.4 Comparison of Nrp1 expression
Horizontal section of PD21 olfactory bulb taken with the Aperio Scanscope compares intensity of Nrp1 antibody staining (red) in mice with an knockout of Nrp1 in OMP-expressing OSNs (A) compared to staining intensity in mice with normal Nrp1-expression (B, M71-IRES-Cre x R26-STOPtauGFP). White arrowheads indicate that Nrp1 is still expressed in the knockout in layers other than glomerular layer. Green signal in B references the medial glomerular position of M71-IRES-Cre expressing OSNs (yellow arrowhead). Scale bars: 250 µm.

7.1.3 Ectopic glomerulus

The phenotype of the Nrp1 knockout in M71-expressing OSNs is a robust and consistent observation in all analyses. A new glomerulus is formed on the medial side in the dorsal anterior bulb. However there are still labeled axons converging onto glomeruli in the posterior area of the OB. In general a

singular glomerulus is formed in a dorsal, central area between the medial and lateral position of the normal M71 glomeruli (Figure 7.5). Often an additional glomerulus is formed in the dorsal medial area close to the area normally occupied by M71-expressing axons.

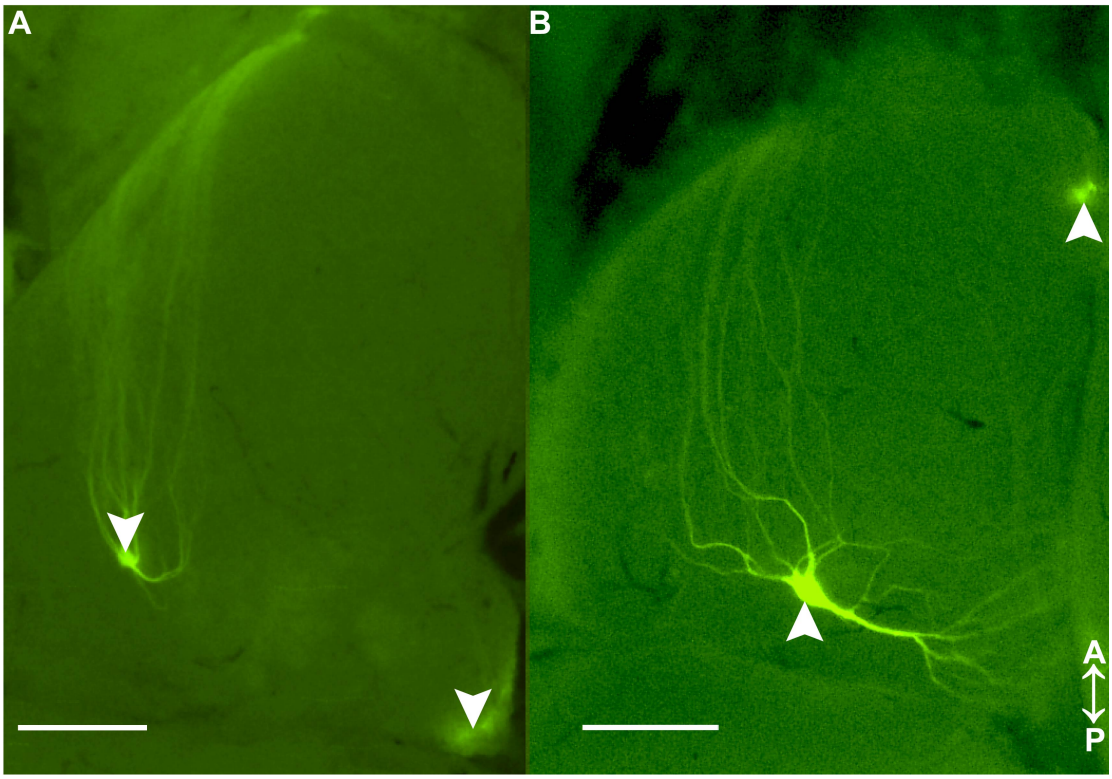

Figure 7.5 Comparison of M71 strains for Nrp1 knockout
(A) Dorsal view of a whole mount of a M71-IRES-Cre x R26-tauGFP PD21 bulb, imaged with NIKON, showing the intrinsic fluorescence. White arrowheads show normal glomerular positions for M71-expressing OSNs. (B) Dorsal view of a n5247MCZ PD21 bulb showing intrinsic fluorescence. White arrowheads show ectopic glomeruli for Nrp1 negative M71 axons. Scale bars: 500 µm.

7.1.4 Mixed glomeruli in conserved glomerular position

The phenotypes of the ectopic anterior glomeruli in dorsal medial position as well as of the shifted lateral glomeruli are conserved in all knockout strains. For more details on the axon composition of the glomeruli of the NMRCZ compound heterozygous animals, 12 µm coronal sections of the bulb at PD21 and PD70 were taken.

The posterior glomeruli in conserved medial M71 position in the NMRCZ strain are heterozygous for the M71 alleles. The shifted glomeruli, which are along the anterior-posterior axis at the same height as the normal M71 glomerular position, are shifted more dorsally and often appear to be

fragmented into several small glomeruli (Figure 7.6). If a glomerulus is formed at the normal M71 position, it is heterozygous for Nrp1-deficient axons and M71 axons with normal Nrp1 expression.

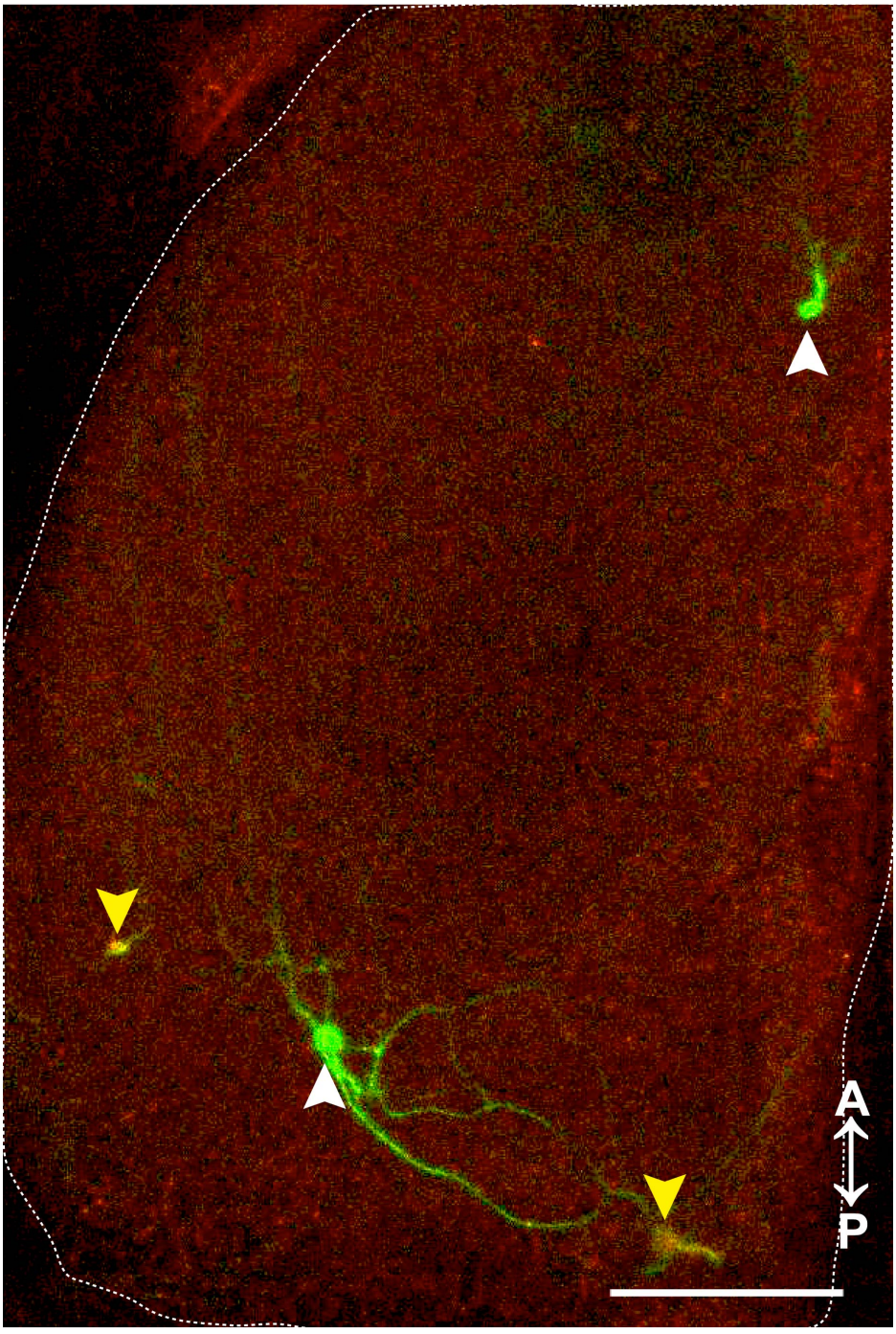

Figure 7.6 Axonal wiring in a whole mount NMRCZ mouse
Confocal image of a whole mount of a PD14 NMRCZ mouse. White arrowheads indicate ectopic glomeruli only formed by M71 axons deficient of Nrp1 (intrinsic fluorescence, green). Yellow arrowheads indicate heterozygous glomeruli at the normal M71 glomerular position, consisting of Nrp1-deficient axons and axons with normal Nrp1 expression (intrinsic fluorescence, green; Nrp1, red). White dashed line shows the outline of the olfactory bulb. Scale bar: 500 µm.

In the heterozygous glomeruli both axons intermingle, only in one single NMRCZ mouse a compartmentalization was observed at PD70 (**Figure 7.7**). This glomerulus shows the different Nrp1 expression levels for the M71 alleles.

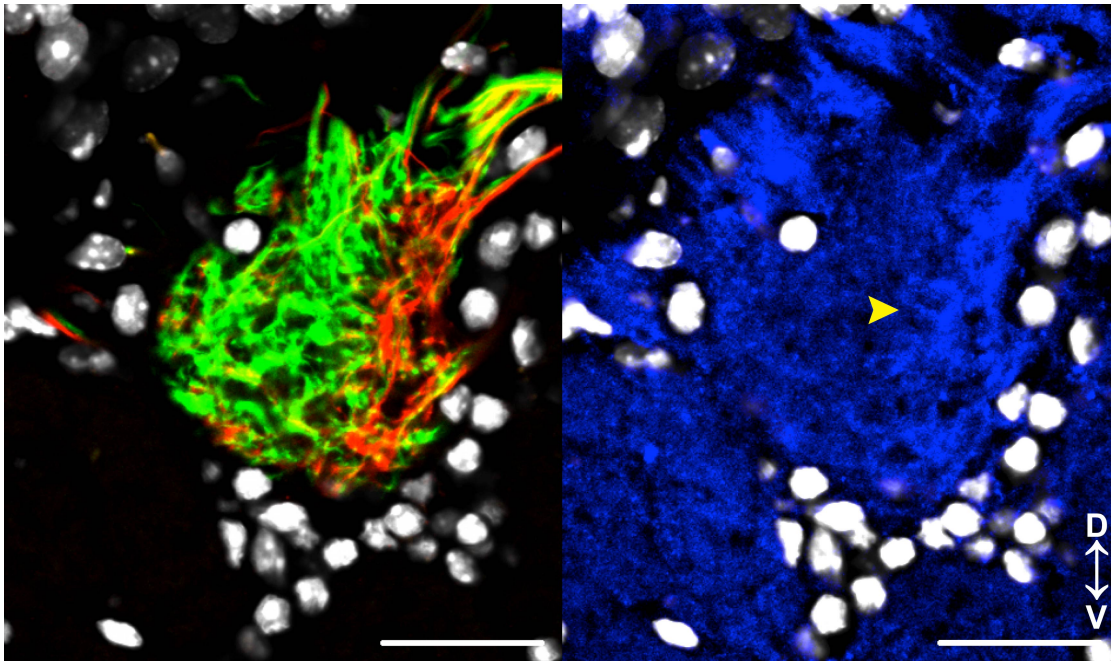

Figure 7.7 Heterozygous NMRCZ medial glomerulus
The left image shows 12 µm coronal section of a NMRCZ mouse at PD70 and axons of both M71 alleles forming a heterozygous glomerulus with Nrp1 deficient axons (intrinsic fluorescence, green) and axons with normal Nrp1 expression (antibody staining for tauRFP2, red). The right image shows the Nrp1 antibody staining in the same glomerulus (blue). A stronger staining for Nrp1 is clearly visible (yellow arrow) at positions occupied by the red axons in the left figure with normal Nrp1 expression. Scale bar: 25 µm.

For all mice analyzed, the ectopic anterior glomeruli consist of GFP stained M71 OSNs, which show only background levels of Nrp1 antibody staining (**Figure 7.8**).

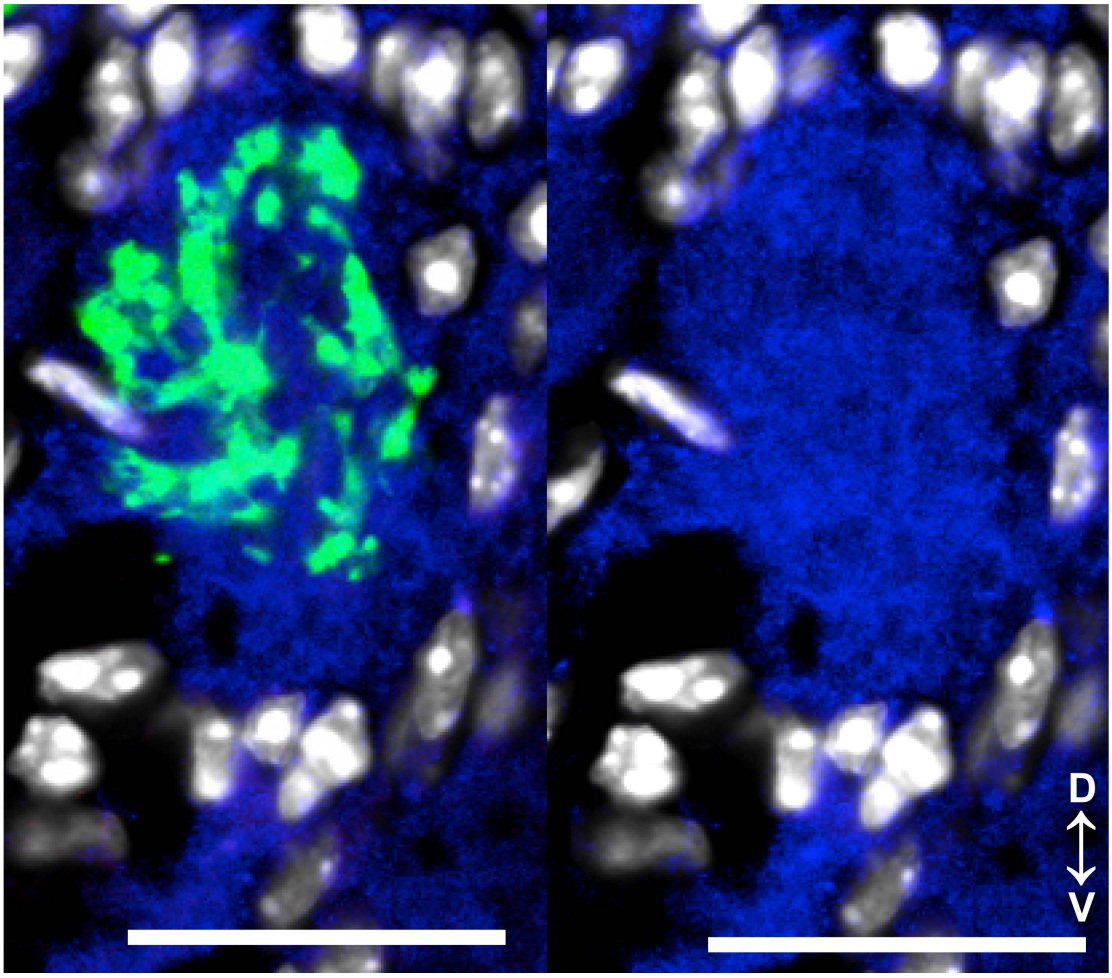

Figure 7.8 M71 OSN ectopic glomerulus
Coronal section of a PD70 ectopic glomerulus of the NMRCZ strain (12 µm thickness). The green M71-IRES-Cre expressing axons form small homogeneous ectopic glomeruli (intrinsic fluorescence, left) while the Nrp1 antibody staining (blue) in that glomerulus is absent from the green axons (right). Scale bar: 25 µm

7.1.5 Nrp1 knock out phenotype at various ages

The phenotype of ectopic anterior glomerulus starts forming directly after birth in n5247MCZ mice. Axons project to the anterior ectopic position as well as to the posterior, normal M71 glomerular position (Figure 7.9).

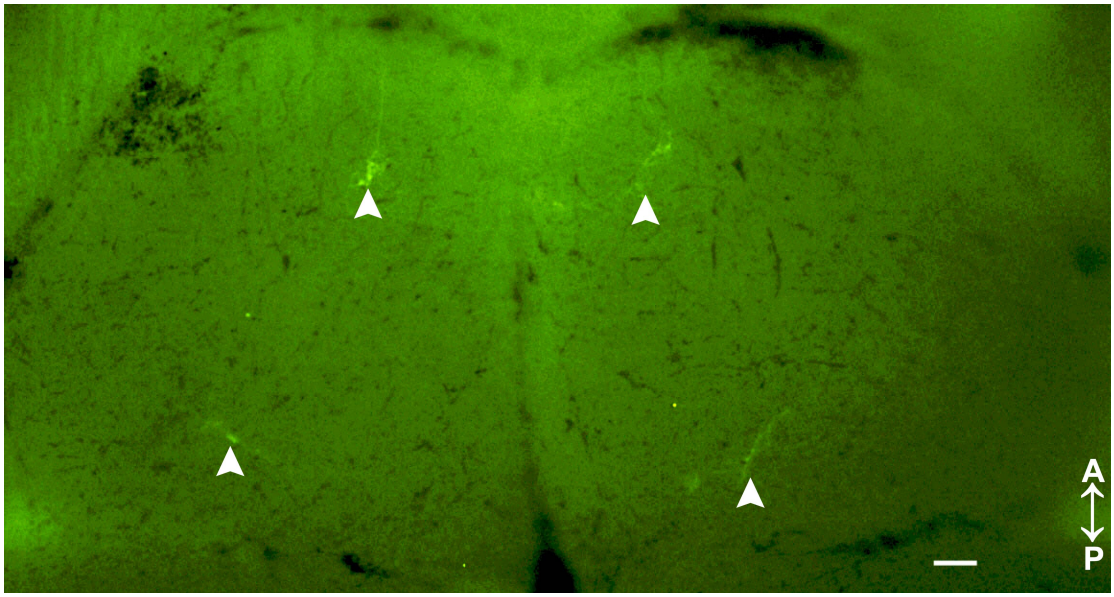

Figure 7.9 Axonal wiring of n5247MCZ mice in neonatal mice
Dorsal view of a whole mount of a of PD0 n5247MCZ mouse. The white arrowheads show nascent glomeruli forming at the ectopic anterior position and the posterior, normal M71 position. Glomeruli are not fully formed yet but already project to the position typical for this phenotype. Scale bar: 100 µm.

Likewise the Nrp1 knockout phenotype remains well conserved at PD140 (Figure 7.10). The ectopic glomeruli are still present and a posterior medial glomerulus is maintained at the normal M71 medial position. The lateral posterior glomerulus is shifted more dorsally and dispersed into several small glomeruli compared to M71.

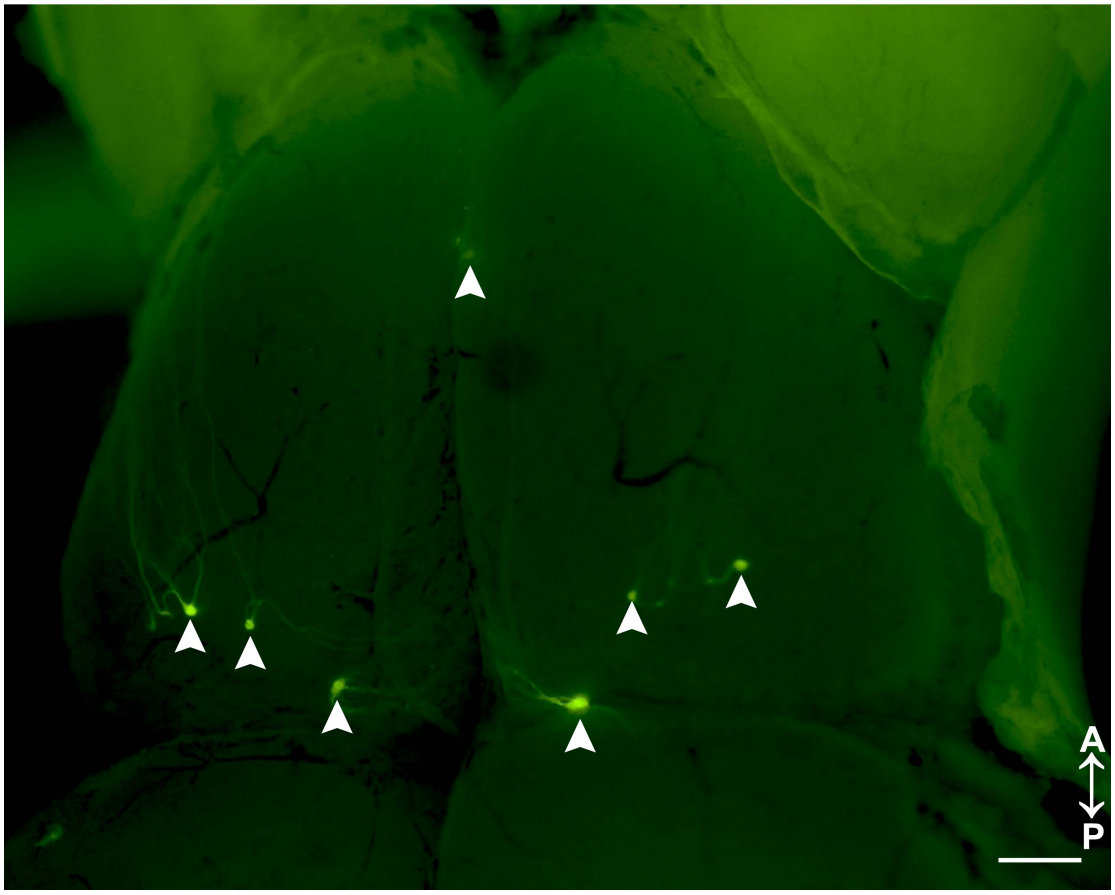

Figure 7.10 Axonal wiring in old NMRCZ mice
Dorsal view of a whole mount the olfactory bulb of a NMRCZ PD140 mouse taken with NIKON stereoscope. White arrowheads indicate glomeruli formed by M71-expressing axons deficient for Nrp1 (intrinsic fluorescence, green). Axons of M71-expressing OSNs with normal Nrp1 expression are not shown in this image. Scale bar: 500 µm

To evaluate for the stability of the phenotype through life, several age groups were chosen for analysis. The compound heterozygous knockout strain NMRCZ was analyzed at young age of PD7, PD14 (the same age as the mice reported by Imai *et al.* (2009)) and PD21, in young adults at PD35 and adults at PD70, and finally in aged mice at PD140. In each age group the reported phenotype is present and well conserved (Table 7.1).

For the homozygous knockout strain n5247MCZ the age PD21 as the lab standard age and PD0 were analyzed. These also show the phenotype (Table 7.1).

Table 7.1 Table of age and number of mice investigated for Nrp1 knock out strain

Strains	PD0	PD7	PD14	PD21	PD35	PD70	PD140
NMRCZ		Ectopic anterior glomeruli Mixed medial posterior glomeruli Ectopic pos. med. Glomeruli	Ectopic anterior glomeruli Mixed medial posterior glomeruli Ectopic pos. med. Glomeruli	Ectopic anterior glomeruli Mixed medial posterior glomeruli Ectopic pos. med. Glomeruli	Ectopic anterior glomeruli Mixed medial posterior glomeruli Ectopic pos. med. Glomeruli	Ectopic anterior glomeruli Mixed medial posterior glomeruli Ectopic pos. med. Glomeruli	Ectopic anterior glomeruli Mixed medial posterior glomeruli Ectopic pos. med. Glomeruli
Numbers		7	7	6	5	5	2
n5247MCZ	Axons branch at ectopic and posterior position Glomeruli are not formed			Ectopic anterior glomeruli (Medial posterior glomeruli) Ectopic pos. med. Glomeruli			
Numbers	3			7			

7.1.6 Control experiments

To test if the knockout of Nrp1 has an effect on OSN numbers, mice from the NMRCZ strain (n=4) and n5247MCZ (n=3) strain where perfused at PD21 and cells were counted as described in Chapter 4.9. There was no significant difference between NMRCZ (t-test, p=0.053), n5247MCZ (t-test, p= 0.76) and M71-IRES-tauGFP mice (**Figure 7.11**). In the case of NMRCZ cells expressing either allele were evaluated separately and there was no significant difference between the OSN numbers between the two alleles (t-test, p=0.85); each contributing half to the total OSN number of the NMRCZ strain, in keeping with the monoallelic property of an OSN.

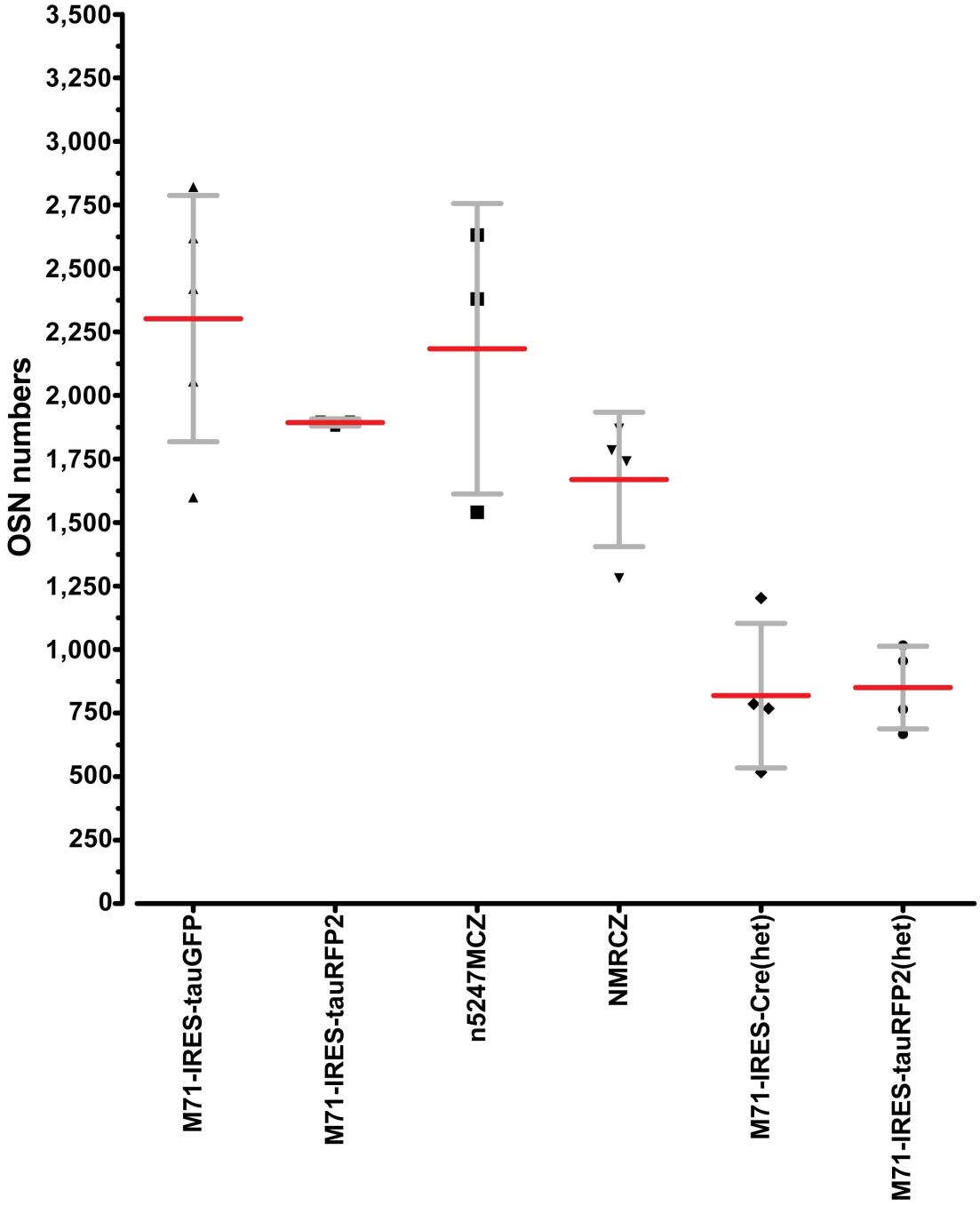

Figure 7.11 OSN numbers for Nrp1 knockout strains
OSN numbers of PD21 Nrp1 knockout strains (±SD). Each symbol represents a single mouse. M71-IRES-tauGFP and M71-IRES-tauRFP2 are the same data as reported in Chapter 6 for comparison. M71-IRES-Cre(het) and M71-IRES-tauRFP2(het) are the OSNs for the individual M71 alleles of NMRCZ, added together totally in the NMRCZ results.

7.2 Discussion

Axonal wiring in the mouse olfactory system remains poorly understood a quarter century after the discovery of OR genes. One of the most impressive feats of the olfactory system is its ability to establish and maintain conserved

glomeruli homogeneous for axons expressing a specific OR in the olfactory bulb, given there are around 1,100 different OSN types. Gradients of cell adhesion molecules are one of several possible explanations for the mechanism of the precise axonal wiring, with Nrp1 being one of the most prominent members. A popular model attributes the glomerular position along the anterior-posterior axis of the olfactory bulb to an increasing gradient of Nrp1 along this axis (Imai et al., 2009). Nakashima et al., 2013 link the expression of Nrp1 to the basal activity of the OR expressed in the OSNs. The higher basal activity in developing OSNs is translated with a signal transduction cascade to a stronger expression of Nrp1 and thus a more posterior position in the OB. However Schwarting et al. (Pasterkamp et al., 1998) reported antibody stainings in rat that show that Nrp1 is not expressed in a simple gradient along the anterior-posterior axis and that the repulsive ligand for Nrp1, Semaphorin 3A (Sema3A), is expressed in a lateral and medial area of the bulb (Schwarting et al., 2004).

The results reported in this chapter also show that the axonal wiring along the anterior-posterior axis is not simply dependent on a Nrp1 gradient. A conditional knockout of Nrp1 in M71-expressing OSNs results in a stable phenotype, where the normal two dorsal posterior M71 glomeruli per bulb (one medial, one lateral) in most cases still exist but other small ectopic glomeruli are formed in addition. Most prominent and stable is the ectopic glomerulus at the anterior tip of the OB. As this ectopic glomerulus this also formed in mice with a homozygous conditional knockout of Nrp1 in M71-expressing OSNs, it is unlikely that the axons with normal Nrp1 expression in the compound heterozygous mice somehow rescue the Nrp1-deficient axons. I speculate that the axons with normal Nrp1 expression help to stabilize the glomeruli at the normal M71 position, because they appear more often in the NMRCZ strain than in n5247MCZ mice. Using a gene-targeting approach these strains are closer to the wild-type situation than transgenic mice. It appears that other factors are also involved in determining the position of a glomerulus. Nrp1 is definitely an important factor in axonal wiring in the OB but it is not the only one, at least for M71.

Another interesting observation is that the phenotype is remarkably similar to a conditional knockout of the adenylyl cyclase 3 (AC3) in OSNs. Both studies, one investigating the axons in M72 mice (Col et al., 2007) and the other one those in M71 mice (Zou et al., 2007), show a similar phenotype of an ectopic glomeruli at the anterior tip of the bulb. Both strains are closely related and axons of their OSNs terminate in the same area of the bulb. In most instances the glomeruli of M71 and M72 are adjacent. As M72 has a higher number of OSNs than M71 (Chapter 6) an additional ectopic glomerulus on the lateral side may be able to form stable in the lateral half (Col et al., 2007).

The similarity of the AC3 knockout phenotype and the phenotype of Nrp1 knockout strongly suggests that the signal transduction cascade mediated by cyclic AMP (cAMP) is an important factor in the expression of Nrp1. Normally Nrp1 does not use cAMP as a second messenger but perhaps another unknown factor is regulated by cAMP. It is possible that this factor is responsible for the complex task to sort 1,100 different kinds of axons into glomeruli at conserved positions, and that this factor is somehow regulated by Nrp1.

In summary the two Nrp1 knockout strains reported in this chapter have an interesting phenotype similar to the effect that an AC3 knockout has on M71-expressing OSNs but unlike the conditional knockout in a transgene mouse reported by Imai and colleagues (2006).

8 Final Discussion

In this thesis I have studied several aspects of the complex mechanisms of axonal wiring in the mouse olfactory system. I set out originally to determine the effect of caGs in M71-expressing OSNs by generating novel strains of gene-targeted strains. My guess is that it would not have shifted the position of M71 glomeruli further posteriorly. However due to persistent difficulties of generating an appropriate targeting vector and because of time constraints I did not continue this project and focussed on the two other aspects reported here.

The second project was a comprehensive empirical study of the distribution and number of OSNs in the olfactory epithelium. Such a study has not been conducted before, and became only possible because of the fortune of a large collection of gene-targeted strains coexpressing tauGFP with individual ORs in the lab. This resource enabled a broad insight into the fundamental constituents (OSNs and glomeruli) of axonal wiring, showing the strong correlation between the two. It also quantified and showed possible pitfalls of sampling of OSN numbers, with determining sampling errors for the strains, showing their different expression patterns and determining the stability of OSN numbers in each strain. My results indicate that OSNs expressing MOR23 should be used for further, quantitative studies because of the stability of this population.

In the third project the role of Nrp1 in axonal wiring was investigated. Recent studies support a direct effect of a Nrp1 gradient on glomerular position along the anterior-posterior axis of the olfactory bulb, but these studies could not explain satisfactorily the monumental task of sorting ~1,100 populations of OSNs so neatly and precisely into glomeruli. The results of a conditional knockout of Nrp1 in M71-expressing OSNs reveal that a simple gradient of Nrp1 cannot be the only factor that determines the anterior-posterior position of a glomerulus. Surveying the research done on axonal wiring in the mouse olfactory system I favour the model of a zip code. Several

molecules contain part of the information to which region within in the glomerular layer the axon has to grow. With the knockout of one molecule or of one signalling cascade, in this case Nrp1 or AC3, axons projected additionally to ectopic positions due to the distorted code.

In conclusion I was able to contribute basic and quantitative empirical data for further research to build upon. I also provided some interesting insights into one of the many aspects of the complex and fascinating mechanism of axonal wiring: Nrp1 is an important factor for OSN axonal pathfinding, however, the mechanism is more complex and a simple gradient of the expression of Nrp1 cannot explain the findings.

9 Literature

Abercrombie, M. (1946). The annotated Abercrombie. The Anatomical Record 94, 239-247

Aoki, M., Takeuchi, H., Nakashima, A., Nishizumi, H., and Sakano, H. (2013). Possible roles of Robo1 +ensheathing cells in guiding dorsal-zone olfactory sensory neurons in mouse. Devel Neurobio, 1–13.

Au, W. W., Treloar, H. B., and Greer, C. A. (2002). Sublaminar organization of the mouse olfactory bulb nerve layer. J. Comp. Neurol. *446*, 68–80.

Bader, A., Bautze, V., Haid, D., Breer, H., and Strotmann, J. (2010). Gene switching and odor induced activity shape expression of the OR37 family of olfactory receptor genes. European Journal of Neuroscience *32*, 1813–1824.

Barnea G., O'Donnell S., Mancia F., Sun X., Nemes A., Mendelsohn M., and Axel R. (2004). Odorant Receptors on Axon Termini in the Brain. Science 304(5676), 1468.

Benes, F. M., and Lange, N. (2001). Two-dimensional versus three-dimensional cell counting: a practical perspective. Trends in Neurosciences *24*, 11–17.

Berghard, A., Buck, L. B., and Liman, E. R. (1996). Evidence for distinct signaling mechanisms in two mammalian olfactory sense organs. Neurology *93*, 2365–2369.

Bozza, T., Feinstein, P., Zheng, C., and Mombaerts, P. (2002). Odorant Receptor Expression Defines Functional Units in the Mouse Olfactory System. The Journal of Neuroscience *22*, 3033–3043.

Bozza, T., Vassalli, A., Fuss, S., Zhang, J.-J., Weiland, B., Pacifico, R., Feinstein, P. (2009). Mapping of Class I and Class II Odorant Receptors to Glomerular Domains by Two Distinct Types of Olfactory Sensory Neurons in the Mouse. Neuron 61(2), 220–233.

Brechbühl J., Klaey M., and Broillet M.C. (2008). Grueneberg ganglion cells mediate alarm pheromone detection in mice. Science *321*(5892), 1092–1095.

Bressel, O.C., Khan, M., Mombaerts, P. (2015). Linear Correlation Between the Number of Olfactory Sensory Neurons Expressing a Given Mouse Odorant Receptor Gene and the Total Volume of the Corresponding Glomeruli in the Olfactory Bulb. The Journal of Comparative Neurology (accepted).

Brunet, L. J., Gold, G. H., and Ngai, J. (1996). Brunet 1996 General Anosmia Caused by a Targeted Disruption of the Mouse Olfactory Cyclic

Nucleotide–Gated Cation Channel. Neuron *17*, 681–693.

Buck, L., and Axel, R. (1991). A novel multigene family may encode odorant receptors: a molecular basis for odor recognition. Cell *65*, 175–187.

Bulfone, A., Wang, F., Hevner, R., Anderson, S., Cutforth, T., Chen, S., Meneses, J., Pedersen, R., Richard, A., and Rubenstein, L. R. (1998). An Olfactory Sensory Map Develops in the Absence of Normal Projection Neurons or GABAergic Interneurons. Neuron *21*, 1273–1282.

Bush, C. F., Jones, S. V., Lyle, A. N., Minneman, K. P., Ressler, K. J., and Hall, R. A. (2007). Bush 2006 Specificity of Olfactory Receptor Interactions with Other G Protein-coupled Receptors. The Journal of Biological Chemistry *282*, 19042–19051.

Chesler, A. T., Zou, D.-J., Le Pichon, C. E., Peterlin, Z. A., Matthews, G. A., Pei, X., Miller, M. C., and Firestein, S. (2007). A G protein:cAMP signal cascade is required for axonal convergence into olfactory glomeruli. PNAS *104*, 1039–1044.

Chess, A., Simon, I., Cedar, H., and Axel, R. (1994). Allelic inactivation regulates olfactory receptor gene expression. Cell *78*, 823–834.

Cho, J. H., Lepine, M., Andrews, W., Parnavelas, J., and Cloutier, J. F. (2007). Requirement for Slit-1 and Robo-2 in Zonal Segregation of Olfactory Sensory Neuron Axons in the Main Olfactory Bulb. Journal of Neuroscience *27*, 9094–9104.

Col, J. A. D., Matsuo, T., Storm, D. R., and Rodriguez, I. (2007). Adenylyl cyclase-dependent axonal targeting in the olfactory system. Development *134*, 2481–2489.

Connelly, T., Savigner, A., & Ma, M. (2013). Spontaneous and sensory-evoked activity in mouse olfactory sensory neurons with defined odorant receptors. *Journal of Neurophysiology*, *110*(1), 55–62. doi:10.1152/jn.00910.2012

Cummings, D. M., and Belluscio, L. (2010). Continuous Neural Plasticity in the Olfactory Intrabulbar Circuitry. Journal of Neuroscience *30*, 9172–9180.

Cutforth, T., Moring, L., Mendelsohn, M., Nemes, A., Shah, N. M., Kim, M. M., Frisén, J., and Axel, R. (2003). Axonal Ephrin-As and Odorant Receptors: Coordinate Determination of the Olfactory Sensory Map. Cell *114*, 311–322.

Dalton, R. P., Lyons, D. B., and Lomvardas, S. (2013). Co-Opting the Unfolded Protein Response to Elicit Olfactory Receptor Feedback. Cell *155*, 321–332.

Dewan, A., Pacifico, R., Zhan, R., Rinberg, D., and Bozza, T. (2013). Non-redundant coding of aversive odours in the main olfactory pathway. Nature, 1–5.

Døving, K. B., and Trotier, D. (1998). Structure and function of the vomeronasal organ. The Journal of experimental biology, 201(Pt 21), 2913–2925.

Ebrahimi, F. A. W., and Chess, A. (2000). Olfactory neurons are interdependent in maintaining axonal projections. Current Biology *10*, 219–222.

Feinstein, P., and Mombaerts, P. (2004). A Contextual Model for Axonal Sorting into Glomeruli in the Mouse Olfactory System. Cell *117*, 817–831.

Feinstein, P., Bozza, T., Rodriguez, I., Vassalli, A., and Mombaerts, P. (2004). Axon Guidance of Mouse Olfactory Sensory Neurons by Odorant Receptors and the β2 Adrenergic Receptor. Cell *117*, 833–846.

Firestein, S., Zufall, F., and Sheperd, G. M. (1991). Firestein 1991 Single Odor-sensitive Channels in Olfactory Receptor Neurons Are also Gated by Cyclic Nucleotides. The Journal of Neuroscience *11*, 3565–3572.

Fuss, S. H., Zhu, Y., and Mombaerts, P. (2010). Odorant receptor gene choice and axonal wiring in mice with deletion mutations in the odorant receptor gene SR1. Molecular and Cellular Neuroscience *56*, 1–13.

Geuna, S. (2000). Appreciating the Difference Between Design-Based and Model-Based Sampling Strategies in Quantitative Morphology of the Nervous System. J. Comp. Neurol. *427*, 333–339.

Grosmaitre, X., Fuss, S. H., Lee, A. C., Adipietro, K. A., Matsunami, H., Mombaerts, P., and Ma, M. (2009). SR1, a Mouse Odorant Receptor with an Unusually Broad Response Profile. Journal of Neuroscience *29*, 14545–14552.

Grosmaitre, X., Vassalli, A., Mombaerts, P., Shepherd, G. M., and Ma, M. (2006). Odorant responses of olfactory sensory neurons expressing the odorant receptor MOR23: a patch clamp analysis in gene-targeted mice. Proc. Natl. Acad. Sci. U.S.A. *103*, 1970–1975.

Gu, C., Rodriguez, E. R., Reimert, D. V., Shu, T., Fritzsch, B., Richards, L. J., Kolodkin, A. L., and Ginty, D. D. (2003). Neuropilin-1 Conveys Semaphorin and VEGF Signaling during Neural and Cardiovascular Development. Developmental Cell *5*, 45–57.

Guillery, R. W. (2002). On counting and counting errors. J. Comp. Neurol. *447*, 1–7.

Henion, T. R., Faden, A. A., Knott, T. K., and Schwarting, G. A. (2011). 3GnT2 Maintains Adenylyl Cyclase-3 Signaling and Axon Guidance Molecule Expression in the Olfactory Epithelium. Journal of Neuroscience *31*, 6576–6586.

Henion, T. R., Raitcheva, D., Grosholz, R., Biellmann, F., Skarnes, W. C., Hennet, T., and Schwarting, G. A. (2005). 1,3-N-

Acetylglucosaminyltransferase 1 Glycosylation Is Required for Axon Pathfinding by Olfactory Sensory Neurons. Journal of Neuroscience *25*, 1894–1903.

Hirota, J., Omura, M., and Mombaerts, P. (2007). Differential impact of Lhx2 deficiency on expression of class I and class II odorant receptor genes in mouse. Molecular and Cellular Neuroscience *34*, 679–688.

Imai, T., and Sakano, H. (2008). Odorant receptor-mediated signaling in the mouse. Current Opinion in Neurobiology *18*, 251–260.

Imai, T., Suzuki, M., and Sakano, H. (2006). Odorant Receptor-Derived cAMP Signals Direct Axonal Targeting. Science *314*, 657–661.

Imai, T., Yamazaki, T., Kobayakawa, R., Kobayakawa, K., Abe, T., Suzuki, M., and Sakano, H. (2009). Pre-Target Axon Sorting Establishes the Neural Map Topography. Science *325*, 585–590.

Jones, S. V., Choi, D. C., Davis, M., and Ressler, K. J. (2008). Learning-Dependent Structural Plasticity in the Adult Olfactory Pathway. Journal of Neuroscience *28*, 13106–13111.

Kaminski, A., Howell, M. T., and Jackson, R. J. (1990). InitiationofencephalomyocarditisvirusRNA translation: the authentic initiation site is not selected by a scanning mechanism. The EMBO Journal *9*, 3753–3759.

Kaneko-Goto, T., Yoshihara, S.-I., Miyazaki, H., and Yoshihara, Y. (2008). BIG-2 Mediates Olfactory Axon Convergence to Target Glomeruli. Neuron *57*, 834–846.

Kawagishi, K., Ando, M., Yokouchi, K., Sumitomo, N., Karasawa, M., Fukushima, N., and Moriizumi, T. (2014). Stereological quantification of olfactory receptor neurons in mice. Neuroscience *272*, 29–33.

Kerr, M. A., and Belluscio, L. (2006). Olfactory experience accelerates glomerular refinement in the mammalian olfactory bulb. Nat Neurosci *9*, 484–486.

Khan, M., Vaes, E., and Mombaerts, P. (2011). Regulation of the Probability of Mouse Odorant Receptor Gene Choice. Cell *147*, 907–921.

Khan, M., Vaes, E., and Mombaerts, P. (2013). Temporal patterns of odorant receptor gene expression in adult and aged mice. Molecular and Cellular Neuroscience *57*, 120–129.

Klenoff, J. R., and Greer, C. A. (1998). Postnatal development of olfactory receptor cell axonal arbors. J. Comp. Neurol. *390*, 256–267.

Lam, R. S., and Mombaerts, P. (2013). Odorant responsiveness of embryonic mouse olfactory sensory neurons expressing the odorant receptors S1 or MOR23. European Journal of Neuroscience *38*, 2210–2217.

Levy, N. S., Bakalyar, H. A., and Reed, R. R. (1991). levy 1991 SIGNAL TRANSDUCTION IN OLFACTORY NEURONS. Journal of Steroid Biochemistry and Molecular Biology *39*, 633–637.

Lewcock, J. W., and Reed, R. R. (2004). A feedback mechanism regulates monoallelic odorant receptor expression. PNAS *101*, 1069–1074.

Li, J., Ishii, T., Feinstein, P., and Mombaerts, P. (2004). Odorant receptor gene choice is reset by nuclear transfer from mouse olfactory sensory neurons. Nature *428*, 393–399.

Liberles, S. D., and Buck, L. B. (2006). A second class of chemosensory receptors in the olfactory epithelium. Nature *442*, 645–650.

Lin, D. M., Wang, F., Lowe, G., Gold, G. H., Axel, R., Ngai, J., and Brunet, L. (2000). Formation of Precise Connections in the Olfactory Bulb Occurs in the Absence of Odorant-Evoked Neuronal Activity. Neuron *26*, 1–1269–80.

Lipscomb, B. W., Treloar, H. B., and Greer, C. A. (2002a). Cell surface carbohydrates reveal heterogeneity in olfactory receptor cell axons in the mouse. Cell Tissue Res *308*, 7–17.

Lipscomb, B. W., Treloar, H. B., and Greer, C. A. (2002b). Novel microglomerular structures in the olfactory bulb of mice. Journal of Neuroscience *22*, 766–774.

Lipscomb, B. W., Treloar, H. B., Klenoff, J., and Greer, C. A. (2003). Cell surface carbohydrates and glomerular targeting of olfactory sensory neuron axons in the mouse. J. Comp. Neurol. *467*, 22–31.

Liu, A. H., Zhang, X., Stolovitzky, G. A., Califano, A., and Firestein, S. J. (2003). Motif-based construction of a functional map for mammalian olfactory receptors. Genomics *81*, 443–456.

Lodovichi, C., Belluscio, L., and Katz, L. C. (2003). Functional Topography of Connections Linking Mirror-Symmetric Maps in the Mouse Olfactory Bulb. Neuron *36*, 265–276.

Lyons, D. B., Allen, W. E., Goh, T., Tsai, L., Barnea, G., and Lomvardas, S. (2013). An Epigenetic Trap Stabilizes Singular Olfactory Receptor Expression. Cell *154*, 325–336.

Ma, M., Grosmaitre, X., Iwema, C. L., Baker, H., Greer, C. A., and Shepherd, G. M. (2003a). Ma 2003 Olfactory Signal Transduction in the Mouse Septal Organ. The Journal of Neuroscience *23*, 317–324.

Ma, M., Grosmaitre, X., Iwema, C. L., Baker, H., Greer, C. A., and Shepherd, G. M. (2003b). Olfactory Signal Transduction in the Mouse Septal Organ. The Journal of Neuroscience *23*, 317–324.

Maritan, M., Monaco, G., Zamparo, I., Pozzan, T., and Lodovich, C. (2009). Maritan 2009 Odorant receptors at the growth cone are coupled to

localized cAMP and Ca2+ increases. PNAS *106*, 3537–3542.

Matsuo, T., Rossier, D. A., Kan, C., and Rodriguez, I. (2012). The wiring of Grueneberg ganglion axons is dependent on neuropilin 1. Development *139*, 2783–2791.

Miyamichi, K., Serizawa, S., Kimura, H. M., and Sakano, H. (2005). Continuous and Overlapping Expression Domains of Odorant Receptor Genes in the Olfactory Epithelium Determine the Dorsal/Ventral Positioning of Glomeruli in the Olfactory Bulb. Journal of Neuroscience *25*, 3586–3592.

Mombaerts, P., Wang F., Dulac C., Chao S. K., Nemes A., Mendelsohn M., Edmondson J., and Axel R. (1996). Visualizing an Olfactory Sensory Map. Cell 84(4), 675-686.

Nagao, H., Yoshihara, Y., Mitsui, S., Fujisawa, H., and Mori, K. (2010). Two mirror-image sensory maps with domain organization in the mouse main olfactory bulb. Chemical Senses *11*, 1–5.

Nakashima, A., Takeuchi, H., Imai, T., Saito, H., Kiyonari, H., Abe, T., Chen, M., Weinstein, L. S., Yu, C. R., Storm, D. R., et al. (2013). Agonist-Independent GPCR Activity Regulates Anterior-Posterior Targeting of Olfactory Sensory Neurons. Cell *154*, 1314–1325.

Nakatani, H., Serizawa, S., Nakajima, M., Imai, T., and Sakano, H. (2003). Developmental elimination of ectopic projection sites for the transgenic OR gene that has lost zone specificity in the olfactory epithelium. Eur. J. Neurosci. *18*, 2425–2432.

Nguyen, M. Q., Zhou, Z., Marks, C. A., Ryba, N. J. P., and Belluscio, L. (2007). Nguyen 2007 Prominent roles for odorant receptor coding sequences in allelic exclusion. Cell *131*, 1009–1017.

Nguyen-Ba-Charvet, K. T., Di Meglio, T., Fouquet, C., and Chedotal, A. (2008). Robos and Slits Control the Pathfinding and Targeting of Mouse Olfactory Sensory Axons. Journal of Neuroscience *28*, 4244–4249.

Nickell, M. D., Breheny, P., Stromberg, A. J., and McClintock, T. S. (2012). Genomics of mature and immature olfactory sensory neurons. J. Comp. Neurol. *520*, 2608–2629.

Omura, M., and Mombaerts, P. (2015). Trpc2-expressing sensory neurons in the mouse main olfactory epithelium of type B express the soluble guanylate cyclase Gucy1b2. Molecular and Cellular Neuroscience *65*, 1–11.

Omura, M., Grosmaitre, X., Ma, M., and Mombaerts, P. (2014). The β2-adrenergic receptor as a surrogate odorant receptor in mouse olfactory sensory neurons. Molecular and Cellular Neuroscience *58*, 1–10.

Pacifico, R., Dewan, A., Cawley, D., Guo, C., and Bozza, T. (2012). An

Olfactory Subsystem that Mediates High-Sensitivity Detection of Volatile Amines. CellReports, 1–18.

Pasterkamp, R. J., De Winter, F., Holtmaat, J. D. G., and Verhaagen, J. (1998). Evidence for a Role of the Chemorepellent Semaphorin III and Its Receptor Neuropilin-1 in the Regeneration of Primary Olfactory Axons. The Journal of Neuroscience *18*, 9962–9976.

Plessy, C., Pascarella, G., Bertin, N., Akalin, A., Carrieri, C., Vassalli, A., Lazarevic, D., Severin, J., Vlachouli, C., Simone, R., et al. (2012). Promoter architecture of mouse olfactory receptor genes. Genome Research *22*, 486–497.

Pomeroy, S. L., LaMantia, A. S., and Purves, D. (1990). Postnatal construction of neural circuitry in the mouse olfactory bulb. J. Neurosci. *10*, 1952–1966.

Potter, S. M., Zheng, C., Koos, D. S., Feinstein, P., Fraser, S. E., and Mombaerts, P. (2001). Structure and emergence of specific olfactory glomeruli in the mouse. Journal of Neuroscience *21*, 9713–9723.

Ressler, K. J., Sullivan, S. L., and Buck, L. B. (1993). A Zonal Organization of Odorant Receptor Gene Expression in the Olfactory Epithelium. Cell *73*, 597–609.

Ressler, K. J., Sullivan, S. L., and Buck, L. B. (1994). Information coding in the olfactory system: evidence for a stereotyped and highly organized epitope map in the olfactory bulb. Cell *79*, 1245–1255.

Richard, M. B., Taylor, S. R., and Greer, C. A. (2010). Age-induced disruption of selective olfactory bulb synaptic circuits. PNAS, 1–12.

Rodriguez-Gil, D. J., Treloar, H. B., Zhang, X., Miller, A. M., Two, A., Iwema, C., Firestein, S. J., and Greer, C. A. (2010). Chromosomal Location-Dependent Nonstochastic Onset of Odor Receptor Expression. Journal of Neuroscience *30*, 10067–10075.

Rolen, S. H., Salcedo, E., Restrepo, D., and Finger, T. E. (2014). Differential localization of NT-3 and TrpM5 in glomeruli of the olfactory bulb of mice. J. Comp. Neurol. *522*, 1929–1940.

Roppolo, D., Vollery, S., Kan, C.-D., Luescher, C., Broillet, M.-C., and Rodriguez, I. (2007). Gene cluster lock after pheromone receptor gene choice. The EMBO Journal *26*, 3423–3430.

Rothman, A., Feinstein, P., Hirota, J., and Mombaerts, P. (2005). The promoter of the mouse odorant receptor gene M71. Molecular and Cellular Neuroscience *28*, 535–546.

Royal, S. J. R., and Key, B. (1999). Royal 1999 Development of P2 Olfactory Glomeruli in P2Internal Ribosome Entry SiteTauLacZ Transgenic Mice. The Journal of Neuroscience *19*, 9856–9864.

Royal, S. J., Gambello, M. J., Wynshaw-Boris, A., and Key, B. (2002). Laminar disorganisation of mitral cells in the olfactory bulb does not affect topographic targeting of primary olfactory axons. Brain Research *932*, 1–9.

Saito, H., Mimmack, M., Kishimoto, J., and Keverne, E. B. (1998). Saito 1998 Expression of olfactory receptors, G-proteins and AxCAMs during the development and maturation of olfactory sensory neurons in the mouse. Developmental Brain Research, 69–81.

Schaefer, M. L., Finger, T. E., and Restrepo, D. (2001). Variability of Position of the P2 Glomerulus Within a Map of the Mouse Olfactory Bulb. J. Comp. Neurol. *436*, 351–362.

Schmitz, C., and Hof, P. R. (2005). Design-based stereology in neuroscience. Neuroscience *130*, 813–831.

Schwarting, G. A., Kostek, C., Ahmad, N., Dibble, D., Pays, L., and Pueschel, A. W. (2000). Semaphorin 3A Is Required for Guidance of Olfactory Axons in Mice. The Journal of Neuroscience *20*, 7691–7697.

Schwarting, G. A., Raitcheva, D., Crandall, J. E., Burkhardt, C., and Puschel, A. W. (2004). Semaphorin 3A-mediated axon guidance regulates convergence and targeting of P2 odorant receptor axons. European Journal of Neuroscience *19*, 1800–1810.

Schwarzenbacher, K., Fleischer, J., and Breer, H. (2005). Formation and maturation of olfactory cilia monitored by odorant receptor-specific antibodies. Histochem Cell Biol *123*, 419–428.

Schwarzenbacher, K., Fleischer, J., Breer, H., and Conzelmann, S. (2004). Expression of olfactory receptors in the cribriform mesenchyme during prenatal development. Gene Expression Patterns *4*, 543–552.

Serizawa, S., Miyamichi, K., Takeuchi, H., Yamagishi, Y., Suzuki, M., and Sakano, H. (2006). A Neuronal Identity Code for the Odorant Receptor-Specific and Activity-Dependent Axon Sorting. Cell *127*, 1057–1069.

Shelly, M., Cancedda, L., Lim, B. K., Popescu, A. T., Cheng, P.-L., Gao, H., and Poo, M.-M. (2011). Semaphorin3A Regulates Neuronal Polarization by Suppressing Axon Formation and Promoting Dendrite Growth. Neuron *71*, 433–446.

Shykind, B. M., Rohani, S. C., O'Donnell, S., Nemes, A., Mendelsohn, M., Sun, Y., Axel, R., and Barnea, G. (2004). Gene Switching and the Stability of Odorant Receptor Gene Choice. Cell *117*, 801–815.

Strotmann, J. (2004). Olfactory Receptor Proteins in Axonal Processes of Chemosensory Neurons. Journal of Neuroscience *24*, 7754–7761.

Strotmann, J., Bader, A., Luche, H., Fehling, H. J., and Breer, H. (2009). The patch-like pattern of OR37 receptors is formed by turning off gene expression in non-appropriate areas. Molecular and Cellular Neuroscience

41, 474–485.

Strotmann, J., Konzelmann, S., and Breer, H. eds. (1996). Laminar segregation of odorant receptor expression in the olfactory epithelium. Cell Tissue Res, 347–354.

Takahashi, H., Yoshihara, S.-I., Nishizumi, H., and Tsuboi, A. (2010). Neuropilin-2 is required for the proper targeting of ventral glomeruli in the mouse olfactory bulb. Molecular and Cellular Neuroscience, 1–19.

Takahashi, T., Fournier, A., Nakamura, F., Wang, L.-H., Murakami, Y., Kalb, R. G., Fujisawa, H., and Strittmatter, S. M. (1999). Plexin-Neuropilin-1 Complexes Form Functional Semaphorin 3A Receptors. Cell *99*, 59–69.

Takeuchi, H., Inokuchi, K., Aoki, M., Suto, F., Tsuboi, A., Matsuda, I., Suzuki, M., Aiba, A., Serizawa, S., Yoshihara, Y., et al. (2010). Sequential Arrival and Graded Secretion of Sema3F by Olfactory Neuron Axons Specify Map Topography at the Bulb. Cell *141*, 1056–1067.

Tan, J., Savigner, A., Ma, M., and Luo, M. (2010). Odor Information Processing by the Olfactory Bulb Analyzed in Gene-Targeted Mice. Neuron *65*, 912–926.

Tian, H., and Ma, M. (2004). Molecular Organization of the Olfactory Septal Organ. Journal of Neuroscience *24*, 8383–8390.

Treloar, H. B., Feinstein, P., Mombaerts, P., and Greer, C. A. (2002). Specificity of glomerular targeting by olfactory sensory axons. Journal of Neuroscience *22*, 2469–2477.

Trinh, K., and Storm, D. R. (2003). Vomeronasal organ detects odorants in absence of signaling through main olfactory epithelium. Nat Neurosci.

Tsuboi, A., Miyazaki, T., Imai, T., and Sakano, H. (2006). Olfactory sensory neurons expressing class I odorant receptors converge their axons on an antero-dorsal domain of the olfactory bulb in the mouse. European Journal of Neuroscience *23*, 1436–1444.

Tucker, E. S., Polleux, F., and LaMantia, A.-S. (2006). Position and time specify the migration of a pioneering population of olfactory bulb interneurons. Developmental Biology *297*, 387–401.

Ukhanov, K., Corey, E. A., Brunert, D., Klasen, K., and Ache, B. W. (2010). Inhibitory Odorant Signaling in Mammalian Olfactory Receptor Neurons. Journal of Neurophysiology *103*, 1114–1122.

Vassalli, A., Rothman, A., Feinstein, P., Zapotocky, M., and Mombaerts, P. (2002). Minigenes impart odorant receptor-specific axon guidance in the olfactory bulb. Neuron *35*, 681–696.

Walz, A., Mombaerts, P., Greer, C. A., and Treloar, H. B. (2006). Disrupted compartmental organization of axons and dendrites within olfactory

glomeruli of mice deficient in the olfactory cell adhesion molecule, OCAM. Molecular and Cellular Neuroscience, 1–14.

Wang, F., Nemes, A., Mendelsohn, M., and Axel, R. (1998). Wang 98 Odorant Receptors Govern the Formation of a Precise Topographic Map. Cell *93*, 47–60.

Wang, S. S. (2004). Genetic disruptions of O/E2 and O/E3 genes reveal involvement in olfactory receptor neuron projection. Development *131*, 1377–1388.

Williams, E. O., Xiao, Y., Sickles, H. M., Shafer, P., Yona, G., Yang, J. Y., and Lin, D. M. (2007). Novel subdomains of the mouse olfactory bulb defined by molecular heterogeneity in the nascent external plexiform and glomerular layers. BMC Dev Biol *7*, 48.

Wynn, E. H., Sánchez-Andrade, G., Carss, K. J., and Logan, D. W. (2012). Genomic variation in the vomeronasal receptor gene repertoires of inbred mice. BMC Genomics *13*, 415.

Yan, Z., Tan, J., Qin, C., Lu, Y., Ding, C., and Luo, M. (2008). Precise Circuitry Links Bilaterally Symmetric Olfactory Maps. Neuron *58*, 613–624.

Yu, C. R., Power, J., Barnea, G., Osborne, J., Axel, R., and Gogos, J. A. (2004). Yu 2004 Spontaneous Neural Activity Is Required for the Establishment and Maintenance of the Olfactory Sensory Map. Neuron *42*, 553–566.

Zhang, J., Huang, G., Dewan, A., Feinstein, P., and Bozza, T. (2012). Uncoupling stimulus specificity and glomerular position in the mouse olfactory system. Molecular and Cellular Neuroscience *51*, 79–88.

Zhang, X., and Firestein, S. (2002). The olfactory receptor gene superfamily of the mouse. Nat Neurosci *5*, 124–133.

Zhao, H., and Reed, R. R. (2001). X Inactivation of the *OCNC1* Channel Gene Reveals a Role for Activity-Dependent Competition in the Olfactory System. Cell *104*, 651–660.

Zheng, C., Feinstein, P., Bozza, T., Rodriguez, I., and Mombaerts, P. (2000). Peripheral Olfactory Projections Are Differentially Affected in Mice Deficient in a Cyclic Nucleotide-Gated Channel Subunit. Neuron *26*, 81–91.

Zou, D. J., Chesler, A. T., Le Pichon, C. E., Kuznetsov, A., Pei, X., Hwang, E. L., and Firestein, S. (2007). Absence of Adenylyl Cyclase 3 Perturbs Peripheral Olfactory Projections in Mice. Journal of Neuroscience *27*, 6675–6683.

Zou, D. J., Feinstein, P., Rivers, A. L., Mathews, G. A., Kim, A., Greer, C. A., Mombaerts, P., and Firestein, S. (2004). Postnatal Refinement of Peripheral Olfactory Projections. Science *304*, 1976–1979.

10 Appendices

10.1 Figures and Tables

10.1.1 Figures

10.1.2 Tables

10.2 Genetic sequences

10.2.1 Vector insert

caGs (1185 bp)

ATGGGCTGCCTCGGCAACAGTAAGACCGAGGACCAGCGCAACGAGGAGAAGGCGCAGCGCGAGGCCAACAAA
AAGATCGAGAAGCAGCTGCAGAAGGACAAGCAGGTCTACCGGGCCACGCACCGCCTGCTGCTGCTGGGTGCT
GGAGAGTCTGGCAAAAGCACCATTGTGAAGCAGATGAGGATCCTGCATGTTAATGGGTTTAACGGAGAGGGCG
GCGAAGAGGACCCGCAGGCTGCAAGGAGCAACAGCGATGGTGAGAAGGCCACTAAAGTGCAGGACATCAAAA
ACAACCTGAAGGAGGCCATTGAAACCATTGTGGCCGCCATGAGCAACCTGGTGCCCCCTGTGGAGCTGGCCAA
CCCTGAGAACCAGTTCAGAGTGGACTACATTCTGAGCGTGATGAACGTGCCGAACTTTGACTTCCCACCTGAAT
TCTATGAGCATGCCAAGGCTCTGTGGGAGGATGAGGGAGTGCGTGCCTGCTACGAGCGCTCCAATGAGTACCA
GCTGATTGACTGTGCCCAGTACTTCCTGGACAAGATTGATGTGATCAAGCAGGCCGACTACGTGCCAAGTGACC
AGGACCTGCTTCGCTGCCGTGTCCTGACCTCTGGAATCTTTGAGACCAAGTTCCAGGTGGACAAAGTCAACTTC
CACATGTTCGATGTGGGCGGCCTGCGCGATGAGCGCCGCAAGTGGATCCAGTGCTTCAATGATGTGACTGCCA
TCATCTTCGTGGTGGCCAGCAGCAGCTACAACATGGTCATTCGGGAGGACAACCAGACTAACCGCCTGCAGGA
GGCTCTGAACCTCTTCAAGAGCATCTGGAACAACAGATGGCTGCGCACCATCTCTGTGATTCTCTTCCTCAACAA
GCAAGACCTGCTTGCTGAGAAAGTCCTCGCTGGCAAATCGAAGATTGAGGACTACTTTCCAGAGTTCGCTCGCT
ATACCACTCCTGAGGATGCGACTCCCGAGCCCGGAGAGGACCCACGCGTGACCCGGGCCAAGTACTTCATTCG
GGATGAGTTTCTGAGAATCAGCACTGCTAGTGGAGATGGGCGCCACTACTGCTACCCTCACTTTACCTGCGCCG
TGGACACTGAGAACATCCGCCGTGTCTTCAACGACTGCCGTGACATCATCCAGCGCATGCATCTCCGCCAATAC
GAGCTGCTCTAA

IRES (589 bp)

CCGCGGCAATTCCGCCCCTCTCCCTCCCCCCCCCCTAACGTTACTGGCCGAAGCCGCTTGGAATAAGGCCGGT
GTGCGTTTGTCTATATGTTATTTTCCACCATATTGCCGTCTTTTGGCAATGTGAGGGCCCGGAAACCTGGCCCTG
TCTTCTTGACGAGCATTCCTAGGGGTCTTTCCCCTCTCGCCAAAGGAATGCAAGGTCTGTTGAATGTCGTGAAG
GAAGCAGTTCCTCTGGAAGCTTCTTGAAGACAAACAACGTCTGTAGCGACCCTTTGCAGGCAGCGGAACCCCCC

ACCTGGCAACAGGTGCCTCTGCGGCCAAAAGCCACGTGTATAAGATACACCTGCAAAGGCGGCACAACCCCAG
TGCCACGTTGTGAGTTGGATAGTTGTGGAAAGAGTCAAATGGCTCTCCTCAAGCGTATTCAACAAGGGGCTGAA
GGATGCCCAGAAGGTACCCCATTGTATGGGATCTGATCTGGGGCCTCGGTGCACATGCTTTACATGTGTTTAGT
CGAGGTTAAAAAAACGTCTAGGCCCCCCGAACCACGGGGACGTGGTTTTCCTTTGAAAAACACGATGATAAT

IRES-gapCFP (1383 bp)

CCGCGGCAATTCCGCCCCTCTCCCTCCCCCCCCCCTAACGTTACTGGCCGAAGCCGCTTGGAATAAGGCCGGT
GTGCGTTTGTCTATATGTTATTTTCCACCATATTGCCGTCTTTTGGCAATGTGAGGGCCCGGAAACCTGGCCCTG
TCTTCTTGACGAGCATTCCTAGGGGTCTTTCCCCTCTCGCCAAAGGAATGCAAGGTCTGTTGAATGTCGTGAAG
GAAGCAGTTCCTCTGGAAGCTTCTTGAAGACAAACAACGTCTGTAGCGACCCTTTGCAGGCAGCGGAACCCCCC
ACCTGGCAACAGGTGCCTCTGCGGCCAAAAGCCACGTGTATAAGATACACCTGCAAAGGCGGCACAACCCCAG
TGCCACGTTGTGAGTTGGATAGTTGTGGAAAGAGTCAAATGGCTCTCCTCAAGCGTATTCAACAAGGGGCTGAA
GGATGCCCAGAAGGTACCCCATTGTATGGGATCTGATCTGGGGCCTCGGTGCACATGCTTTACATGTGTTTAGT
CGAGGTTAAAAAAACGTCTAGGCCCCCCGAACCACGGGGACGTGGTTTTCCTTTGAAAAACACGATGATAATAT
GCTGTGCTGTATGAGAAGAACCAAGCAGGTGGAAAAGAACGATGAGGACCAGAAGATCGTGAGCAAGGGCGAG
GAGCTGTTCACCGGGGTGGTGCCCATCCTGGTCGAGCTGGACGGCGACGTAAACGGCCACAAGTTCAGCGTG
TCCGGCGAGGGCGAGGGCGATGCCACCTACGGCAAGCTGACCCTGAAGTTCATCTGCACCACCGGCAAGCTG
CCCGTGCCCTGGCCCACCCTCGTGACCACCCTGACCTGGGGCGTGCAGTGCTTCAGCCGCTACCCCGACCAC
ATGAAGCAGCACGACTTCTTCAAGTCCGCCATGCCCGAAGGCTACGTCCAGGAGCGCACCATCTTCTTCAAGGA
CGACGGCAACTACAAGACCCGCGCCGAGGTGAAGTTCGAGGGCGACACCCTGGTGAACCGCATCGAGCTGAA
GGGCATCGACTTCAAGGAGGACGGCAACATCCTGGGGCACAAGCTGGAGTACAACTACATCAGCCACAACGTC
TATATCACCGCCGACAAGCAGAAGAACGGCATCAAGGCCAACTTCAAGATCCGCCACAACATCGAGGACGGCA
GCGTGCAGCTCGCCGACCACTACCAGCAGAACACCCCCATCGGCGACGGCCCCGTGCTGCTGCCCCGACAACC
ACTACCTGAGCACCCAGTCCGCCCTGAGCAAAGACCCCAACGAGAAGCGCGATCACATGGTCCTGCTGGAGTT
CGTGACCGCCGCCGGGATCACTCTCGGCATGGACGAGCTGTACAAGTAAAGCGGCCAATCCCGCGG

IRES-tauGFP-ACNF (6267 bp)

CGCCCCCCCCCCCCCCCCCCCCTCTCCCTCCCCCCCCCCTAACGTTACTGGCCGAAGCCGCTTGGAATAAGGCC
GGTGTGCGTTTGTCTATATGTTATTTTCCACCATATTGCCGTCTTTTGGCAATGTGAGGGCCCGGAAACCTGGCC
CTGTCTTCTTGACGAGCATTCCTAGGGGTCTTTCCCCTCTCGCCAAAGGAATGCAAGGTCTGTTGAATGTCGTG
AAGGAAGCAGTTCCTCTGGAAGCTTCTTGAAGACAAACAACGTCTGTAGCGACCCTTTGCAGGCAGCGGAACCC
CCCACCTGGCGACAGGTGCCTCTGCGGCCAAAAGCCACGTGTATAAGATACACCTGCAAAGGCGGCACAACCC
CAGTGCCACGTTGTGAGTTGGATAGTTGTGGAAAGAGTCAAATGGCTCTCCTAAGCGTATTCAACAAGGGGCTG
AAGGATGCCCAGAAGGTACCCCATTGTATGGGATCTGATCTGGGGCCTCGGTGCACATGCTTTACATGTGTTTA
GTCGAGGTTAAAAAAACGTCTAGGCCCCCCGAACCACGGGGACGTGGTTTTCCTTTGAAAAACACGATGATAAT
ATGGCCACAACCATGGCTGAGCCCCGCCAGGAGTTCGACGTGATGGAAGATCATGCTCAGGGGGACTACACCC
TGCAAGACCAGGAGGGTGACATGGACCCCGGCCTGAAAGAGTCTCCCCTGCAGACCCCGGCCGATGATGGAT
CTGAGGAACCAGGCTCTGAAACCTCTGATGCTAAGAGCACTCCGACGGCGGAAGATGCGACAGCACCCTTAGT
GGATGAGGGAGCCCCCGGTGAGCAGGCGGCCGCTCAGGCCCCCGCGGAGATCCCAGAAGGAACCGCAGCTG
AAGAAGCAGGCATTGGCGACACGTCCAACCTGGAAGACCAAGCTGCCGGACACGTGACCCAAGCTCGCATGGT
CAGTAAAGGCAAAGATGGGACTGGACCCGATGACAAAAAAACCAAGGGGGCGGATGGTAAGCCTGGAACGAAG
ATTGCCACACCCCGGGGAGCAGCCCCTCCAGGCCAGAAAGGCCAGGCCAACGCCACCCGGATTCCAGCAAAA
ACCACTCCCACCCCGAAGACCTCGCCAGGTGAATCTGGGAAATCCGGGGACCGCAGCGGCTACAGCAGCCCC
GGCTCCCCAGGCACTCCGGGCAGCCGCTCCCGCACACCCTCCCTGCCGACCCCGCCCACCCGGGAGCCCAA
GAAGGTGGCGGTGGTCCGCACTCCCCCCAAGTCGCCGTCTGCAGCCAAGAGCCGCCTGCAGGCCGCTCCCGG
GCCCATGCCAGACCTGAAGAACGTCAAGTCCAAAATCGGCTCCACGGAAAACCTGAAGCACCAGCCAGGAGGT
GGCAAGGTGCAGATAATTAATAAGAAGCTGGATCTTAGCAACGTCCAGTCCAAGTGTGGCTCAAAGGATAATAT
CAAACACGTGCCAGGAGGCGGCAGTGTGCAAATAGTCTACAAACCAGTGGATCTGAGCAAGGTGACCTCCAAG
TGTGGCTCATTAGGCAACATCCATCATAAGCCAGGAGGTGGCCAAGTGGAAGTGAAATCTGAGAAGCTGGACTT
CAAGGATAGAGTCCAGTCGAAGATTGGGTCCCTGGACAACATCACACACGTCCCTGGCGGAGGGAATAAAAAG
ATCGAAACCCACAAGCTGACCTTCCGCGAGAACGCCAAAGCCAAGACCGACCACGGGGCGGAGATCGTGTCC
GGGGATCCACCGGTCGCCACCATGGTGAGCAAGGGCGAGGAGCTGTTCACCGGGGTGGTGCCCATCCTGGTC
GAGCTGGACGGCGACGTAAACGGCCACAAGTTCAGCGTGTCCGGCGAGGGCGAGGGCGATGCCACCTACGGC
AAGCTGACCCTGAAGTTCATCTGCACCACCGGCAAGCTGCCCGTGCCCTGGCCCACCCTCGTGACCACCCTGA
CCTACGGCGTGCAGTGCTTCAGCCGCTACCCCGACCACATGAAGCAGCACGACTTCTTCAAGTCCGCCATGCC
CGAAGGCTACGTCCAGGAGCGCACCATCTTCTTCAAGGACGACGGCAACTACAAGACCCGCGCCGAGGTGAAG
TTCGAGGGCGACACCCTGGTGAACCGCATCGAGCTGAAGGGCATCGACTTCAAGGAGGACGGCAACATCCTGG
GGCACAAGCTGGAGTACAACTACAACAGCCACAACGTCTATATCATGGCCGACAAGCAGAAGAACGGCATCAAG
GTGAACTTCAAGATCCGCCACAACATCGAGGACGGCAGCGTGCAGCTCGCCGACCACTACCAGCAGAACACCC
CCATCGGCGACGGCCCCGTGCTGCTGCCCGACAACCACTACCTGAGCACCCAGTCCGCCCTGAGCAAAGACC
CCAACGAGAAGCGCGATCACATGGTCCTGCTGGAGTTCGTGACCGCCGCCGGGATCACTCTCGGCATGGACGA
GCTGTACAAGTAAAGCGGCCGCGACTCTAGAGATTCGAGATCTAGATATCGATGAATTCATAACTTCGTATAATG
TATGCTATACGAAGTTATGGATCTGTCGATCGACGGATCGATCCGAACAAACGACCCAACACCCGTGCGTTTTAT
TCTGTCTTTTTATTGCCGATCCCCTCAGAAGAACTCGTCAAGAAGGCGATAGAAGGCGATGCGCTGCGAATCGG
GAGCGGCGATACCGTAAAGCACGAGGAAGCGGTCAGCCCATTCGCCGCCAAGCTCTTCAGCAATATCACGGGT
AGCCAACGCTATGTCCTGATAGCGGTCCGCCACACCCAGCCGGCCACAGTCGATGAATCCAGAAAAGCGGCCA
TTTTCCACCATGATATTCGGCAAGCAGGCATCGCCATGGGTCACGACGAGATCCTCGCCGTCGGGCATGCGCG
CCTTGAGCCTGGCGAACAGTTCGGCTGGCGCGAGCCCCTGATGCTCTTCGTCCAGATCATCCTGATCGACAAG
ACCGGCTTCCATCCGAGTACGTGCTCGCTCGATGCGATGTTTCGCTTGGTGGTCGAATGGGCAGGTAGCCGGA
TCAAGCGTATGCAGCCGCCGCATTGCATCAGCCATGATGGATACTTTCTCGGCAGGAGCAAGGTGAGATGACA
GGAGATCCTGCCCCGGCACTTCGCCCAATAGCAGCCAGTCCCTTCCCGCTTCAGTGACAACGTCGAGCACAGC
TGCGCAAGGAACGCCCGTCGTGGCCAGCCACGATAGCCGCGCTGCCTCGTCCTGCAGTTCATTCAGGGCACC
GGACAGGTCGGTCTTGACAAAAAGAACCGGGCGCCCCTGCGCTGACAGCCGGAACACGGCGGCATCAGAGCA
GCCGATTGTCTGTTGTGCCCAGTCATAGCCGAATAGCCTCTCCACCCAAGCGGCCGGAGAACCTGCGTGCAAT

CCATCTTGTTCAATGGCCGATCCCATATTGGCTGCACGGATCCTGAACGGCAGAGGTTACGGCAGTTTGTCTCT
CCCCCTTCCGGGAGCCACCTTCTTCTCCAACCGTCCCGGTCGCGCTCTCGGCGCTTCTGAGGAGAGAACTGGC
TGAGTGACGCCCTTTATAGATTCGCCCTTGTGTCCCGCCCCTTCCTTTCCCGCCCTCCCTTGCGCTACGGGGCC
GCCCGCACCGGCCTACACGGAGCGCGCGCGGCGGAGTTGTTGACGCTAGGGCTCCGGCTCCCTGGTTGGGT
GTTCTTTCTGACGCGACAGGAGGAGGAGAATGTCCTGGTCCTGTCGTCCTCCTTTCGGGTTTCCCGTGCACTCA
AACCGAGGACTTACAGAACGGAGGATAAAGTTAGGCCATTTTTACTCAGCTTCGGAGTTCAGGCTCATTTTTCAG
CTAAAGTCTCTCATTAGTATCCCCCCACACACATCGGGAAAATGGTTTGTCCTACGCATCGGTAATGAAGGCGG
GGCCCTTCGGGTCCTCCGGAGCGGGTTCCGGGGGTGGGGGGAAGGAGGGAGGGACGGGACGGGCCTCGTTC
ATGAATATTCAGTTCACCGCTGAATATGCATAAGGCAGGCAAGATGGCGCGTCCAATCAATTGGAAGTAGCCGT
TATTAGTGGAGAGGCCCCAGGACGTTGGGGCACCGCCTGTGCTCTAGTAGCTTTACGGAGCCCTGGCGCTCGA
TGTTCAAGCCCAAGCTTTCGCGAGCTCGACCGAACAAACGACCCAACACCCGTGCGTTTTATTCTGTCTTTTTAT
TGCCGCTCAGCTTTACAGTGACAATGACGGCTGGCGACTGAATATTAGTGCTTACAGACAGCACTACATATTTTC
CGTCGATGTTGAAATCCTTTCTCATATGTCACCATAAATATCAAATAATTATAGCAATCATTTACGCGTTAATGGCT
AATCGCCATCTTCCAGCAGGCGCACCATTGCCCCTGTTTCACTATCCAGGTTACGGATATAGTTCATGACAATAT
TTACATTGGTCCAGCCACCAGCTTGCATGATCTCCGGTATTGAAACTCCAGCGCGGGCCATATCTCGCGCGGCT
CCGACACGGGCACTGTGTCCAGACCAGGCCAGGTATCTCTGACCAGAGTCATCCTAAAATACACAAACAATTAG
AATCAGTAGTTTAACACATTATACACTTAAAAATTTTATATTTACCTTAGCGCCGTAAATCAATCGATGAGTTGCTT
CAAAAATCCCTTCCAGGGCGCGAGTTGATAGCTGGCTGGTGGCAGATGGCGCGGCAACACCATTTTTTCTGACC
CGGCAAAACAGGTAGTTATTCGGATCATCAGCTACACCAGAGACGGAAATCCATCGCTCGACCAGTTTAGTTAC
CCCCAGGCTAAGTGCCTTCTCTACACCTGCGGTGCTAACCAGCGTTTTCGTTCTGCCAATATGGATTAACATTCT
CCCACCGTCAGTACGTGAGATATCTTTAACCCTGATCCTGGCAATTTCGGCTATACGTAACAGGGTGTTATAAGC
AATCCCCAGAAATGCCAGATTACGTATATCCTGGCAGCGATCGCTATTTTCCATGAGTGAACGAACCTGGTCGAA
ATCAGTGCGTTCGAACGCTAGAGCCTGTTTTGCACGTTCACCGGCATCAACGTTTTCTTTTCGGATCCGCCGCAT
AACCAGTGAAACAGCATTGCTGTCACTTGGTCGTGGCAGCCCGGACCGACGATGAAGCATGTTTAGCTGGCCC
AAATGTTGCTGGATAGTTTTTACTGCCAGACCGCGCGCCTGAAGATATAGAAGATAATCGCGAACATCTTCAGGT
TCTGCGGGAAACCATTTCCGGTTATTCAACTTGCACCATGCCGCCCACGACCGGCAAACGGACAGAAGCATTTT
CCAGGTATGCTCAGAAAACGCCTGGCGATCCCTGAACATGTCCATCAGGTTCTTGCGAACCTCATCACTCGTTG
CATCGACCGGTAATGCAGGCAAATTTTGGTGTACGGTCAGTAAATTGGACACCTTCCTCTTCTTCTTGGGCATGG
CCGCAGGAAAGCAGAGCCCTGAAGCTCCCATCACCGGCCAATAAGAGCCAAGCCTGCAGTGTGACCTCATAGA
GCAATGTGCCAGCCAGCCTGACCCCAAGGGCCCTCAGGCTTGGGCACACTGTCTCTAGGACCCTGAGAGAAAG
ACATACCCATTTCTGCTTAGGGCCCTGAGGATGAGCCCAGGGGTGGCTTGGCACTGAAGCAAAGGACACTGGG
GCTCAGCTGGCAGCAAAGTGACCAGGATGCTGAGGCTTTGACCCAGAAGCCAGAGGCCAGAGGCCAGGACTT
CTCTTGGTCCCAGTCCACCCTCACTCAGAGCTTTACCAATGCCCTCTGGATAGTTGTCGGGTAACGGTGGACGC
CACTGATTCTCTGGCCAGCCTAGGACTTCGCCATTCCGCTGATTCTGCTCTTCCAGCCACTGGCTGACCGGTTG
GAAGTACTCCAGCAGTGCCTTGGCATCCAGGGCATCTGAGCCTACCAGGTCCTTCAGTACCTCCTGCCAGGGC
CTGGAGCAGCCAGCCTGCAACACCTGCCTGCCAAGCAGAGTGACCACTGTGGGCACAGGGGACACAGGGTGG
GGCCCACAACAGCACCATTGTCCACTTGTCCCTCACTAGTAAAAGAACTCTAGGGTTGCGGGGGGGTGGGGGAG
GTCTCTGTGAGGCTGGTAAGGGATATTTGCCTGGCCCATGGAGATCCATAACTTCGTATAATGTATGCTATACGA
AGTTATAAGCTTTCGCGAGCTCGA

10.2.2 Plasmids & Genes

M71 coding sequence (930 bp)

ATGACTGCAGAGAATCAATCTACAGTGACAGAGTTTATCCTCGGGGGGCTAACTAACAGGCCAGAGCTCCAGCT
ACCCCTCTTCCTCCTCTTTCTGGGGATCTACGTAGTCACCATGGTAGGAAACCTGGGCATGATCACCTTGATTG
GACTCAACTCACAGCTTCACACCCCCATGTACTTCTTCCTCAGTAACCTGTCACTCGTGGATCTCTGCTACTCCT
CTGTCATTACCCCTAAAATGCTCATCAACTTTGTGTCCCAAAGAAACCTCATCTCCTATGTGGGATGCATGTCTCA
GCTATACTTCTTCCTGGTTTTCGTCATTGCTGAGTGTTACATGCTCACTGTGATGGCCTATGACCGCTATGTGGC
CATCTGTCAACCCTTGCTTTATAACATCATCATGTCTCCTGCCCTCTGCTCTCTGCTGGTGGCTTTTGTCTATGCC
GTAGGACTCATCGGTTCAGCAATTGAGACTGGCCTCATGTTGAAATTAAACTATTGTGAGGACCTCATCAGCCAC
TACTTCTGTGACATCCTCCCCCTCATGAAGCTCTCTTGCTCTAGTACCTATGATGTAGAAATGGCTGTCTTCTTTT
TAGCTGGATTTGACATTATCGTCACAAGCTTAACCGTACTCATTTCCTATGCATTCATCCTGTCCAGCATCCTTCG
CATCAGCTCCAATGAGGGCAGGTCCAAAGCCTTCAGCACCTGCAGCTCCCACTTTGCAGCTGTGGGCTTGTTCT
ATGGATCCACAGCATTCATGTACTTAAAGCCTTCTACAGCTAGTTCCCTGGCCCAGGAGAATGTAGCTTCTGTGT
TCTACACCACAGTGATCCCCATGTTCAACCCCCTGATCTACAGCCTGAGAAACAAGGAGGTGAAGACCGCACTG
GACAAAACACTGAGGAGAAAAGTCTTTTGA

LA (4532bp)

GATCTTCCAGAAGCAATGAGCTTCTCTGGCATCAGATTCACATTCCTGGGGGTGTCATTTCCCTACTGAAAGAACC
AAGATTCTTGGTGAAATGAATGACTCAGCTCTGAAGAATGAAAAGAATGTGGTAAAGTCACAACATCTTGTCATA
CCAGATGGTAAGGAAGATATTAGAGACTAGTATATTAAGTTCAGAGACAAATTGAGAAGTCCAGAGACTGTCAAT
ACCTGGGGCAGTAGCTTACTGGTTAAGTGTGCGCACTGCTGTTGCTGAGCACCTGAGTGTGGTTCTCAGCACAT
AGCTCAACTTATAACTCAAGGTCCAAGGGGGAATTTATTGCTGTCCCCTCCAAAGGTATTTGTGTTCATGTGAAC
ATACCAACACAGACACATGTACAATTTAAAATAATGAAAATAAAATGTAAAACATAAAATTAAATTCTGATAAAAGC
ATAGTAATTGTATTGGGCTGAAGCACATTAAATATGTTCACACTAGTGAATTTATAAAGGGGGGGATATAAGAAAC
CAACTATTGTTTTTAAATTATAAAACATATCTTTTTATTATAACTGTAATAGCAAATACAGGAACTATTCTGTTGAAT
AGATAGCACAAAAATAAGCACCAAAATGAGTGTGATTAAAATTGGAGAGCTCTGAATAAAATTAAAACTAGTGTCA
ATATTCTGGCCATGATGAGTACAGCTGTTTTCAAAGACATTACTCTCTCCCCGGGAAGGAATTTTAGCAACAGGC
TTCCACTTTGTGCTTCAAGTTAAACTTGCAAAACAAAGAAGCCAGGACCTGAATTTGAGAAATAATGTGTGTCATT
TGTCTTTCTGTCCCTGAGTTGCCTCACTTGGCAAAACTTTGTTTCAACAAAACTCTTTAAAACAAGCATGTCAAGG
CTAGCTCATGATGCATCATGGTGACTAGCTAACAATATGTAATAACCATCATGGCACTGAGAATGATGTTGCTGG
TAGTTACTGTGGTGCCTATTGAGATGAAAATGACAATAATGATAATACATCAGTAGTAAAGGTGATAGCCATGGT
CATAATGGTAATGATGATAAGGATGGGTGGGTAGTGGTGATGGATGGTTGGTGGTGGTGGTGGTGATGGTAGT

GGTAGGGGGGGTAATGGTGGTGGTAACGGCTCTGTTGATGCTAAATTGTTCATTGCCCCATTATATTCTAAGTTTC
TGAAACTGAAAGATGACTTTTACAGATAAAAGAAGAATTAACACACTTGGGAAATAAAACATGATTCACAGAACAA
GAGAAAACATGAACTAATTGTTACTTTAGAGACAACAATGGTCTCTAGAGTGACTATATCCCAGGAGATGATCCA
CACACACACACACATATATATAAACAGAACCCCCAATTTTTAGTCATATTATATCACCTTTCCAAATGACAATCTCC
TTTTCTGGACTAGACTGGGCTCTTTAAGTAAATTTTGTGGTGTATACACATCTGCATACTTCTAGAATTTACTGAAT
ATTGAAGCCACAGACATTGCCTGAAGTTTCATTTGAGACGCTGTTTCATTTCCTTCAGCACAGGTATTTTGTCTAA
AAATTAGATGAGAAAATATCTTCTCTTGTGAGCTCTTCTTTATAGTTTAGACTATTTATGACCATATGTTGACAGTT
AACTTTTAATGCTCTGTTCTATGTGATGTACTCTCTTCAGAAAAAATCCTGAGCTTCTGAAAGCTTGATAATAATAG
CTAATACACATAGGAACTCAGAAGGTATGTGTGGTCCTAGTTGGGTCTTTTATATCATTAGAAAATTTAAGCTGTAC
CTGATAGCTAACACTGCTACCTGTATTTTCAGCACTTGGTCAGCTAAGGCAGGAGAATCATTACAAGCTGAAGGT
TAACCTGGGCTTTGGAGTGAGATCTTGTCTCAAAAAACAGTAGTGGGAGACCTGGAGAGGTGGCTCAGCAGTTA
AGAGCACTGACTGCTCATCCAGAGGTCATGAGTTCAAATCCCAAAAACCATCTGTAATGAGATCTGATGCCCTCT
TCTGGTGTATCTGAAGACAGCAACAGCAACAGTGTATTCATAAGCATAAAATAAATAAATACATCTTTAAAAAGAA
TCAGTAGTGGGGAAAAAGACAAGAATAAAAAGCTGCAGAAGAAGATTATATAAGCAAAAAAAAAAAATTGAGACTA
GCTGTCTGAGCTCATTCTACAAGAATGTATTCTCATCTACATTGCACTGGGTATATAACATTTACCCTGACCTGAT
TTACAAAGTATTTTAATCTCTGCTAATGGTTACTGAATATGTTTCTTATAATATTAAGAAGCAGAGATTCCATAAAG
AGGGATAGGTAATATTTTTAATTATTCATCATCTAGATAAAAATCATTTTGTAGCCGGGCTTGGTGGCACACGCCT
TTAATCCCAGCACTTGGGAGGCAGAGGCAGGCAGATTTCTGAGTTCAAGGCCAGCCTGGTCTACAAGGTGAGTT
CCAGGACAGCCAGGGCTATACAGAGAAACTCTGTCTCAAAAATTAAAAAAAGATCATTTTGTAGTAAATAAAAATA
ATATTCAAGATCATACCGATCTGTGATATGTCAATATGTAACTTTAGTTAAGAAACGTTCTATCACTAATTCAATAT
GTAAACCCTACATATAACACATATGTTCTAATATTCAAAATATTCCAAAGATGTTAAAGATTCTCTTATACTTAAGA
AAAAGGAAGTCACTTGACTCAGTAGATAAAGCCATTTTCCATCAAATCTTAAAACTTGAGTTTTATCCCTAGAAGC
TTTAAGAAACAAGGAGAAAGCCAATTTCTGCAAGTTGTATATACACACACAACACAGCACAGCACACTCGCTATA
CACAAAATCTCTTTTCACAAAACTGGTACTATAAGTGACTTTTGAAAGAATGAACTGAAGATGTGTCAATAATTAAT
AATTGTATCAAAAACAATTACCATAGTGAGATTCCTGCTATGCCTTAAGAAATGTATCCCATACTGTACAGGGGCA
GCACATGGCTGCAATCCCAGCCAGCAGGAAGAAGAAGAAGGGGTAAGTTCAAGGAAAACCAATGCTACATAGA
AAGACTTAACTTTCAAAAAAAGAAAAAGAAAAATAGAAAGAAATAGAGAATAATACCTCAGATATGAGAATTTAATT
TAATATGTATCACATCTACTAATAACAACACATGCTTCTTAGGAAAATATACTATATATGTATATATAATATGTATGA
TTTGACATAGTGATAAATGGTGCAATGGTTTAGGATCTAAAAATAATAGCTAAAATTAACAACAAAGTGCTTGCTG
ATCCCACAATAAGCAACTACTCATCAAATATGACAGGACAGCAGTAAGAAATACAGAACTTGGCCCTTTACTAAG
CTTTAAGGCCTCTGAAACCCTAAGGGCTGGTCCTTCTGTCAGCAAGAAGCAACAGTATAGAGAAGATATGTGTG
CCACAGCCAGAATAGCTCAGCAAGTGTCAAATGCAGAAAACCAGCTCTCCAAGCAGGGCAAGAACAGCCATTCA
CAAACTCCTTCTCTCCCACCACACAGGCTTCCCACCCAGACACAATGACTGCAGAGAATCAATCTACAGTGACA
GAGTTTATCCTCGGGGGGCTAACTAACAGGCCAGAGCTCCAGCTACCCCTCTTCCTCCTCTTTCTGGGGATCCT
CGTAGTCACCATGGTAGGAAACCTGGGCATGATCACCTTGATTGGACTCAACTCACAGCTTCACACCCCCATGT
ACTTCTTCCTCAGTAACCTGTCACTCGTGGATCTCTGCTACTCCTCTGTCATTACCCCTAAAATGCTCATCAACTT
TGTGGCCCAAAGAAACCTCATCTCCTATGTGGGGTGCATGTCTCAGCTATACTTCTTCCTGGTTTTCGTCATTGC
TGAGTGTTACATGCTCACTGTGATGGCCTATGACCGCTATGTGGCCATCTGTCAACCCTTGCTTTATAACATCAT
CATGTCTCCTGCCCTCTGCTCTCTGCTGGTGGCTTTTGTCTATGCCGTAGGACTCATCGGTTCAGCAATTGAGAC
TGGCCTCATGTTGAAATTAAACTATTGTGAGGACCTCATCAGCCACTACTTCTGTGACATCCTCCCCCTCATGAA
GCTCTCTTGCTCTAGTACCTATGATGTAGAAATGGCTGTCTTCTTTTTAGCTGGATTTGACATTATCGTCACAAGC
TTAACCGTACTCATTTCCTATGCATTCATCCTGTCCAGCATCCTTCGCATCAGCTCCAACGAGGGCAGGTCCAAA
GCCTTCAGCACCTGCAGCTCCCACTTTGCAGCTGTGGCTTGTTCTATGGATCCACAGCATTCATGTACTTAAAGC
CTTCTACAGCTAGTTCCCTGGCCCGGGAGAATGTAGCTTCTGTGTTCTACACCACAGTGATCCCCATGCTCAAC
CCCCTGATCTACAGCCTGAGAAACAAGGAGGTGAAGACCGCACTGGACAAAACACTGAGGAGAAAAGTCTTTTG
ATGT

RA (3807bp)

AAATGCTGATCTTTCTTCATGTAAAAGTAAGTGGTTATGCACACCTGTATGATAACCTCTGCAAGCTCACCCAACT
CTGAACAGGAAACAGGAATCATTGCTCTCCATTGTTGGGCTCAAGGCCAATCTCCTTGTCCTCATTCTCATCTTC
TCTACCATTGGTTCTATTTATAATTACTCGATTTTAAGATAATTTTTATATTATTGGGTCTCTGTCCTCTATATGAGG
CCAATGGTAAGCAATTTTATAATTTTTACTATTAATATTTCATCTATTATATAATGTATTTGATCATATTCACCCCCA
CCCTCTTCTTCTCTTTCATTATCACCCCCTATATATCTACCTCCCATTTTCATGTCCTCTTTTTTTTTTAATAACCAA
CTGCATCCAATTAATACTGTTTATATTCACATTAGTGTCTGGCCATGCATGGGAGCATGGGTAACCTACTAGCAA
ATCTCACACAAATTCATTTAATTAGTGGAATCTAAATTACTTCTAGGGTACTAGTTGCAAGTGATTCTGAGAAATG
CAGTTTCCAGCTTGTTGACACTAAATAGAATGTGTATTAAAGGGTTAGTAGGACAGTCTCACTTAAATAGCTTTTT
ACTCATTTTCTTCTGACCTTTCCCCAACAAAAGAAGAAATTGCTACCACTGTTGATATGCTCTAATTAGAACTAAA
GGTAGGAAACTATCTCAGAGGGAGACCTCTCGATGCAACAACAACAACAACAACAACAAAAAGGCAAAAGTGTA
ATTCTGAGTTAGAATACATGCCTGAAGAGGGTGAGGCACTGAATTTGACGTGATGTAATCAGTTTCACAATTTAC
TTATATTGGTTTTAAATATTGTAATCTGCAAAGTGGGCAAAACCAGGGAAAGATAATTCTGTGTTCCAGACAAGAC
AGAACAATCAGATCCAAATCTGTAGAGCAGGTTATTTCCACAGAAACATAGTGCTTCTCAGTTCAAGCTGCTCGC
CCAAATAAAGCTCTGGAGAGGCGACTTGTGAAGCATGGAACACCTCACTAGACTGCCCAAGGATTTTAGCCCAA
GAAAAGTCTTTGTCACCAGAGCTAGGACATTTAGTTTTATTTCCTGGTTAGTCATGAATTTTCCCTCTTAAACTTTA
CCTTTTCATAGAGTTGACTCCACTATACTTAGAACCACAAACTCTCACCGTCAACAACAGCATCCTCATTGTGAAT
ACCTTCCATGGAAAGACCAGAAGTCTTTTCTCTTTAGCCTTGACTTTACTTCAGTTTATTACAAGCACAAATGTATT
TTTTTCATTATTTGGAATTGATCAATTTGATGGCATTGTGCAAATTGCTTTACCAATTGGATGAATTTTCTCAAAAG
TGTAGTTTTTAAAGAGAAGTTTATTTTGAAGATCTTTATGAAACTGCCTATAATAGAGAGGAGCTGTGGCAGACTA
AACACCAAAAATCTTTCCTCTGCCTTTGTGCTAAAACTGTTGTTTCTAACACACGCACACAAAAATCTCCAACAGT
AGGCGTACATAATCTGGCATACATCACTGCTCTTAAAAACTTTTTAAACTGCCGGGCAGTGGTGGTGCATGTCTT
TAATCCCAGCATTTGGGAAGCAGAGGCAGGCAAATTTCTGAGTTCAAAGCCAGCCTGGTCTACAGAGAGAGTTC
CAGAACAGCCCAGGTTATACAACGAAACCCTGTCTCAAATAAATAAATAAATAAATAAATAAATAAATAAATAATA
ACCTTTTAAACTAATGTTAGTATCTTCATGATCTCAAACTGATTTAGGAAAATAACGTGTCCTTCTTTAGTGTTTGG
TATAGAGAGTATAGGCTCTTCACTAAATATTTACAGGAATCCTTTGTGAATAACTTCAAAGTATACAAGGCCATTC
CTAAATTTATAAGCTTGCACTATAGATTTTTGTTGAACTGTAGTCACACATCTTGTGGTTTTCAAAAATAGTATATC
TAACTTATGAAATGTATTATTAGCCCTTTTCTTCTTTTCCCCTTCTTTTCTCATGACTGAAGGTATGAAGCCAGTTC

AATGATGTGTTCATCTGTGTACTAAATACTGATAGTGTTTGTGTGCACAAAGGCTAAAAAGGCAAAAATTTTTGGA
AGAAGAGTTTGCTCTACCTGAAACCTGTAAAATACAGTCTTTAAATGACTATGTAACAGTGAAAGGTTCTTTTGTA
CTAAGCACTTAGAAGGTGAGTGACAACAATGTAGGAGAAAACTAATTTAAGGTCATTTCCAGTCCTTCCTCTTAG
CCACTCAAGAGTACAACTGTCCATCACTCCTAAAATGTCCACCCTCTTGAACATCTGTGAAATTCCCTTTTTCCCT
TAATTACCTTCTAAATAGTCTCAATTCCTCACATATACCTTCTATTTTATTTTTTGCTTCTGGTCTTCACTAGGACAC
TGTGTCTGACAGTTTGGCCTTGCCCACCACATTCACATAGCTGTCGAGTAATGGCTCCACATCACCCAAGCCTTC
CCCAGCATCTCCGCTGTCAACAAGCTGATGCCTTTTATGGACATGTTAAGGGAAACTTTCAGCAGTGATTTTTTT
GTAGGTTTTCATCTAAGGGTTAGGTCTTATGAAGTTTCCTCAATCTACATTTATCAGCTGATGTCATTACACAGGT
CTTGTTGAGGTTGTCACAATTTTATAGGTGCAGCTTCTTCGTTGCCATATCCAAAGATGCTATCTCATAGCAGGTA
GCCGGTTCCTCTAGCTCTTATAATCTTTCCACCACTCTTCCATGATGATCCCTGAGACTTAAATATAGTGTCTACA
TGTAGTTGCGAATATCTGCCATAGTGTCAGATATGAATCCCCTCCTAGTTAGCAAGCCTTAAGACTTTGAGGTTG
TTGCCATTCCCTAGCTACTGTGAGTAAAGTGGAAATGAACACAGTCAAGCAAGTATCTGTTGAGGAGAACACCCA
GTCCTTTGGCAATATACCAAAGAAGAATACAGCTAGATCCTGTGATAATCCAGTTATAACTTTCTGTGAATCCTCC
ACAGTGATTACCATAGAGGCTTCCCTATTTGCAACCCTAGCAACAATCAATAAGTCTTTTTGCCTTTCTCTGAATC
CTAGACATTTGTTTCAGTTGTTTTCTTAATCCTAACCATCTGACTGGAGTAAGGCAAAATCTAAAAGCAGTTTTAAT
TTGCATTTTCATAGTTGCAAAGGAAGTTAAACACATTTTTACATATTTGTCAGCCATTTTTATTTCTTCCTCTGAGA
TCTTTCTCTTCAAATCCAGGGCCTATTAGGGGTGGGGAGTGGTCAGTTAATGACCTTAATGACTGAGCAAATGGA
GTCTTTCTCAGAAAGTCTTTTACTACATCTCTATCTTAGAGGGGACTGCCTGTGTACTCTTCAAGCGGTTTTAGCA
TTTAACGTTGCCCATGGAAGTTTTTGATCCATTTGGAATTTTTGTACCAAATAATAGATGTGGGACTATTTTTATTC
TTCTACATGTGGACATCCAGTTTTACCAGCACAATTTGTTGAAGAGTTTGTCTTTATACCAGTGTATATGTTTAACA
TTTTTGTCAAATATCAGATGGCTAAACTCATGTTTCAGTTTTCTGTTCTGTTACTCTGATTTAAATGCCTGTTGGTT
TGGCCATTTATTTTGCTTTGTTTTGTTGCCAGTACCATGCAATTTTTATTACTATAGCTCTATAACACTGGTTGAAA
CTGTGTTCTATCTCTCTAGCATTGTTCTTTCTGCTCAGGATTTCTTTGGTTATCCTTAGTCTCTTATGGTTCCATAT
GG

pBluescript Phagemid Vector (2015)
http://www.genomics.agilent.com/GenericB.aspx?PageType=Vector&SubPageType=Vector&PageID=32

11 Acknowledgements

I would like to thank Dr. Peter Mombaerts for giving me the opportunity to work in his lab and on such versatile projects. His support, his belief in the projects, his scholarly advice and the inspiring discussions made this thesis possible.

I would like to thank Professor Bodo Laube for being my contact to the TUD and guiding me through this thesis. Even at a distance he was always supportive. His scholarly advice and fruitful discussions and open ears for my worries helped a lot.

I would like to thank Professor Paul G. Layer, for agreeing to evaluate this thesis and for his scholarly advise in the process.

A great thanks goes to my supervisor Dr. Mona Khan. Her advice, training, guidance and long discussions helped substantially for writing this thesis. Thank you for always taking the time for me.

Another great thanks goes to Dr. Martin Vogel. Thanks you for being always helpful and supportive. You are not only a good colleague but also a good friend.

I would also like to thank the members of the Max Planck Research Unit for Neurogenetic (Guido, Elisabeth, Isabelle, Diane, Bartos, Christian, Anna H., Anna D., Andrea, Markela, Marta, Mario, Maria, Masayo, Bolek, Kia, Evelien, Florian, Tobias, Zhaodai, Jiangwei, Zheng, Bassim, Sachiko, Alex, Jan and Vicky) for all their timely helpful advice and unconditional support for my research. A special thanks to the animal caretakers Rebecca L., Rebecca W., Steffi, Mandy, Caroline, Annelie and Ali for helping in handling all the various mice strains and advising me in breeding strategies.

Last but not least I would like to thank my family and friends. I wouldn’t have made it without the unconditional support from my parents. Thank you for listening to my science rambling. Also thank you to my friends for keeping up with me during the stressful periods in research and writing. Especially thanks to Christine for support and advice on writing and Damaris for cheering me up when work got tough.

Thank you all.

12 Ehrenwörtliche Erklärung:

Ich erkläre hiermit ehrenwörtlich, dass ich die vorliegende Arbeit entsprechend den Regeln guter wissenschaftlicher Praxis selbstständig und ohne unzulässige Hilfe Dritter angefertigt habe.

Sämtliche aus fremden Quellen direkt oder indirekt übernommenen Gedanken sowie sämtliche von Anderen direkt oder indirekt übernommenen Daten, Techniken und Materialien sind als solche kenntlich gemacht. Die Arbeit wurde bisher bei keiner anderen Hochschule zu Prüfungszwecken eingereicht.

Olaf Christian Bressel

Darmstadt, den ……

13 Curriculum vitae

1. Family name Bressel

2. First name Olaf Christian

3. Date of birth October 16, 1982

4. Nationality German

5. Civil status Not married

6. Education Elementary school,
Prälat-Diehl-Schule Groß-Gerau, German “Gymnasium“ leaving certificated with “Abitur”
Student of Biology at the Technische Universität Darmstadt

7. Language skills German (mother tongue), English (good), Latin (good)

8. Present position Ph.D. student at the Max Planck Research Unit for Neurogenetics since November 2009 in cooperation with TU Darmstadt

9. Key qualifications Advanced practicum in genetics
Advanced practicum in animal physiology, partial at the Max Planck Institute for Brain Research, Frankfurt, Germany
Advanced practicum in plant physiology
2.5 months lab practicum at University of New South Wales, Sydney, Australia
8 months diploma thesis at University of New South Wales, Sydney Australia
Graduated the Preliminary Diploma Examination at Semester 4
Graduated

10. Professional experience record
Practicum at the Institute of Pathology, Darmstadt, 2 weeks
Part-time IT-Job, Dresdner Bank Frankfurt, 3 weeks
German army, 9 months, Pioneer “Obergefreiter”, 2 medals for disaster aid
Part-time job retail Games Workshop, Frankfurt, 5 years
Proxy project leader for S1 Security at Max Research Unit for Neurogenetics (since 2015)

11. Others archery, roleplaying